Master Thesis
LIU-IEI-TEK-A–19/03400—SE

# Control of a Hydraulic Hybrid System for Wheel Loaders

**Christopher Reichenwallner**
**Daniel Wasborg**

Department of Management and Engineering
Division of Fluid and Mechatronic Systems
Linköping University, SE-58183, Linköping, Sweden

Supervisors: **Liselott Ericson**
IEI, Linköping University
**Karl Uebel**
Volvo Construction Equipment
**Martin Rohdin**
Volvo Construction Equipment

Examiner: **Petter Krus**
IEI, Linköping University

July 2019

# Abstract

In recent years many companies have investigated the use of hybrid technology due to the potential of increasing the driveline's efficiency and thus reducing fuel consumption. Previous studies show that hydraulic hybrid technology can be favourable to use in construction machinery such as wheel loaders, which often operate in repetitive drive cycles and have high transient power demands. Parallel as well as Series hybrid configurations are both found suitable for wheel loader applications as the hybrid configurations can decrease the dependency on the torque converter. This project has investigated a novel hydraulic hybrid concept which utilizes the wheel loaders auxiliary pump as a supplement to enable both Series and Parallel hybrid operation. Impact of accumulator sizes has also been investigated, for which smaller accumulator sizes resembles a hydrostatic transmission. The hybrid concept has been evaluated by developing a wheel loader simulation model and a control system based on a rule-based energy management strategy. Simulation results indicate improved energy efficiency of up to 18.80 % for the Combined hybrid. Moreover, the accumulator sizes prove to have less impact on the energy efficiency. A hybrid system with decreased accumulator sizes shows improved energy efficiency of up to 16.40 %.

# Acknowledgements

This thesis serves as the final part of a master's degree at the Division of Fluid and Mechatronic Systems (Flumes) at Linköping university. The work has been carried out at Volvo Construction Equipment AB in Eskilstuna, Sweden. We are very grateful for the opportunity to perform our thesis at Volvo CE, the time spent has been nothing less than excellent much thanks to our supervisors Karl Uebel and Martin Rohdin. Thank you very much for all your support, knowledge and valuable discussions throughout the work. A special thanks to Vilhelm Fredriksson for sharing your knowledge and for the time spent supporting us. The list of helpful people at Volvo CE can be made very long, we would like to thank you all for your contribution and help.

A big thank you Liselott Ericson for your supervision and support during the thesis. We will also always be grateful for the opportunities you have given us during our study time at Flumes. Thank you Petter Krus for your insightful and interesting input. We would also like to thank Henrique Raduenz for your interest in our work and helpful comments from many miles away.

*Linköping, July 2019*
Christopher Reichenwallner
Daniel Wasborg

# Contents

# Nomenclature

| | | |
|---|---|---|
| $A$ | Valve area | $[m^2]$ |
| $c_v$ | Real gas specific heat | $[kJ/kg \cdot K]$ |
| $c_v^0$ | Ideal gas specific heat | $[kJ/kg \cdot K]$ |
| $C_q$ | Flow coefficient | $[-]$ |
| $D_{m1}$ | Machine 1 displacement | $[m^3/rev]$ |
| $D_{m2}$ | Machine 2 displacement | $[m^3/rev]$ |
| $\Delta p$ | Pressure difference | $[Pa]$ |
| $\Delta V_g$ | Difference in gas volume | $[m^3]$ |
| $\Delta V_{oil}$ | Difference in oil volume | $[m^3]$ |
| $\varepsilon_{m1}$ | Machine 1 displacement setting | $[-]$ |
| $\varepsilon_{m2}$ | Machine 2 displacement setting | $[-]$ |
| $\varepsilon_{ref}$ | Reference displacement setting signal | $[-]$ |
| $F_{brk}$ | Breakaway friction force | $[N]$ |
| $F_C$ | Coulomb friction force | $[N]$ |
| $F_{conventional}$ | Conventional traction force | $[N]$ |
| $F_{hybrid}$ | Hybrid traction force | $[N]$ |
| $F_S$ | Stribeck friction force | $[N]$ |
| $F_{traction}$ | Traction force | $[N]$ |
| $F_{translational}$ | Translational force | $[N]$ |
| $F_{transMax}$ | Maximum translational force | $[N]$ |
| $F_V$ | Viscous friction force | $[N]$ |
| $i_C$ | C-axle gear ratio | $[-]$ |
| $i_{FD}$ | Final Drive gear ratio | $[-]$ |
| $i_{PTO}$ | Power Take-Off gear ratio | $[-]$ |
| $i_{tra}$ | Transmission gear ratio | $[-]$ |
| $i_{WH}$ | Work Hydraulics gear ratio | $[-]$ |
| $\eta$ | Efficiency | $[-]$ |
| $\eta_{hm}$ | Hydro-mechanical efficiency | $[-]$ |
| $\eta_{vol}$ | Volumetric efficiency | $[-]$ |
| $\eta_{ix}$ | Arbitrary gear ratio efficiency | $[-]$ |

| | | |
|---|---|---|
| $m_{nitrogen}$ | Nitrogen mass | $[kg]$ |
| $\mu_{TC}$ | Torque Converter torque amplification factor (Torque Ratio) | $[-]$ |
| $n$ | Polytropic exponent | $[-]$ |
| $n_{FD}$ | Final Drive rotational speed | $[rev/s]$ |
| $n_{ICE}$ | Internal Combustion Engine rotational speed | $[rev/s]$ |
| $n_{impeller}$ | Impeller rotational speed | $[rev/s]$ |
| $n_{m1}$ | Machine 1 rotational speed | $[rev/s]$ |
| $n_{m2}$ | Machine 2 rotational speed | $[rev/s]$ |
| $n_{turbine}$ | Turbine rotational speed | $[rev/s]$ |
| $\nu_{TC}$ | Torque Converter slip ratio (Speed Ratio) | $[-]$ |
| $P_{ICE}$ | Internal Combustion Engine power | $[W]$ |
| $P_{in}$ | Power in | $[W]$ |
| $P_{out}$ | Power out | $[W]$ |
| $P_{WH}$ | Work Hydraulics power | $[W]$ |
| $p_0$ | Initial charge pressure | $[Pa]$ |
| $p_{acc}$ | Node A pressure | $[Pa]$ |
| $p_B$ | Node B pressure | $[Pa]$ |
| $p_C$ | Node C pressure | $[Pa]$ |
| $p_D$ | Node D pressure | $[Pa]$ |
| $p_{acc}$ | Accumulator pressure | $[Pa]$ |
| $p_g$ | Gas pressure | $[Pa]$ |
| $p_{init}$ | Pressure at start of simulation | $[Pa]$ |
| $p_{ref}$ | Reference pressure signal | $[-]$ |
| $p_{reservoir}$ | Reservoir pressure | $[Pa]$ |
| $Q$ | Energy | $[J]$ |
| $q_{fuel}$ | Fuel flow | $[m^3/s]$ |
| $q_{m1}$ | Machine 1 flow | $[m^3/s]$ |
| $q_{m2}$ | Machine 2 flow | $[m^3/s]$ |
| $R$ | Universal gas constant | $[J/kg \cdot K]$ |
| $r_{tire}$ | Tire radius | $[m]$ |
| $\rho$ | Oil density | $[kg/m^3]$ |
| $S$ | Entropy | $[J/K]$ |

| | | |
|---|---|---|
| $T_{FD}$ | Final Drive torque | $[Nm]$ |
| $T_g$ | Gas temperature | $[K]$ |
| $T_{ICE}$ | Internal Combustion Engine torque | $[Nm]$ |
| $T_{impeller}$ | Impeller torque | $[Nm]$ |
| $T_{in}$ | Input torque | $[Nm]$ |
| $T_{m1}$ | Machine 1 torque | $[Nm]$ |
| $T_{m2}$ | Machine 2 torque | $[Nm]$ |
| $T_{out}$ | Output torque | $[Nm]$ |
| $T_s$ | Ambient temperature | $[K]$ |
| $T_{WH}$ | Work Hydraulics torque | $[Nm]$ |
| $\tau_{BWR}$ | BWR temperature time constant | $[s]$ |
| $\tau_{disp}$ | Displacement setting time constant | $[s]$ |
| $U$ | Internal energy | $[J]$ |
| $V$ | Volume | $[m^3]$ |
| $V_0$ | Initial charge gas volume | $[m^3]$ |
| $V_g$ | Accumulator gas volume | $[m^3]$ |
| $V_{init}$ | Volume at start of simulation | $[m^3]$ |
| $v$ | Velocity | $[m/s]$ |
| $v_{brk}$ | Breakaway velocity | $[m/s]$ |
| $v_{Coul}$ | Velocity at maximum Coulomb friction | $[m/s]$ |
| $v_{St}$ | Velocity at maximum Stribeck friction | $[m/s]$ |
| $v_{veh}$ | Vehicle velocity | $[m/s]$ |
| $W$ | Work | $[J/kg]$ |
| $\omega_{out}$ | Output rotational speed | $[rev/s]$ |
| $\omega_{in}$ | Input rotational speed | $[rev/s]$ |

## Abbreviations

| | |
|---|---|
| ACC | Accumulator |
| BWR | Benedict-Webb-Rubin |
| DP | Dynamic Programming |
| EMS | Energy Management Strategy |
| EPS | Displacement Setting |
| ETA | Efficiency |
| FD | Final Drive |
| HP | High Pressure |
| ICE | Internal Combustion Engine |
| LP | Low Pressure |
| NC | Normally Closed |
| NO | Normally Open |
| PRV | Pressure Relief Valve |
| PTO | Power Take-Off |
| REF | Reference |
| SHHS | Supplementary Hydraulic Hybrid System |
| SLC | Short Loading Cycle |
| SOC | State Of Charge |
| SR | Slip Ratio |
| TC | Torque Converter |
| TR | Torque Ratio |
| TRA | Transmission |
| WH | Work Hydraulics |

# 1 Introduction

Increased environmental awareness and higher fuel prices are some reasons leading to rising demand for fuel efficient vehicles with low emissions [1, 2]. Due to the awareness a lot of development in the automotive industry has turned towards alternative fuels and hybrid technology. Electric powertrains are commonly used in cars because of its high efficiency [3] and the renewable potential of electricity. In construction machinery however, other type of hybridization technologies, such as hydraulic hybrid technology, may be favourable due to short, repetitive drive cycles with high transient power outputs [2, 4]. A previous study has shown fuel efficiency advantages with a Parallel hydraulic hybrid concept in a wheel loader [5]. This project has investigated a novel hydraulic hybrid concept which enables both Series/Parallel operation.

Vehicles using Internal Combustion Engine's (ICE) most often require a transmission to transfer rotational speed and torque to the wheels and to decouple the engine from the wheels. The two most common types of transmissions are the manual and automatic transmissions. Using a manual transmission in a wheel loader is not realizable due to high traction forces and repetitive drive cycles with many start and stops which would lead to excessive clutch wear. Hence, wheel loaders commonly uses automatic transmissions. The substitute for the mechanical clutch is known as the Torque Converter (TC). However, the TC is a big contributor to power losses due to its low efficiency during high slip operations, especially when used in wheel loaders [4]. High slip, i.e. when the TC's output shaft is rotating much slower than its input shaft, may occur when large tractive forces are needed, for instance during bucketfill operation. Expectations are that a Series/Parallel hydraulic hybrid concept can reduce power losses in the TC by introducing an alternative power path. Possible advantages are, among others, lower fuel consumption and increased productivity as well as potential for reduced component wear.

## 1.1 Project scope and aim

The aim of this project is to investigate the possibility for energy savings using hydraulic hybrid technology while maintaining an acceptable operability in a wheel loader application. The scope includes development of an Energy Management Strategy (EMS) for the hydraulic hybrid concept for a wheel loader drive cycle. Based on the EMS a control system is developed, which control relevant hardware components, such as valves and hydraulic machines. The control system is evaluated in a simulation environment for which a wheel loader simulation model is developed. Included in the scope is also how smaller accumulator sizes affects the energy savings. The aim can be translated into the following research questions:

- **Q1:** To what extent can energy losses in the driveline be decreased by using a series/parallel hydraulic hybrid system in a wheel loader?
- **Q2:** How can the operability of the wheel loader be preserved during a short loading cycle?
- **Q3:** When should the energy storage be charged/discharged and with what configuration?
- **Q4:** What is a suitable control system architecture for the hydraulic hybrid system?

## 1.2 Delimitations

The project is limited to evaluate the hybrid system for a short loading cycle using the bucket tool for transportation of gravel material. Strategies for gear shifts, auxiliary power consumers and work hydraulics are not considered. Recuperation of energy will only consider kinetic energy. The reference conventional driveline is limited to address one engine, an automatic transmission and a TC.

## 1.3 Method

The following methods are used throughout the project.

- Literature study
- Modeling
- Simulation
- Control engineering

A literature study is conducted to gain sufficient theoretical background about hybrid vehicle technology, EMS and driveline components. A wheel loader simulation model and

control system is developed for the proposed concept. In parallel, the opportunities of the concept is analysed and an EMS is defined. The EMS and control system is then further refined in an iterative development process in a simulation environment, namely Matlab/Simulink. The wheel loader simulation model provides the opportunity for rapid evaluation of the EMS and control system's functionality. Lastly, an evaluation of results acquired from the simulations is made and the performance for the hybrid concept is benchmarked against the conventional driveline in terms of energy efficiency.

## 1.4 Thesis outline

Relevant theory is presented for the reader to gain sufficient background knowledge about the material presented in the thesis. The theory includes general information about wheel loaders, drive cycle, mechanical and hydraulic components as well as hybrid vehicles. In the third chapter the hybrid system concept is introduced. Followed by the fourth chapter which concerns energy management strategies.

Chapter five focuses on modelling, control system architecture and simulation. The simulation results are presented in chapter six followed by discussion and conclusions in chapters seven and eight. Lastly, future work possibilities are suggested in chapter nine.

# 2 Theory

The section briefly covers relevant theory that is addressed throughout the project.

## 2.1 Wheel loaders

Wheel loaders are off-road vehicles with pivoted rear axle, rubber tires and a hydraulically controlled load assembly for the work functions [6]. Wheel loaders are often articulated between the front and rear axle which allow narrow turns. Large wheel loaders often have four wheel drive [6] and use the counter weight principle to be able to carry mass. Generally, wheel loaders are highly versatile machines, capable of handling many different types of tasks and they are a common sight on workplaces such as mine quarries, paper mills and construction sites. The main enabler for wheel loaders versatility is a high level of modularity of the machines load assembly which enable mounting of a wide variety of tools. One of the most common tools is the bucket. Other commonly used tools are forks, grapples, handling arm and pickup-sweeper, Figure 2.1 displays usage of some of these tools.

Figure 2.1: Examples of applications for wheel loaders and the various type of tools that can be used. In the top left picture timber is transported using grapples, in the top right picture a pick-up sweeper tool is used and in the bottom picture a bucket is used. Picture source: [7].

This project focuses on wheel loaders using the bucket tool for the purpose of transporting gravel. For this application, the fuel consumption and potential productivity of the wheel loader is linked to a large number of factors, for example machine specification, pile characteristics and skill level of the operator just to mention some. Previous studies show that fuel efficiency can differ up to 200 % and productivity up to 700 % between novice and professional operators when operating a Short Loading Cycle [8]. The Short Loading Cycle will be presented in Section 2.2.

The wheel loaders size is a key factor in how much load that the machine can carry.

Especially the counterweights mass is important for the load capacity [9]. Depending on the mass the wheel loader is specified for, driveline, chassis and work functions have to be dimensioned accordingly. Increased mass capacity requires larger engine, counterweight, hydraulic load assembly and stronger chassis.

Regarding pile characteristics one study shows that the degree of rock fragmentation and material uniformity has an effect on machines productivity. The study concludes that large particle sizes and low uniformity of the material affects the productivity negatively. Small particle sizes and uniform material is preferred from a productivity point of view. [10]

## 2.2 Short Loading Cycle

One of the most common drive cycles for wheel loaders is the Short Loading Cycle (SLC). The SLC is used when the wheel loader loads material (often gravel or stone) onto a hauler that in turn transports the material to another location for processing. The SLC is characterized by a low cycle time, frequent starts and stops and high transient power demands. Cycle time is generally not more than 25-40 seconds. During that time the wheel loader operator has filled the bucket, driven the machine to the hauler, unloaded the load and driven the machine back to the pile.

The driving pattern of the SLC is visualized in Figure 2.2. To explain the different phases of one cycle the numbers in the figure will be used. Green colour illustrates drive, i.e when the operator is accelerating/travelling at constant speed. Brake is illustrated by red colour. The cycle starts at (1) when the operator enters the pile to gather material, this phase is referred to as bucketfill. (2) The operator shifts to reverse and reverses out from the pile. (3) The operator lines the machine up towards the hauler, brakes and shifts to forward. (4) While travelling towards the hauler, the operator lifts the bucket to prepare for unloading of the bucket's load. (5) The operator shifts to reverse and reverses the machine. (6) The operator brakes and shifts to forward to line the machine up for bucketfill operation once again. The cycle is completed at (7) and the machine is ready for yet another cycle. In Figure 2.3 a simplified velocity profile of the cycle can be seen.

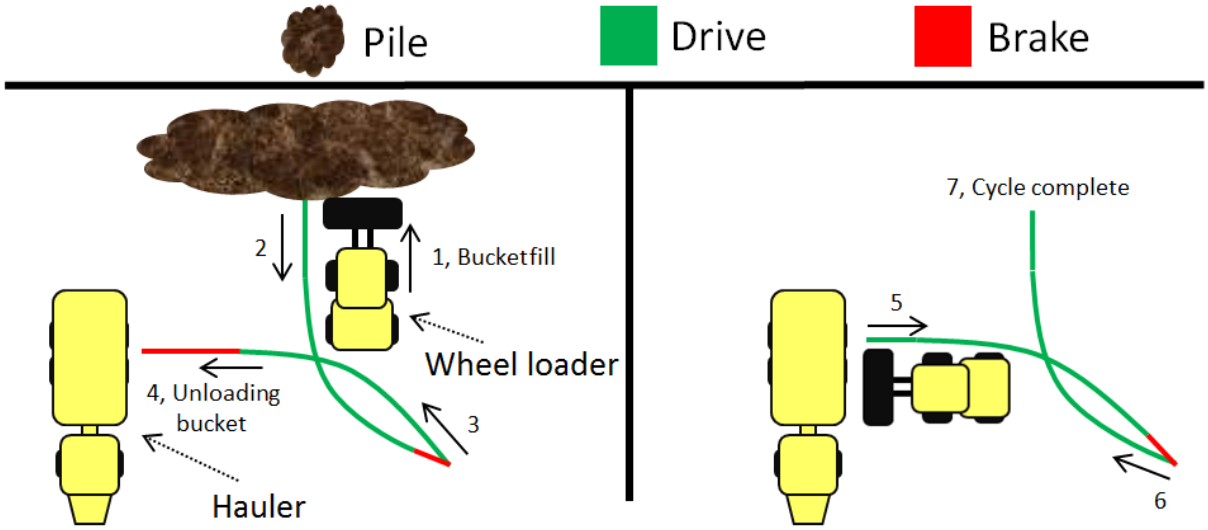


Figure 2.2: One of the most common drive cycles for wheel loaders, the short loading cycle. Green colour illustrates drive. Red illustrates braking and brown a gravel pile. One cycle consist of: (1) Bucketfill ⇒ (2) Reverse from pile ⇒ (3) Approaching hauler ⇒ (4) Unloading bucket ⇒ (5) Reverse from hauler ⇒ (6) Approaching gravel pile ⇒ (7) cycle complete.

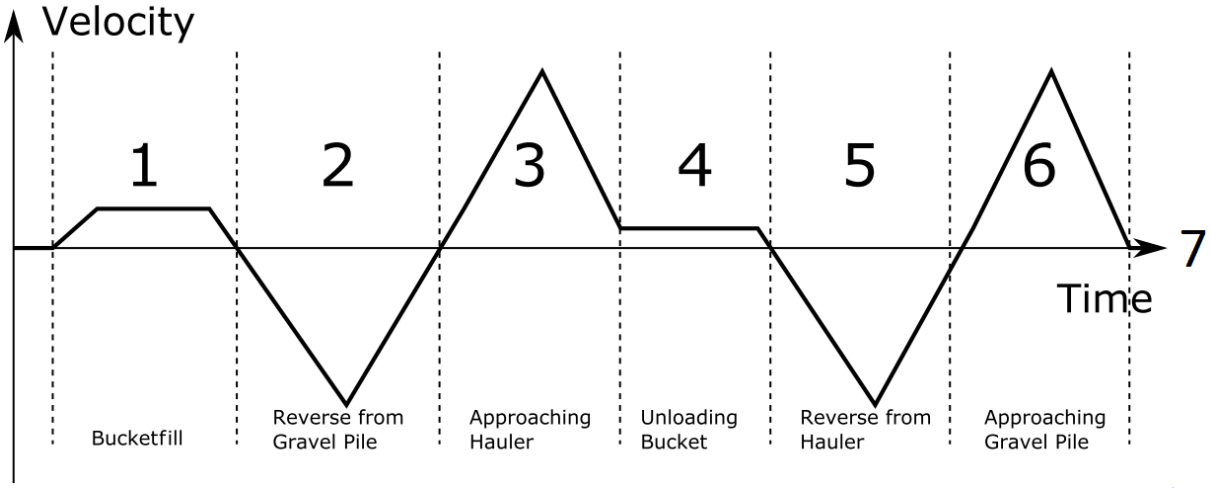


Figure 2.3: Simplified velocity profile of the short loading cycle. Picture source [5].

## 2.3 Driveline components

A schematic illustration of the Conventional wheel loader driveline with representation of the work hydraulics can be studied in Figure 2.4. The main components of the Conventional wheel loader driveline is:

- Internal Combustion Engine which converts diesel power to rotational mechanical power.
- Torque Converter (TC) which amplifies torque
- Transmission with multiple gear ratios
- Final Drive (FD) which splits and amplifies the provided torque to the wheels.

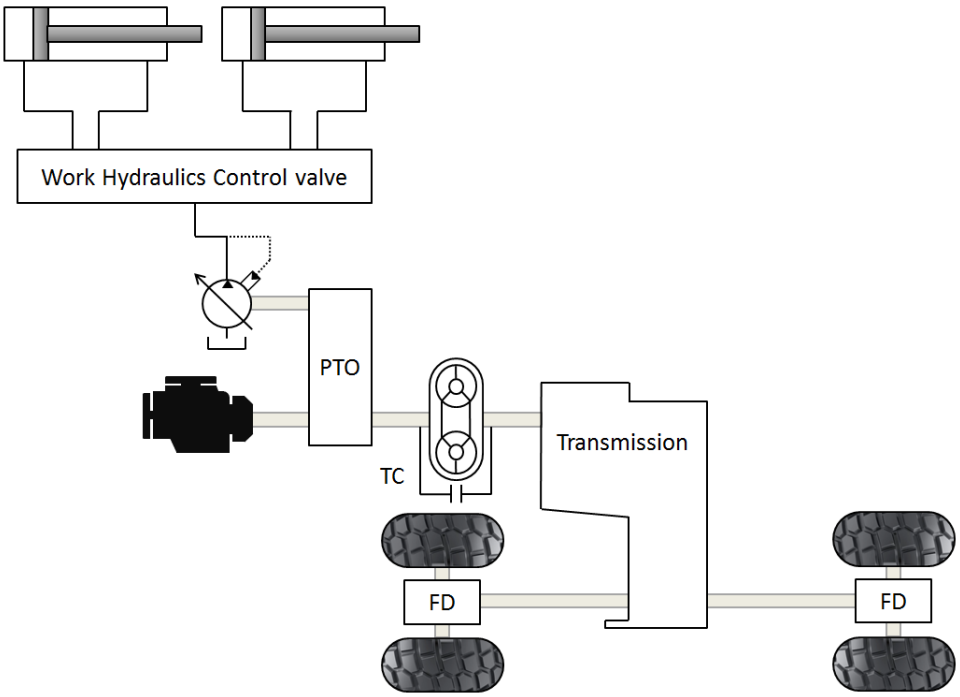


Figure 2.4: Schematic illustration of the conventional wheel loader driveline.

The TC is considered the most relevant component for this project and will therefore be further explained.

### 2.3.1 Torque Converter

The TC is a hydrodynamic coupling which has the function to transfer power from the ICEs crankshaft to the transmission. It is an important component in the driveline for mainly two reasons, torque amplification and mechanical decoupling of the ICE from the wheels [11]. Regarding decoupling the TC can be compared to the function of a clutch in a manual transmission. TCs working principle can be exemplified by two identical electric

fans. One fan, which is powered blows air (fluid) towards another fan which is switched off. When the fluid reaches the fan which is switched off it will start to rotate and power is transferred. TCs use the same principle for transferring power, the powered fan represents the ICE shaft and the switched off fan represents the transmission shaft [11, 12]. TCs are commonly used together with an automatic transmission in cars, trucks, wheel loaders and many more vehicles. In heavy applications such as wheel loaders and other construction machinery the TC is often used because of its low cost, well known behaviour and robust design [13].

The TC consist of three main components; impeller, turbine and stator, see Figure 2.5. The impeller and turbine is situated inside a casing which is filled with oil. The impeller is connected directly to the ICE output shaft and the turbine is connected to the transmission input shaft. When the ICE makes the impeller rotate oil flows into the impeller and is pressurized by centrifugal forces. The pressurized oil is directed towards the turbine. The impact between the pressurized oil and the turbine blades applies large forces on the turbine blades, which results in turbine motion. The fluid is then directed back into the stator. The stator's function is to slow down the speed of the fluid and channel it back to the impeller, completing the loop. As the TC provides mechanical decoupling between engine and wheels it enables gears to be fully engaged even though the vehicle is moving very slowly or standing still. [11, 12]

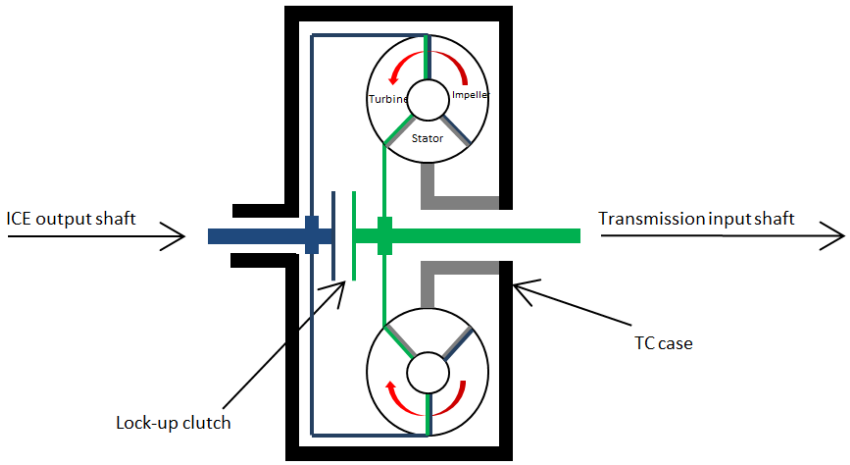


Figure 2.5: Side crop of a TC, the main components are the impeller which is connected to the ICE shaft, the turbine which is connected to the transmission shaft and the stator which is mounted between the impeller and turbine.

TCs have three stages of operation; stall, acceleration and coupling. Stall occurs when the impeller spins but the turbine is held stationary by the brakes or high traction forces. At stall maximum torque amplification may be achieved, stall speed is the maximum speed difference between impeller and turbine speed. Acceleration is when the turbine starts to speed up, torque amplification decreases but turbine speed is increased. Coupling is when the lock-up function is used. The torque amplification becomes 1:1, and the wheels are mechanically coupled to the ICE. [12]

Efficiency of hydraulic and mechanical components may be calculated using Equation 2.1 which is equivalent to Equation 2.2.

$$\eta = \frac{P_{out}}{P_{in}} \tag{2.1}$$

$$\eta = \frac{T_{out} \cdot \omega_{out}}{T_{in} \cdot \omega_{in}} \tag{2.2}$$

For TCs the efficiency can be described in an alternative, perhaps more intuitive way. Equation 2.2 happens to include two more quantities, namely the slip ratio and the torque ratio, described in Equation 2.3 and 2.4 respectively.

$$\nu = \frac{\omega_{out}}{\omega_{in}} \tag{2.3}$$

$$\mu = \frac{T_{out}}{T_{in}} \tag{2.4}$$

Substituting the slip and torque ratio equations into Equation 2.2 yields Equation 2.5.

$$\eta = \mu \cdot \nu \tag{2.5}$$

The main disadvantage with TCs are poor efficiency at low values of $\nu$, indicated in Figure 2.6. At low efficiency operations, a large amount of power is dissipated as heat. In fact, the poor efficiency is the reason for the lock-up function invented in the 1980's [11]. Studies show that the lock-up function can significantly decreases the fuel consumption for a wheel loader application [14].

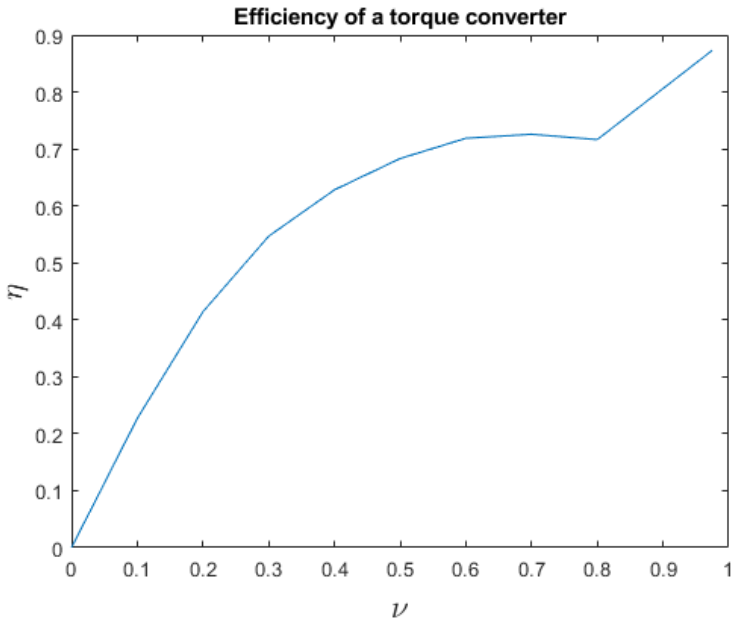


Figure 2.6: Example of TC efficiency characteristic.

Negative slip is a common phenomenon for TCs in wheel loaders. The phenomenon occur if the operator flips the gear lever from reverse to forward or vice versa while the vehicle is still in motion. This results in the turbine side of the TC starting to spin in the opposite direction of the impeller. The consequence is that both sides of the TC starts to pressurize the fluid in attempt to push the fluid to the opposing side. Negative slip causes wear on the TC [15] as well as increased fuel consumption as the component is used for braking the wheel loader [16].

## 2.4 Hydraulic components

A hydraulic hybrid concept requires several hydraulic components to function. Accumulators, hydraulic machines and valves are key components to make the hybrid concept reality. The relevant components are presented in this chapter.

### 2.4.1 Accumulators

Fluids can not practically be compressed for energy storage purposes in hydraulic systems. Instead, accumulators are used to store energy in hydraulic circuits. Hydraulic accumulators are characterized by high capacitance just as their electric equivalent, the supercapacitor. One of the main advantages of hydraulic accumulators is their potential to store and release energy in very short time intervals, i.e they have high specific power. The main disadvantage with hydraulic accumulators compared to, for example electric batteries is the poor specific energy, i.e they require large volume to store high amounts of energy. This can be an issue in applications which are sensitive to weight and size, such as vehicles. [21]

There are various different applications that reflects the potential of hydraulic accumulators high capacitance. In hydrostatic circuits they provide capacitance if flow fluctuations occur [17, 21]. Moreover they can be used as shock cushioning/pulsation absorption, as hydraulic systems in many cases are exposed to pressure peaks. Accumulators can effectively absorb these pressure peaks, which potentially could damage the other components in the hydraulic circuit such as hoses [17]. There is also potential to even out the power demand over the drive cycle. If the drive cycle contains large variations in power the accumulator could be charged during the periods that the pump is idling, which provides possibilities for energy savings and pump downsizing. [17, 21]

Thermodynamic processes affect accumulators pressure level since heat will either dissipate i.e energy is lost or be absorbed i.e energy is gained depending on the accumulators gas temperature in relation to the surrounding temperature.

*Hydro-pneumatic accumulators* are the most common type of accumulator. These type of accumulators utilize gas, often nitrogen, as compressible medium. They are both superior in performance and more compact than for example *spring loaded accumulators*. There are different types of hydro-pneumatic accumulators, namely piston and bladder type, see Figure 2.7. There are also the less common diaphragm accumulator made for applications

where small volumes and flexible placement is desired. [17]

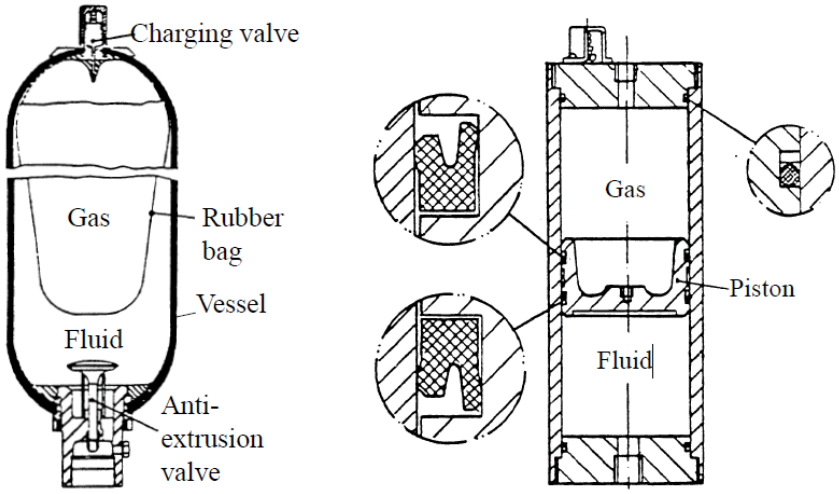


Figure 2.7: Hydro-pneumatic accumulators, the most common accumulator type in hydraulic system [17]. In the Figure two types of hydro-pneumatic accumulators can be seen, to the left bladder type and to the right piston type. Picture source: [21].

*Piston hydro-pneumatic accumulators* uses a piston plate to separate the oil from the compressible gas. Depending on the oil's pressure, the piston will be displaced to a certain degree, compressing the gas. This type of accumulator is highly sensitive to contamination that could damage the seal between piston and cylinder [21]. The *bladder hydro-pneumatic accumulators* separates the oil from the compressible gas with a rubber bladder. Increasing oil pressure compresses the rubber bladder and thus the gas. Decreasing oil pressure results in expatiation of the bladder, extruding the oil. If pressure drops too low there is a risk that the bladder extrudes from the accumulator. Hence a safety valve is used to close the accumulator if the bladder press against it, stabilizing the pressure. [17, 21]

### 2.4.2 Hydraulic machines

Hydraulic machines are key components for the hybrid system. An hydraulic machine either operate as pump converting mechanical rotary power into hydraulic power or as motor converting hydraulic power into rotary mechanical power [21]. Hydraulic power is defined by two central physical quantities, pressure and flow. The flow provided by hydraulic pumps is described by Equation 2.6. The torque required for pumps to maintain certain pressures is described by Equation 2.7 [22]. Hydraulic pumps deliver flow but not pressure. Pressure is a consequence of the resistance to flow occurring in pipes and at the flow consumer. Hence the pump only maintains the essential pressure. [23]

$$q = \varepsilon D n \eta_{vol} \tag{2.6}$$

$$T = \varepsilon D \frac{\Delta p}{2\pi} \eta_{hm} \tag{2.7}$$

The quantities in the equations are described as follows: $\varepsilon$ denotes the displacement setting of the hydraulic machine, $D$ the machine displacement, $n$ rotational speed, $\Delta p$ pressure difference, $\eta_{vol}$ the volumetric efficiency and $\eta_{hm}$ the hydromechanical efficiency.

Rotational speed, pressure, displacement setting and viscosity are all examples of quantities affecting the efficiency of the hydraulic machine. Hydromechanical losses are influenced by pressure differences over the machine and frictional losses in the machine while volumetric losses are caused by machine leakage and compressibility of the fluid. [21]

Hydraulic machines can be divided into two groups, rotational- and piston machines. The difference between the types correlates with the movement of the work element. Rotational machines uses rotating work elements while in piston machines the work element performs linear movements. Another major difference between the two types is the sealing gaps. Smaller and fewer sealing gaps allows the machine to work on higher rotational speeds and higher pressure with maintained high efficiency. Normally, rotational machines has larger and more sealing gaps compared to piston machines implying piston machines to be more suitable for high speed and high pressure operations [21]. Gear and vane machines are two examples of rotational machines while in-line and bent-axis machines are two examples of piston machines which fall under the category of piston machines.

For hydraulic hybrid vehicles, the displacement control is of importance to avoid disturbances in the vehicle speed which can have negative effects on the operability. Fast and accurate displacement controllers are therefore essential [18]. Control of hydraulic hybrid vehicles has also been stated to be more complex than for an electric hybrid vehicle, see [2, 18], which can make the control challenging.

*In-line machines* are characterized by the pistons and the input shaft being aligned, see Figure 2.8. A tiltable swash plate realize the variability of the machine and negative displacement is relatively easy obtained. Due to the low moment of inertia of the moving parts in the in-line machine displacement control is accurate and easily accomplished [24].

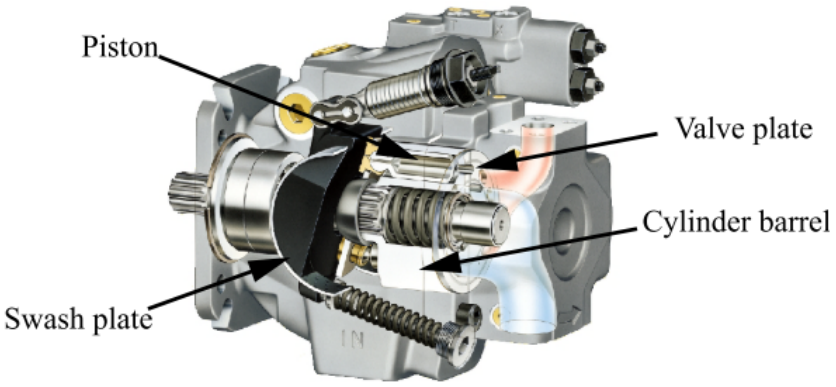


Figure 2.8: Axial piston machine of in-line type. Picture source: [21].

*Bent-axis machines* are instead characterized by the pistons being in an angle to the input shaft, which enables the machine to displace fluid, see Figure 2.9. This principle allows the bent-axis machine to obtain larger angles compared to the in-line machine, which is beneficial from en efficiency and power density point of view. Another advantage of the

bent-axis machine is its high torque and efficiency at low rotational speeds, which makes it favourable for motor operations. However, the design of the bent-axis machine makes displacement setting angles bulkier to alter since the whole cylinder house needs tilting, which specifically complicates negative displacements. [24]

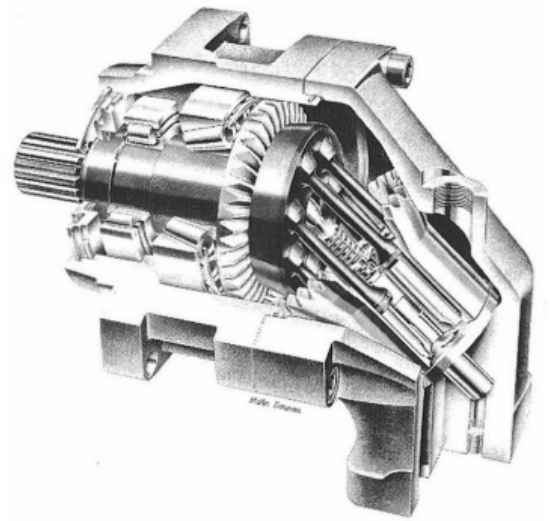

Figure 2.9: Axial piston machine of bent-axis type. Picture source: [21].

### 2.4.3 Valves

There are a large amount of various kinds of valves for hydraulic applications, the valves relevant to this project will be briefly explained in this chapter. In Figure 2.10 four different type of valves can be seen.

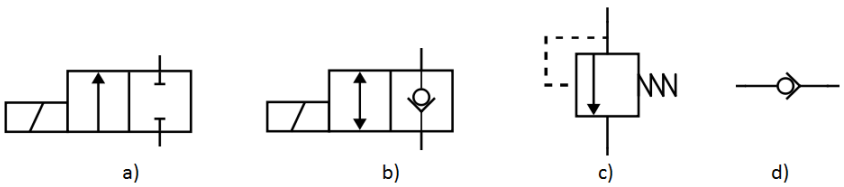


Figure 2.10: Some of the most common valves for hydraulic circuits. a) On/off valve, b) On/off valve with integrated check valve, c) Pilot operated pressure relief valve and d) check valve.

*Directional On/Off Valve* are either opened or closed depending on if they are energized, in contrary to proportional valves for which the opening can be continuously controlled. On/Off valves can either be normally closed (NC) or normally open (NO). If the valve is NC it requires energization to open and vice versa for the NO valve. There are On/Off valves with integrated pressure relief valves, see Figure 2.10. [21]

*Pressure Relief Valves* (PRV) are often used as safety function in hydraulic systems. The valve is normally closed and is only opened if the system pressure reaches a certain level, decided by the PRVs spring pre-tension. Consequently the pressure will decrease until it has reached level below the pre-tension. There different types of PRVs, one of the most

common being pilot controlled PRVs. Pilot controlled PRVs utilize a small hole in the cone which the spring is mounted in. The pilot controlled PRVs function can keep the spring size down. [21]

*Check Valves* only allow flow in one direction. A spring loaded piston seals against a seat to assure that flow can only flow in one direction. Ideally the pressure drop over the valve should be as low as possible to keep the system losses down. [21]

## 2.5 Hybrid vehicles

Hybrid technology relies on two, or more, different on-board energy carriers. Commonly the primary energy carrier is a long term energy storage often consisting of fossil fuel while the secondary energy carrier is of short term. The secondary energy carrier is of reversible type which in turn enables regenerative braking and thus recuperation of energy, which can be beneficial for fuel savings. [3, 14, 19]

Propulsion system design is influenced by the energy density of the on-board energy carrier. High energy density may be favourable from a vehicle design point of view, however not always from an environmental point of view, at least not with the technology level of today. Fossil fuel are often characterized by relatively high energy density, see Figure 2.11, making them suitable alternatives for the on-board energy carrier in vehicles [3].

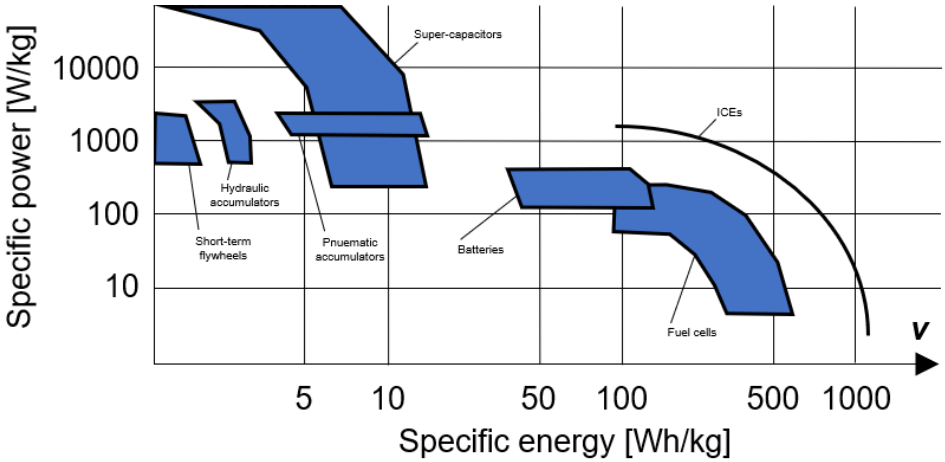


Figure 2.11: Specific energy to specific power for different energy carriers. Picture inspired by [3].

Combustion engines are not characterized by high efficiency nor contributing to a better environment [3]. Pathways to improved fuel economy and thus pathways to address the drawbacks fossil fuels entails are among others

- Improve powertrain component efficiencies.
- Enable recuperation of potential and kinetic energy.
- Optimize component sizes for a certain powertrain configuration [3].

All of which hybrid technology can address. An early definition of configurations are Parallel, Series and Combined hybrids [3]. These configurations will be further explained.

### 2.5.1 Parallel hybrids

In Parallel hybrids configuration the primary and secondary mover are mechanically connected. The primary mover, e.g. an internal combustion engine, powers the vehicle normally through conventional driveline while the secondary mover assists the propulsion and provides energy recuperation capability [3, 14]. Figure 2.12 and 2.13 exemplifies the Parallel hybrid configuration with electrical respectively hydraulic hybrid supplementary. The Parallel hybrid configuration entails advantages such as downsizing of individual components and the need of fewer components, compared to the Series configuration. Drawbacks with the configuration is however the mechanical connection between both movers which can result in negative effects one mover, mainly the ICE, operating on suboptimal operating points [3].

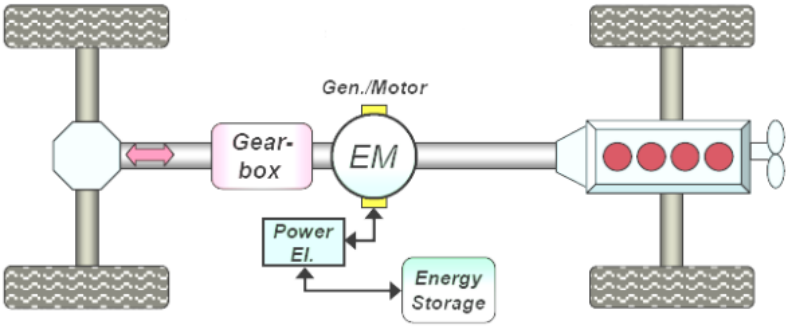


Figure 2.12: Electric Parallel hybrid configuration. Picture source: [2].

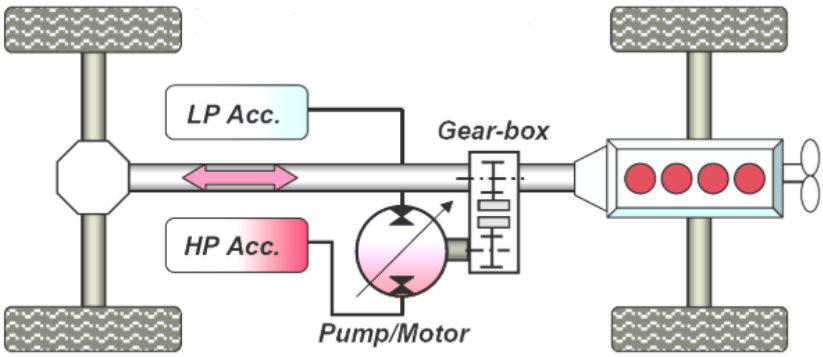


Figure 2.13: Hydraulic Parallel hybrid configuration. Picture source: [2].

### 2.5.2 Series hybrids

Series hybrids have no mechanical connection between the movers. Instead, the coupling between the primary mover and the wheels is established by another type of element but mechanical. Figure 2.14 and 2.15 presents examples of electrical and hydraulic Series

hybrids. The mechanical power provided by the ICE is converted to either electrical or hydraulic power and transferred to an energy storage. Electric or hydraulic power is then transferred from the energy storage and converted back to mechanical power provided to the wheels when propulsion is demanded. Mechanical decoupling between the ICE and wheels allows the ICE to operate on a point with optimal efficiency and optimal emissions at all times, which constitutes an advantage for the Series hybrid configuration. However, due to the absence of a mechanical connection more components, such as electrical or hydraulic machines is required. Propulsive power from the engine will thus be transferred through more components and may suffer increased power losses due component efficiencies, which is a disadvantage for the Series hybrid configuration [3]. Recuperation of energy functions in the same way as for the Parallel hybrid configuration.

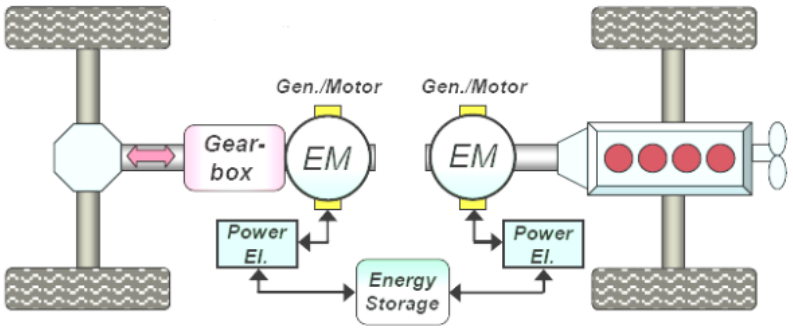


Figure 2.14: Electric Series hybrid configuration. Picture source: [2].

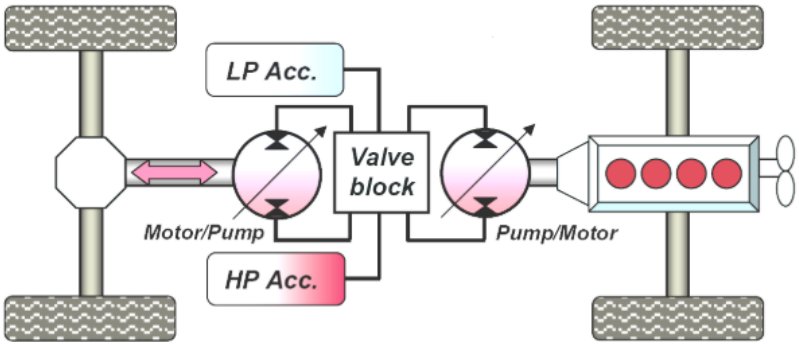


Figure 2.15: Hydraulic Series hybrid configuration. Picture source: [2].

### 2.5.3 Combined hybrids

Combined hybrids conducts a combination of the Parallel and Series configurations. Figure 2.16 presents a schematic of a hydraulic Combined hybrid configuration. By the clutch on the mechanical shaft the vehicle can be operated either as Parallel or Series hybrid and can draw advantages from both configurations. With the clutch engaged the configuration can also run on a power-split mode utilizing both the Parallel and Series configurations simultaneously, similar to a power-split hydromechanical transmission [18].

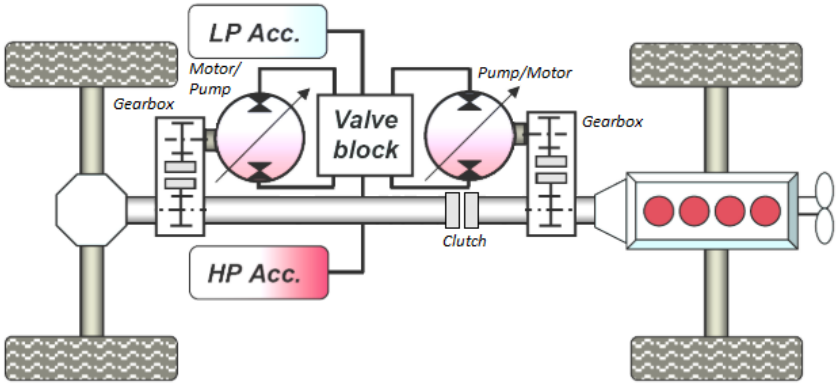


Figure 2.16: Hydraulic Combined hybrid configuration. Picture inspired by [2].

# 3 Hybrid system concept

The hydraulic hybrid system concept that is investigated during this project is realized by adding a Supplementary Hydraulic Hybrid System (SHHS) to a conventional wheel loader driveline. To be able to utilize the SHHS for both Series and Parallel operation the hydraulic machines are mechanically connected to the driveline at two locations. One pressure regulated machine connected on a Power Take-Off (PTO) at the ICE and one displacement controlled machine connected to the transmission. An accumulator is used for energy storage. This type of configuration is commonly referred to as a secondary controlled system [20]. No modifications are done to the conventional driveline components. Hence, the SHHS has a low impact on the overall wheel loader composition which enables favourable benefits for low effort and cost.

The concept of the Series/Parallel hydraulic hybrid wheel loader is presented in Figure 3.1. Compared to Figure 2.13 it is possible to differentiate how the machine connected to the transmission is composing the Parallel configuration and compared to Figure 2.15 how the machine connected to the ICE PTO is composing the Series configuration. Both configurations combined compose the counterpart to the Combined hydraulic hybrid presented in Figure 2.16.

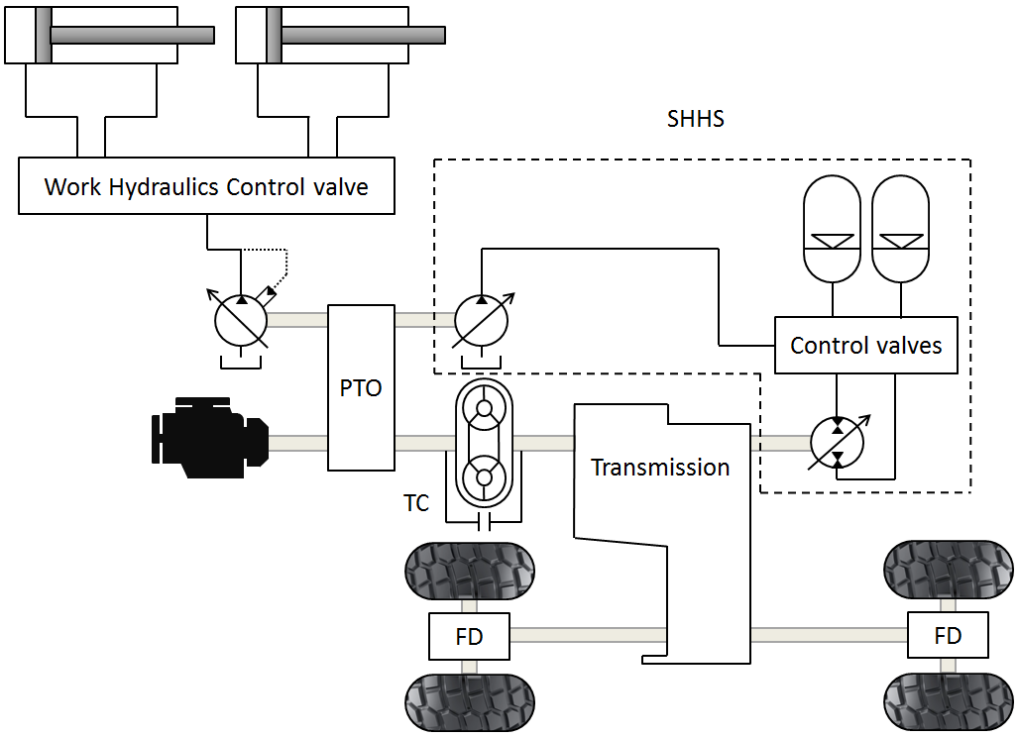


Figure 3.1: Hydraulic hybrid wheel loader driveline.

A presentation of the SHHS is found in Figure 3.2 and contains the following components:

- Hydraulic bent axis machine (Machine 1)
- Hydraulic in-line pump (Machine 2)
- Five hydraulic valves
  - Two NO valves (3, 4)
  - Three NC vales with built in check vales (1, 2, 5)
- High pressure accumulator of bladder type (HP)
- Low pressure accumulator of bladder type (LP)
- Two Pressure relief valves
  - High pressure to low pressure
  - Low pressure to tank
- Check valve

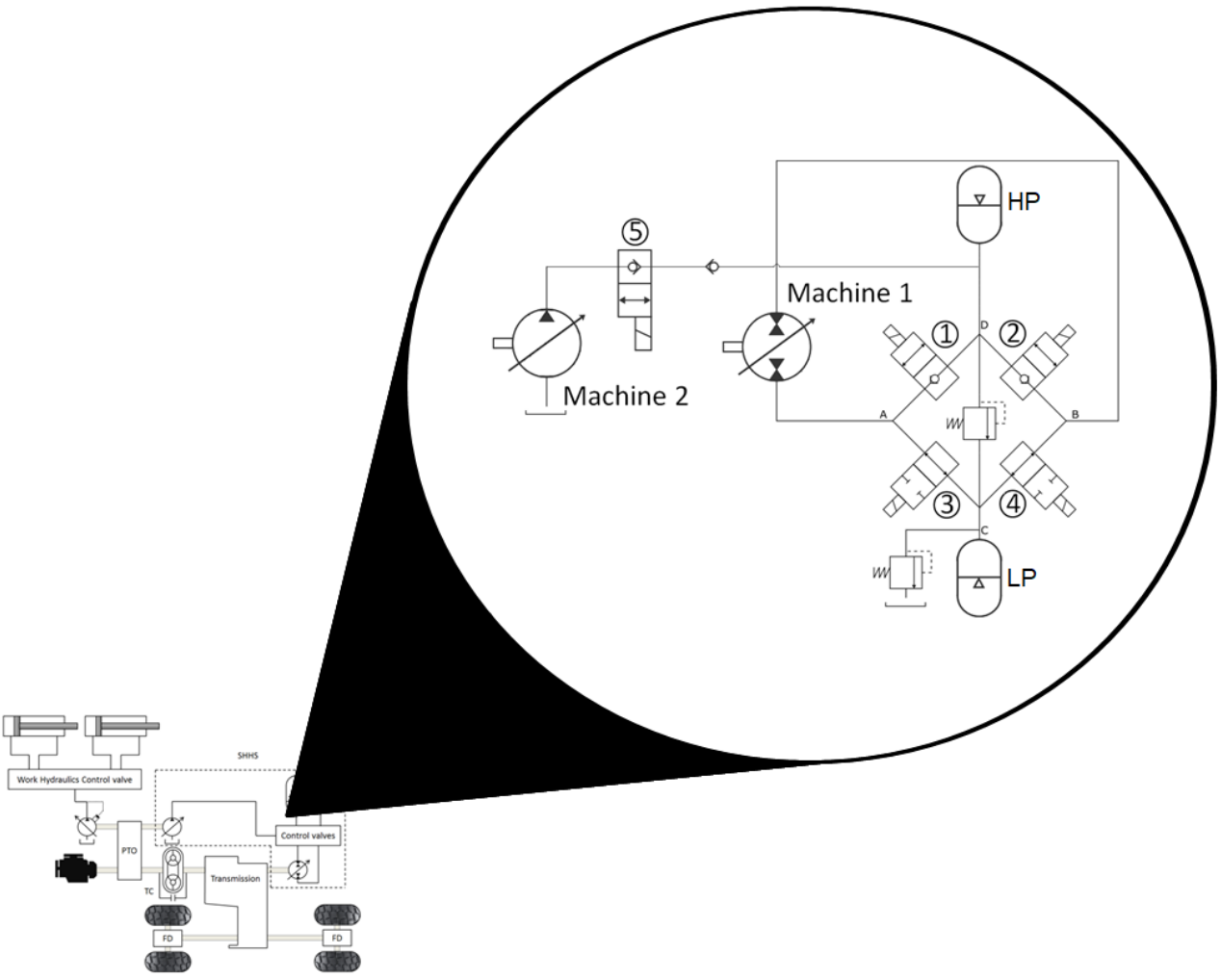


Figure 3.2: The Supplementary Hydraulic Hybrid System.

Propulsive torque is essential during bucket fill operations, i.e. during low speed operations. By this fact an axial piston machine of bent-axis type is recommended and favourable for the hydraulic variable machine, Machine 1. A bent-axis machine contribute with high starting torque and high efficiency at low speeds but slightly complicates the SHHS configuration due to its limitations in over center displacement setting control. The valve bridge seen in the SHHS in Figure 3.2 is thus a consequence of the usage of the bent-axis machine.

With the suggested SHHS configuration oil can move from the low pressure accumulator to the high pressure accumulator or vice versa. Oil can also be provided to the high pressure accumulator by Machine 2 and also directly to Machine 1. Flow is however not possible from the high pressure accumulator to Machine 2 due to the check valve. Machine 2 is mechanically connected to the ICE which implies that it will operate at high speeds. An axial piston machine of in-line type is therefore recommended for Machine 2 since fast and accurate displacement setting changes is prioritized over high efficiency at low speeds.

NO vales are used as a safety feature. If the wheel loader suddenly looses power, the vales will automatically open and even out any pressure difference over Machine 1.

Figure 3.3 exemplifies different flow paths for potential operation modes. Valve 5 control if Series configuration should be utilized while Valves 1-4 control the direction of oil flow over Machine 1. If Valve 5 is closed the SHHS can only utilize its Parallel configuration but if Valve 5 is open both Series and Parallel combined or only Series configuration can be utilized, depending on the flow demand of Machine 1. The systems also provides possibility to charge the accumulator in an Series pump operation if Valve 5 is open and all other valves are closed.

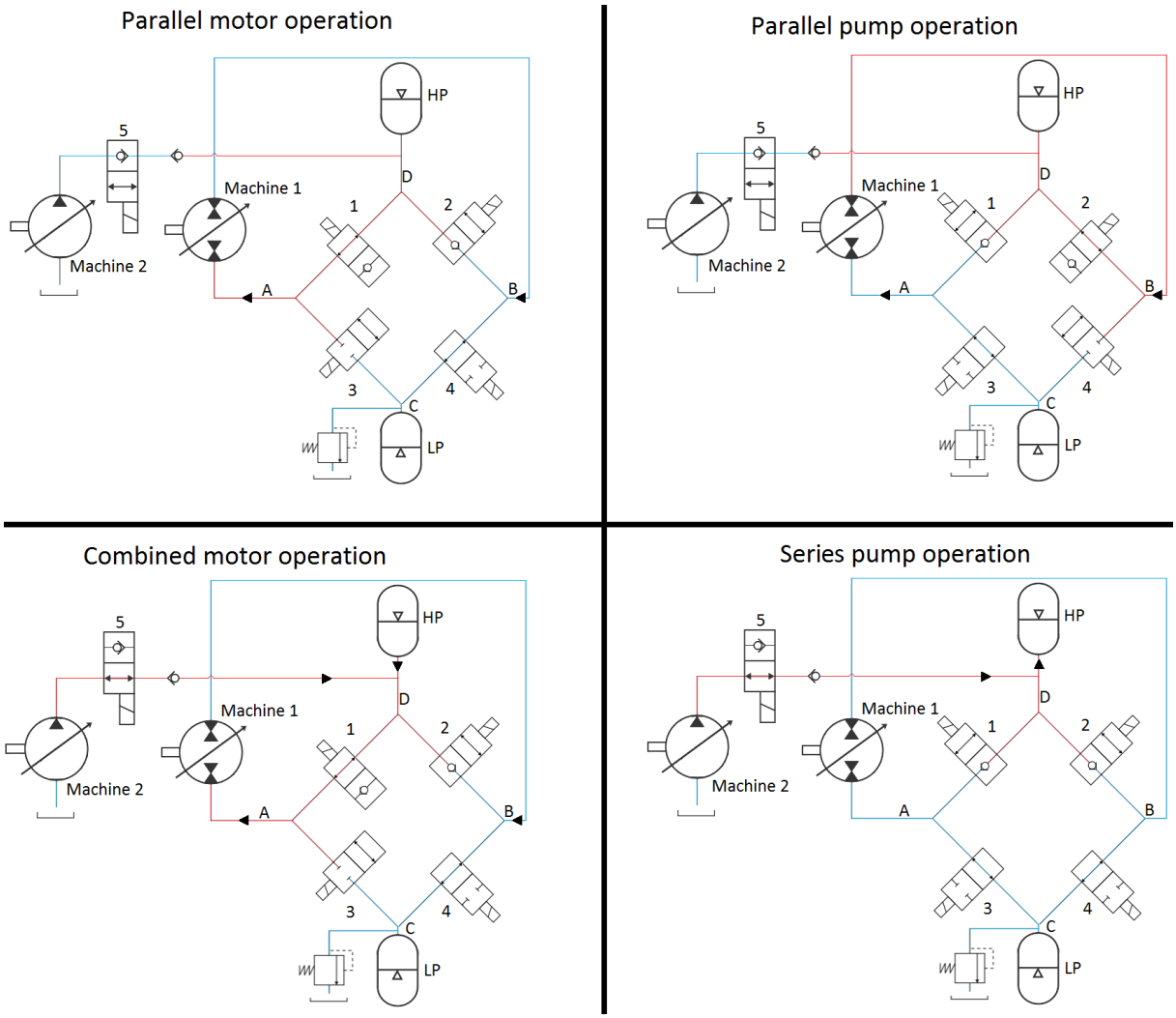


Figure 3.3: Examples of possible flow paths. Red color indicates high pressure, blue color indicates low pressure and arrows indicate flow direction. More paths are available for other modes. PRVs and tank for the LP accumulator is excluded.

## 3.1 Potential hydraulic hybrid work cycle

To be able to utilize the SHHS optimally it is essential to be aware of the potential functionalities of the SHHS during each part of the drive cycle. The SLC illustrated in Figure 2.2 consists of six active phases. Each phase will be presented along with the potential SHHS functionality for that particular phase.

1. **Bucketfill:** As much propulsive force as possible is desired. Recuperated energy in the high pressure accumulator should be utilized and power flow through the TC should be minimized, hence the following functionalities are best suited for this phase.
   (a) Parallel motor operation
   (b) Combined motor operation
2. **Reverse from gravel pile:** Bad TC efficiency during acceleration from the pile induces power flow through the TC to be minimized. Recuperating as much kinetic energy possible during braking is desired. Also, it is desirable to reach a pressure level in the high pressure accumulator enabling hydraulic power assist during next acceleration.
   (a) Series motor operation
   (b) Parallel pump operation
   (c) Combined pump operation
3. **Approaching hauler:** Bad TC efficiency during acceleration from low velocity induces power flow through the TC to be minimized. Also, it is desirable to utilize the energy stored in the accumulator for acceleration. Next phase has good potential in charging the accumulator which is why recuperation of energy only during braking is sufficient.
   (a) Combined motor operation
   (b) Parallel pump operation
4. **Unloading bucket:** During unloading of bucket the wheel loader often has a very low velocity or stands completely still. However, to increase the velocity of work hydraulic functions the accelerator pedal is usually pressed and the engine rotational speed increased. Instead of dissipating excessive energy provided by the ICE in the frictional brakes the energy can be stored in the high pressure accumulator.
   (a) Combined pump operation
   (b) Parallel pump operation
5. **Reverse from hauler:** Bad TC efficiency during acceleration from low velocity induces power flow through the TC to be minimized. The accumulator will have a sufficient state of charge to be able to assist during acceleration. Recuperating as much kinetic energy possible during braking is desired.
   (a) Combined motor operation
   (b) Parallel pump operation
6. **Approaching gravel pile:** Bad TC efficiency during acceleration from low velocity induces power flow through the TC to be minimized. The highest possible high pressure accumulator state of charge is desired to be achieved before the bucketfill phase, which is why acceleration assisted by the high pressure accumulator may not be desirable.
   (a) Series motor operation
   (b) Combined pump operation

## 3.2 Dimensioning of the Supplementary Hydraulic Hybrid System

The calculations presented in this chapter are mainly for the purpose of dimensioning the SHHS. In Figure 3.4 the conventional wheel loader driveline including ICE, TC, transmission, FD and tire together with the two machines of the SHHS can be seen.

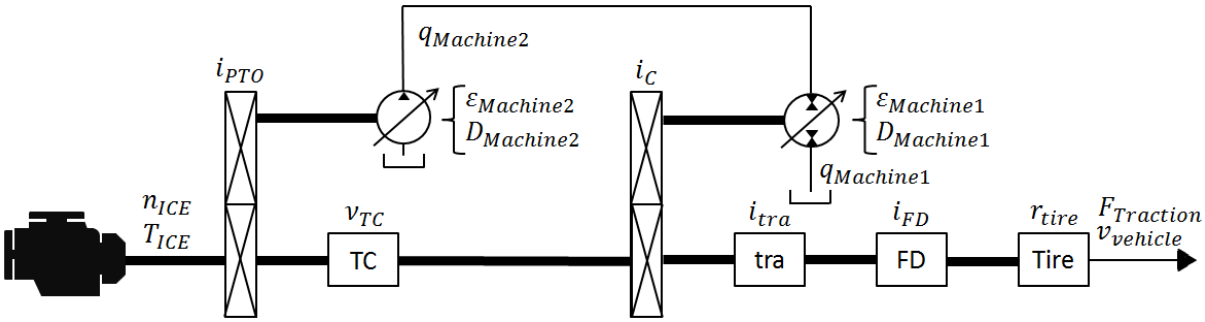


Figure 3.4: The conventional driveline including ICE, TC, transmission, FD and Tire together with the two machines of the SHHS.

### 3.2.1 Machine 1

Machine 1 is mechanically connected to the wheels. Hence, the size of Machine 1 will determine the magnitude of torque that can be delivered by the hybrid system and is therefore of interest for dimensioning purposes. The torque delivered from Machine 1 is described by Equation 3.1.

$$T_{m1} = \frac{\varepsilon_{m1} \cdot D_{m1}}{2 \cdot \pi} \cdot \Delta p \cdot \frac{1}{\eta_{hm}} \cdot \frac{1}{i_C} \tag{3.1}$$

For dimensioning purposes, the relationship between $T_{m1}$, $D_{m1}$ and $\Delta p$ is of interest. Therefore, Equation 3.1 is simplified to Equation 3.2 by assuming $\varepsilon_{m1} = 1$, $i_C = 1$ and neglecting the efficiency $\eta_{hm}$.

$$T_{m1} = \frac{D_{m1}}{2 \cdot \pi} \cdot \Delta p \tag{3.2}$$

By plotting Equation 3.2 the relationship between $T_{m1}$ for varying $D_{m1}$ and $\Delta p$ is Visualized. See Figure 3.5.

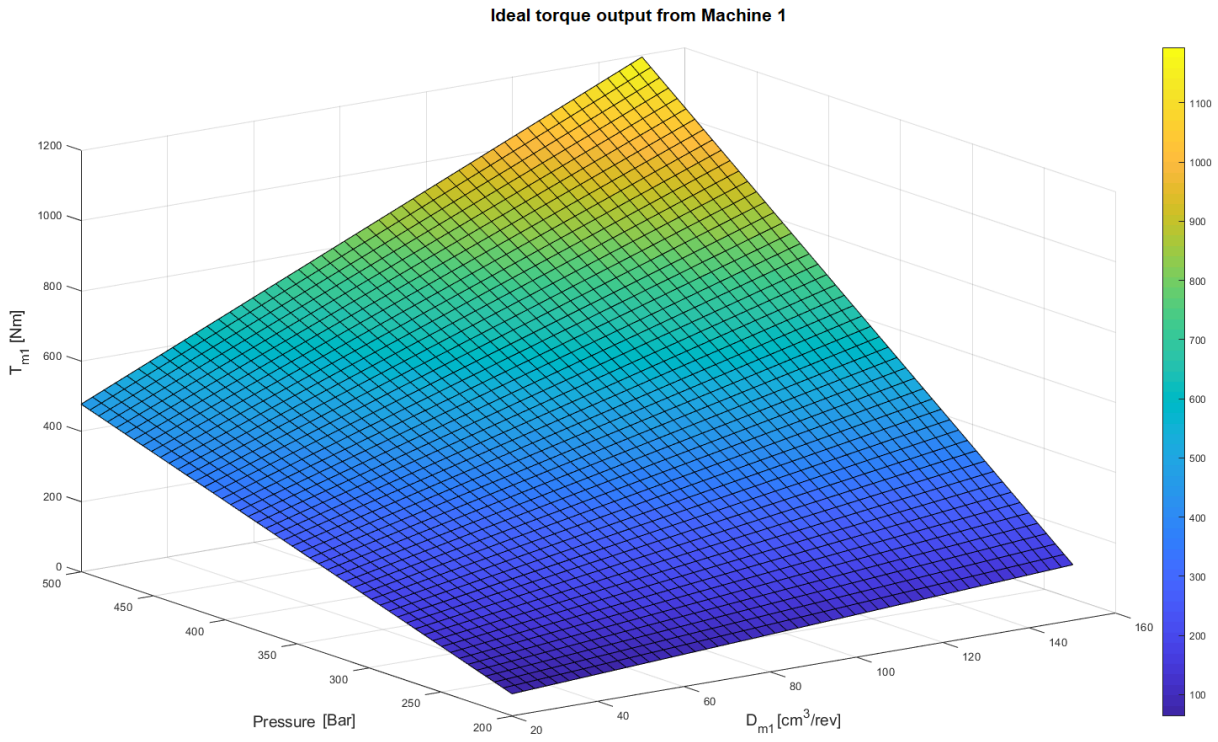


Figure 3.5: Relationship between $T_{m1}$, $D_{m1}$ and $\Delta p$ for hydraulic machines which is of interest when dimensioning the hydraulic hybrid system.

To obtain a better understanding on how to dimension Machine 1, it is of interest to study the tractive demand from the drive cycle. One approach is to model the translational friction between moving bodies. When the translational forces acting on the wheels during operation is known it can be used as a tool to choose a suitable Machine 1 size. The translational force can be described as a function of velocity and be approximated by the sum of Stribeck, Coulomb and viscous friction, see Figure 3.6. This model captures the stick-slip phenomenon which occurs at acceleration from zero.

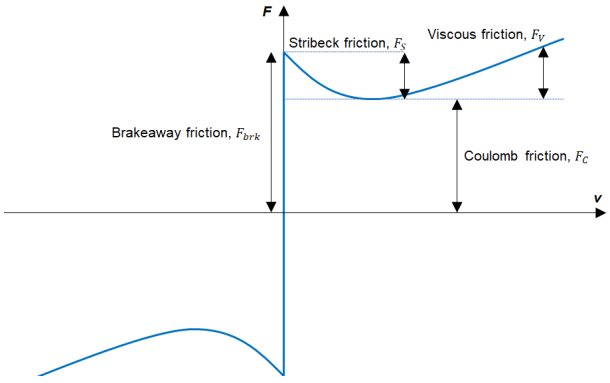


Figure 3.6: Translational friction between moving bodies as a function of velocity can be described by the sum of Stribeck, Coulomb and viscous friction. Picture inspired by [26].

Where the Stribeck friction $F_S$ describes the characteristics at low velocities [25]. $F_C$ is the Coulomb friction, a constant force acting to oppose motion on the system at all velocities. $F_V$ is the viscous friction which opposes motion proportionally to the relative

velocity. $F_{brk}$ is referred to as the breakaway friction and is the sum of the Coulomb and Stribeck frictions in close proximity to zero velocity. In Equation 3.3, 3.4 and 3.5 the equations describing the translational forces can be seen. [26]

$$F_{translational} = \sqrt{2 \cdot e} \cdot (F_{brk} - F_c) \cdot e^{-1 \cdot \left(\frac{v}{v_{St}}\right)^2} \cdot \frac{v}{v_S t} + F_C \cdot arctan\left(\frac{v}{v_{Coul}}\right) + F_v \cdot v_{veh} \quad (3.3)$$

$$v_{St} = v_{brk} \cdot \sqrt{2} \quad (3.4)$$

$$v_{Coul} = \frac{v_{brk}}{10} \quad (3.5)$$

When the forces required has been approximated using Equation 3.3 they can be compared to the tractive forces exerted on the wheels by the driveline. The total tractive force delivered by the driveline can be described by Equation 3.6.

$$F_{traction} = F_{hybrid} + F_{conventional} \quad (3.6)$$

$F_{hybrid}$ can be calculated by Equation 3.7 which is derived from the configuration in Figure 3.4. $T_{m1}$ is calculated using Equation 3.2.

$$F_{hybrid} = T_{m1} \cdot \eta_{hm} \cdot \frac{1}{i_C \cdot i_{tra} \cdot i_{FD}} \cdot \eta_{ix} \cdot \frac{1}{r_{tire}} \quad (3.7)$$

According to the principle presented in Figure 3.4, $F_{conventional}$ can be calculated using Equation 3.8 .

$$F_{conventional} = T_{ICE} \cdot \nu_{TC} \cdot \frac{1}{i_{tra} \cdot i_{FD}} \cdot \eta_{ix} \cdot \frac{1}{r_{tire}} \quad (3.8)$$

Values of $\eta_{hm}$ and $\eta_{ix}$ can be set to arbitrary approximative values. Figure 3.7 presents three different sizes of Machine 1 and their corresponding tractive force capability calculated according to Equation 3.7 plotted together with an arbitrary translational force calculated using Equation 3.3.

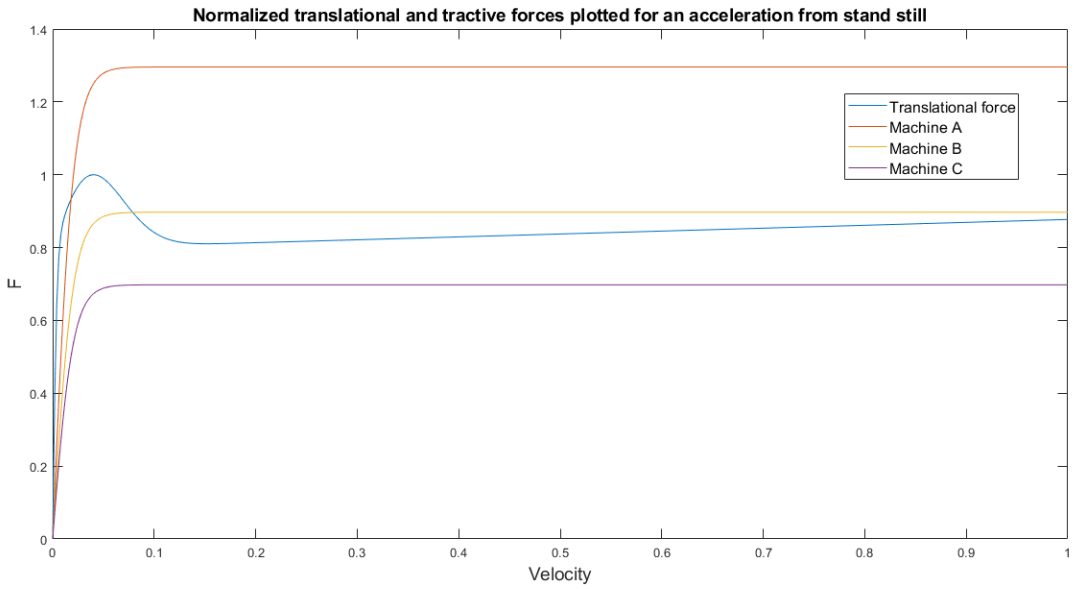


Figure 3.7: Translational force for an acceleration from stand still against the traction force exerted from three arbitrary machines, *Machine A* which has potential for full hybrid operation, *Machine B* which require assist from the conventional driveline at acceleration from zero and *Machine C* which always require assist from the conventional driveline.

Considering only translational forces exerted during an acceleration from stand still as in Figure 3.7 some conditions on the hybrid systems functionality can be formulated. If full hybrid operation is desired, the tractive forces delivered by the hybrid system must be greater or equal to the transitional forces acting on the wheels. Thus the condition for full hybrid operation is:

$$F_{hybrid} \geq F_{translational}$$

If this condition is not fulfilled, assist from the conventional driveline is to some degree necessary to meet the requirements of $F_{translational}$. The tractive force demand from the conventional driveline can be approximated by:

$$F_{conventional} \geq F_{translational} - F_{hybrid}$$

One noteworthy aspect for a wheel loader application is the translational force during bucketfill operation. The force is significantly greater during bucketfill operation compared to a regular acceleration from stand still due to the friction between the bucket and the material. This has to be considered when dimensioning the driveline. To ensure that the driveline can fulfill the maximum torque demand the following relation has to be fulfilled:

$$F_{hybrid} + F_{conventional} \geq F_{tranMax}$$

Transversal, aerodynamic or other disturbance forces could also be taken into account but is neglected in this report for simplification.

Depending on the magnitude of the translational forces and the desired purpose of the hybrid system the engineer can select a suitable size for Machine 1 together with a reasonable system pressure by using the equations and plots presented in this chapter. Other parameters to keep in mind is that fast and accurate displacement controllers of the hydraulic machine is important for the functionality of the hybrid system [18].

### 3.2.2 Machine 2

This chapter will go through an approach which can be adapted to dimension Machine 2. The ideal flows of Machine 1 and 2 can be explained by Equation 3.9 and 3.10.

$$q_{m1} = n_{ice} \cdot \nu_{TC} \cdot i_C \cdot \varepsilon_{m1} \cdot D_{m1} \tag{3.9}$$

$$q_{m2} = n_{ice} \cdot i_{PTO} \cdot \varepsilon_{m2} \cdot D_{m2} \tag{3.10}$$

The relation $q_{m1} = q_{m2}$ is valid if assuming no leakage, which in turn formulates Equation 3.11.

$$n_{ice} \cdot \nu_{TC} \cdot i_C \cdot \varepsilon_{m1} \cdot D_{m1} = n_{ice} \cdot i_{PTO} \cdot \varepsilon_{m2} \cdot D_{m2} \tag{3.11}$$

Which is equivalent to Equation 3.12.

$$\frac{\varepsilon_{m2}}{\varepsilon_{m1}} = \frac{\nu_{TC} \cdot i_C \cdot D_{m1}}{i_{PTO} \cdot D_{m2}} \tag{3.12}$$

Assuming that both machines have max displacement setting, $\varepsilon_{m2} = \varepsilon_{m1} = 1$, Equation 3.12 can be simplified to Equation 3.13.

$$\frac{D_{m2} \cdot i_{PTO}}{D_{m1} \cdot i_C} = \nu_{TC} \tag{3.13}$$

Assuming a slip $\nu_{TC} \approx 0.3$ during bucketfill phase formulates Equation 3.14.

$$\frac{D_{m2} \cdot i_{PTO}}{D_{m1} \cdot i_C} = 0.3 \tag{3.14}$$

$i_{PTO}$ and $i_C$ can be neglected in this stage. Hence, a suitable relationship between $\frac{D_{m2}}{D_{m1}}$ should reasonably be in the range seen in Equation 3.15 below.

$$0.25 \leq \frac{D_{m2}}{D_{m1}} \leq 0.4 \tag{3.15}$$

Considering varying pump efficiencies, arbitrary gear ratios $i_{PTO}$ and $i_C$ can be set accordingly after dimensioning the hydraulic machines.

### 3.2.3 High pressure accumulator

The accumulators size, in particular the high pressure accumulator, will play a key role in how the hybrid system can be utilized. If the hybrid system is to be used mainly for Parallel hybrid operation one design suggestion is to measure the approximate time for the bucketfill in field and then calculate the volume of oil that is required to fulfil the demand using Equation 3.16.

$$V_{accForParallel} = \int_{t_0}^{t} q_{m1} dt \tag{3.16}$$

$q_{m1}$ can be approximated by using Equation 3.9. Another alternative is to use Equation 3.17:

$$q_{m1} = v_{vehBF} \cdot \frac{1}{r_{tire} \cdot 2 \cdot \pi \cdot i_{FD} \cdot i_{tra} \cdot i_C \cdot \eta_{ix}} \tag{3.17}$$

For Series/Parallel hybrid operation, the accumulator size could be determined by downsizing the accumulator proportionally to the flow delivered from Machine 2. For this approach, the engineer has to decide to what degree Series hybrid operation is desired. Equation 3.18 could be used for calculation of the volume required.

$$V_{accForCombined} = \int_{t_0}^{t_1} q_{m1} dt - \int_{t_2}^{t_3} q_{m2} dt \tag{3.18}$$

$q_{m1}$ and $q_{m2}$ can be approximated using Equation 3.17 and 3.10 respectively. The integration intervals $[t_0, t_1, t_2, t_3]$ can be approximated and determined through studying empirical data from machine tests, where $[t_0, t_1]$ denotes the time interval in which Machine 1 is used and $[t_2, t_3]$ the time interval in which Machine 2 is used.

Large accumulator size provide high potential for energy recuperation. However large accumulators must then be mounted on the wheel loader which increase weight and could prove difficult to install. With the Series configuration, accumulator sizes could be decreased according to Equation 3.18. If pure hydrostatic transmission configuration is desirable, the accumulator sizes can be decreased to a volume of $0.75 \leq V_{acc} \leq 1$ litre [27].

# 4 Energy Management Strategies

Hybrid vehicles require a supervisory controller to determine the power requirements from each of the energy carriers [3] as another degree of freedom is introduced to the conventional control strategy [13]. The controllers purpose is mainly to reduce the overall energy consumption while satisfying the power demands of the driveline [3]. Maintaining acceptable driving conditions is also important from an operator point of view. Consideration to various type of component and system characteristics also has to be made, for example response time, hysteresis, gear shift points and so on. These type of component and system characteristics can be difficult to capture in simulation [18].

Control strategies may be classified based on their dependency on knowledge about future situations. If exact knowledge is known in advance about the drive cycle, which might be the case for public transportation or other vehicles with set drive cycles non-causal controllers can be used. In cases when the exact drive profile is unknown or cannot be predicted in advance causal controllers are used. [3]

Controllers can also be sorted among heuristic, optimal and sub-optimal controllers [3].

## 4.1 Heuristic controllers

Heuristic controllers are causal and the control is based on boolean, sometimes referred as fuzzy rules. Heuristic controllers are simple but can still prove competitive in terms of fuel efficiency for hybrid vehicles [28]. Decision making is based on defined rules depending on various vehicle parameters or operating conditions. For a hydraulic hybrid wheel loader application, typical conditions could be:

- below a certain accumulator state of charge the hydraulic hybrid system can not be used for propulsion (charge is required);
- above a certain state of charge the accumulator can not be charged;
- if a certain gear is engaged the hydraulic hybrid system is engaged to assist propulsion;
- if the brake pedal is applied, recuperation of energy should be made possible

Some of the main advantages with heuristic controllers robustness and easy implementation [3].

## 4.2 Optimal and sub-optimal controllers

Every driving mission for a hybrid vehicle has an optimal solution to when the hybrid system should be used and to what extent to minimize fuel consumption. Hence, the controller has to be non-causal to find the optimal solution. Dynamic programming (DP) is a numerical optimization method that can be used to find an optimal solution for a certain state variable in multi-stage problems [29]. DP is a deterministic algorithm and requires discrete values of state variables (often State of Charge) and time [3]. An optimal trajectory is then calculated at each time and state of the system [29]. By integrating the trajectory over the course of the drive cycle the global optimum fuel consumption for the drive cycle can be found. DP provides a good basis for designing and benchmarking heuristic and sub-optimal control strategies, as the optimal solution can be used as reference [30]. DP is relatively computational heavy as the computational cost increases exponentially with the number of state variables. However, it only increase linearly for increased time [3].

Most often optimal controllers cannot practically be used in hybrid vehicles. Instead, sub-optimal controllers may be utilized as they have causal properties. Analytical optimization methods can be used to formulate minimization functions which, due to their quick computational time, make real-time decisions to achieve minimized fuel consumption [3]. One analytical optimization method which is often used in hybrid vehicles is the Equivalent-Consumption Minimization (ECMS), see [31]. The principle of ECMS is based on the use of an analytically determined function, often referred to as the Hamiltonian, which is minimized with respect to the control function (often fuel consumption) at each time while still fulfilling set constraints of the hybrid vehicle [3]. These functions will minimize the fuel consumption for each time, i.e provide the local optimal solution for the current time. Compared to dynamic programming which provide the global optimal solution for the complete drive cycle.

## 4.3 Controllers suitable for hydraulic hybrid wheel loaders

Vehicle type, application and energy carriers affects the choice of controller. Previous studies has concluded that a simple rule-based strategy is most robust and adequate to use in a hydraulic hybrid wheel loader to minimize the fuel consumption. The study concludes that ECMS could be a better choice over a rule-based strategy if the size of the energy storage is greatly increased [14]. However, this imposes a significant increase in accumulator volume as accumulators have low specific energy. The consequence of increasing the accumulator size is increased weight and potential lack of mounting space, which could prove not feasible.

# 5 Modelling and simulation

The principle used for the simulation model can be seen in Figure 5.1. Velocity and traction forces are fed from a drive cycle to the model, which will trigger corresponding sensor signals. Sensor signals are for example; current gear, shaft speeds, hybrid system state and more. The sensor signals are sent to the control system for decision making and corresponding control signals are returned to the wheel loader model. The control signals used are displacement setting for Machine 1, reference pressure signal for Machine 2, valve signals for the valves and engine limitation signal to the ICE. In Section 5.1 the wheel loader simulation model is presented and in Section 5.2 the control system's architecture and functionality will be further explained.

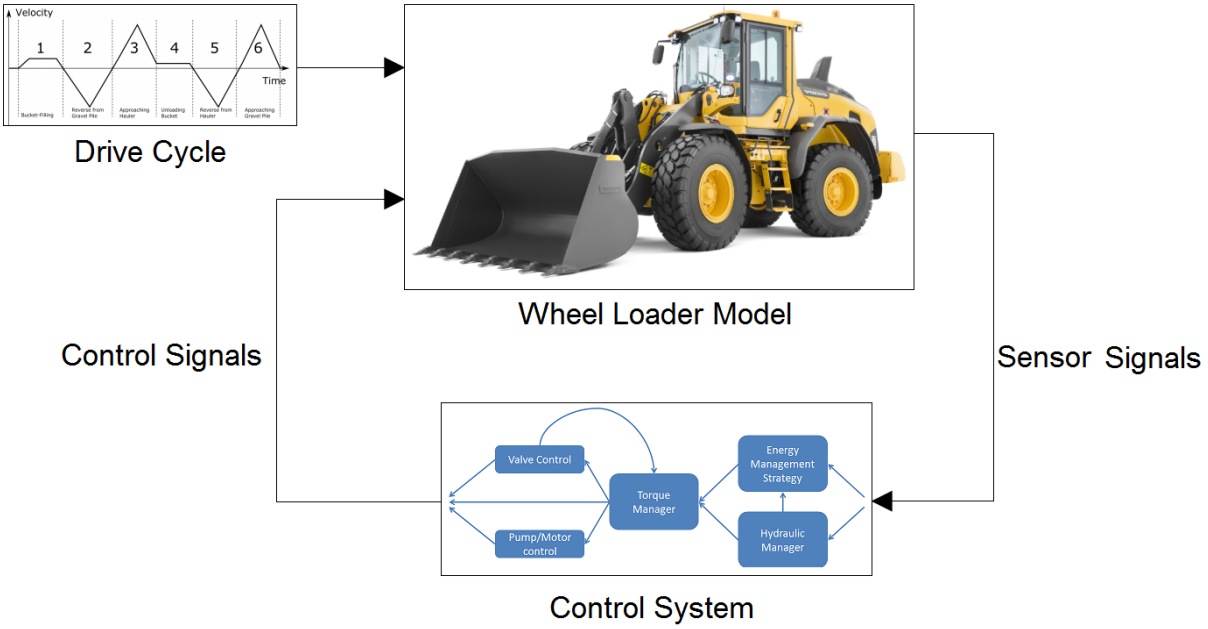


Figure 5.1: Wheel loader simulation model principle. Picture source drive cycle: [5] Picture source wheel loader: [7].

## 5.1 Wheel loader model

The purpose of the wheel loader simulation model is to provide a realistic description of the wheel loaders behaviour. With a simulation model in place the proposed hybrid concept can be evaluated rapidly in simulation before choosing a final design [13]. The simulation model also serves as a rapid evaluation tool of the control system's functionality. The working principle of the backward-facing wheel loader simulation model can be seen in Figure 5.2. Some of the components in the wheel loader have been described with physical equations which capture their behaviour. For other components look-up tables are used, which rely on measured data from each specific component at different operating points.

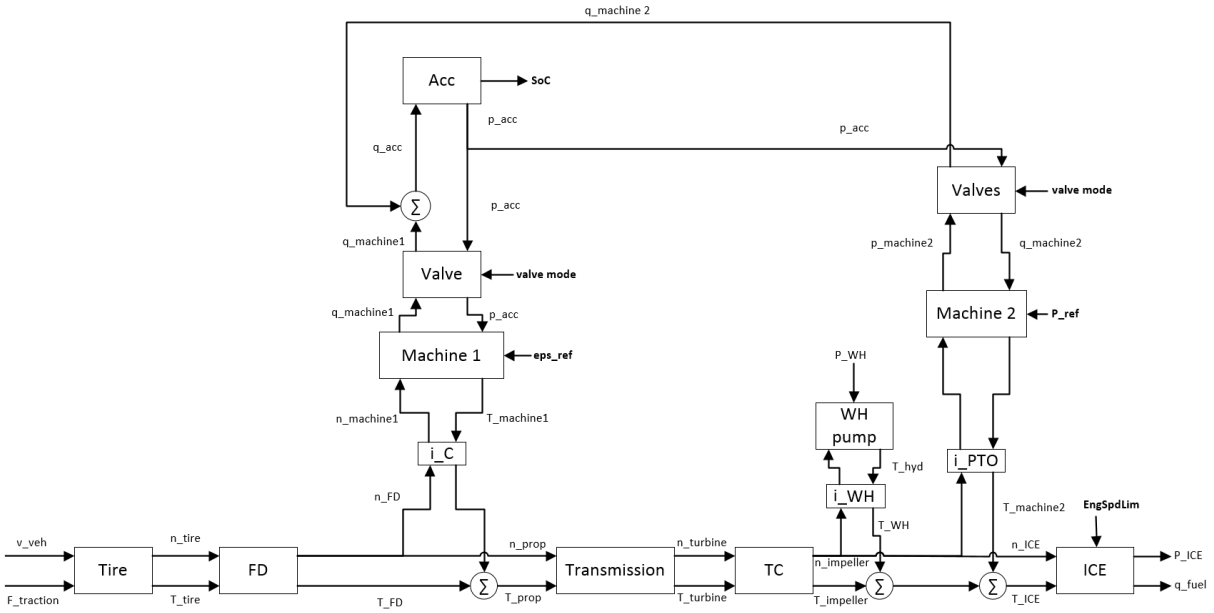


Figure 5.2: Backward-facing wheel loader simulation model.

When using backward facing simulation the input variables are the physical outputs of the vehicle i.e traction force and velocity. The direction of computation goes backward from the wheels, through each component of the driveline to obtain the required control inputs. In contrary to forward facing simulation, which rely on control signals as input which result in corresponding physical outputs. One of the main advantages with backward facing simulation is that it does that no feedback control is required, which forward simulation most often does. Hence the control system can be evaluated for different drive cycles and various vehicle sizes without the need to redesign the control for each change, which could be cumbersome. [32]

The wheel loader model, as modelled in Simulink can be seen in Figure 5.3. The simulation model is based on the principle presented in Figure 5.2 and partly adapted from a previous study [5]. The drive cycle feeds the wheel loader model with vehicle velocity, traction forces, gear and power demand from the work hydraulic system while the control system provide the appropriate control signals. This chapter will go through the different parts of the wheel loader simulation model.

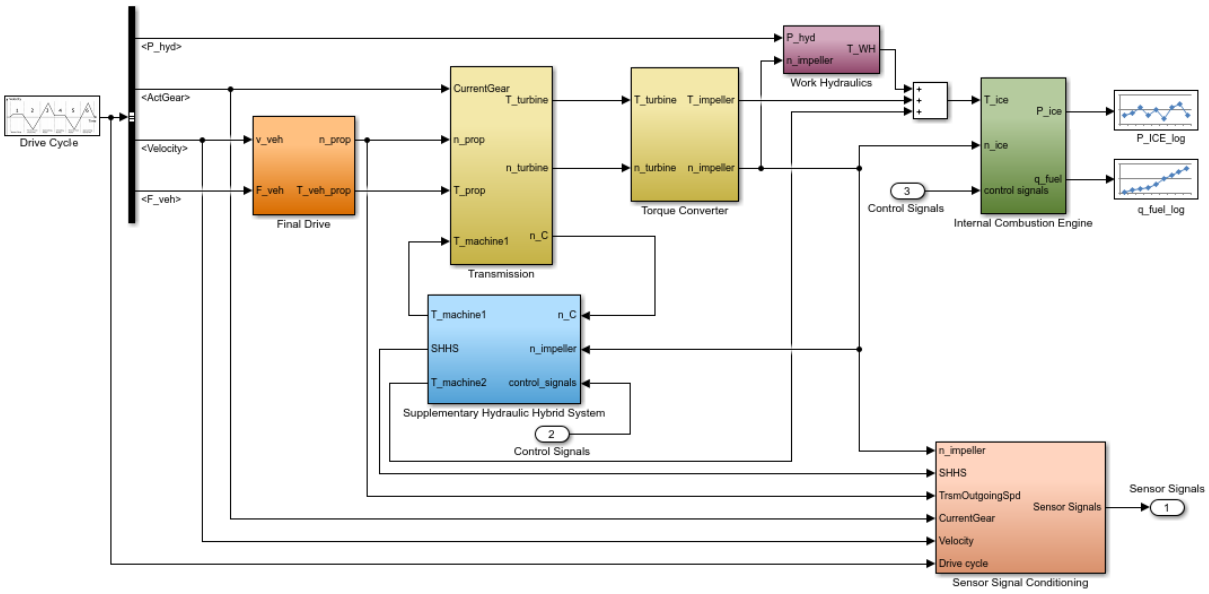


Figure 5.3: The backward-facing wheel loader simulation model as modelled in Simulink.

### 5.1.1 Tire and Final Drive

In the FD-block, the torque and shaft speed of the transmission's outgoing shaft is calculated. The shaft speed, $n_{FD}$ is calculated using Equation 5.1

$$n_{FD} = \frac{v_{veh} \cdot i_{FD}}{r_{tire} \cdot \pi \cdot 3.6} \cdot 30 \tag{5.1}$$

The outgoing torque is calculated using Equation 5.2.

$$T_{FD} = \frac{F_{traction} \cdot r_{tire}}{\eta_{FD} \cdot i_{FD}} \tag{5.2}$$

### 5.1.2 Transmission

The transmission block, as modelled in Simulink can be seen in Figure 5.4. Calculations of the torque and speed on the turbine shaft of the TC are conducted in this block.

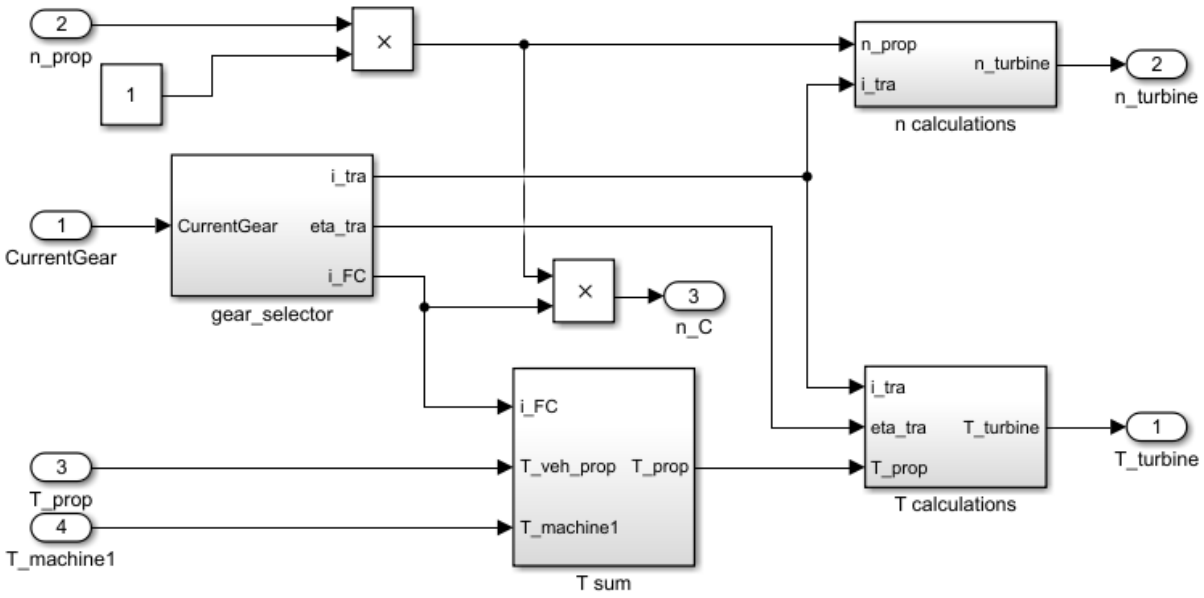


Figure 5.4: Transmission as modelled in Simulink.

The current gear engaged is fed to the wheel loader model from the drive cycle, it is then sent to the gear selector block to determine gear ratios for both the turbine axle and the C axle of the transmission. The SHHS is connected to the C axle of the transmission and the C axle is mechanically connected to the turbine shaft of the transmission with a gear ratio $i_C$. The gear ratios are set by look-up tables where each gear simply correspond to a certain gear ratio, the gear selector block also determines $\eta_{tra}$ by a look-up table as each gear has different efficiency. $n_{turbine}$ and $n_C$ is calculated by Equation 5.3 and 5.4.

$$n_{turbine} = n_{FD} \cdot i_{tra} \tag{5.3}$$

$$n_C = n_{FD} \cdot i_C \tag{5.4}$$

According to Figure 5.2 $T_{FD}$ and $T_{m1}$ should be summarized before calculating $T_{turbine}$. This is done in the T sum block using Equation 5.5.

$$T_{prop} = T_{FD} - \frac{T_{m2}}{i_C} \tag{5.5}$$

$T_{turbine}$ is then calculated using Equation 5.6.

$$T_{turbine} = \frac{T_{prop}}{i_{tra} \cdot \eta_{tra}} \tag{5.6}$$

### 5.1.3 Supplementary Hydraulic Hybrid System

The SHHS as modelled in Simulink can be seen in Figure 5.5. Machine 1 is displacement controlled which implies that the displacement control signal will control the flow and torque of Machine 1. Machine 2 is pressure controlled, thus a different calculation approach than for Machine 1 is required. A reference pressure is set by the control system and sent to Machine 2 which in turn forwards the reference to the valve system where a flow is calculated depending on the pressure drop over the valve.

The two valve systems control the opening and closing of each of the five valves, the active valve configuration is set by the control signals from the control system. The flow from each machine is sent to the accumulator system for pressure calculation of node C and D, recall Figure 3.2 for the node placements. Pressures for the A and B nodes are set in Machine 1's valve system. Outputs from the SHHS system include pressure in each nodes A, B, C, D as well as sensor signals from the machines. For Machine 1 displacement setting and shaft speed and for Machine 2 torque and shaft speed.

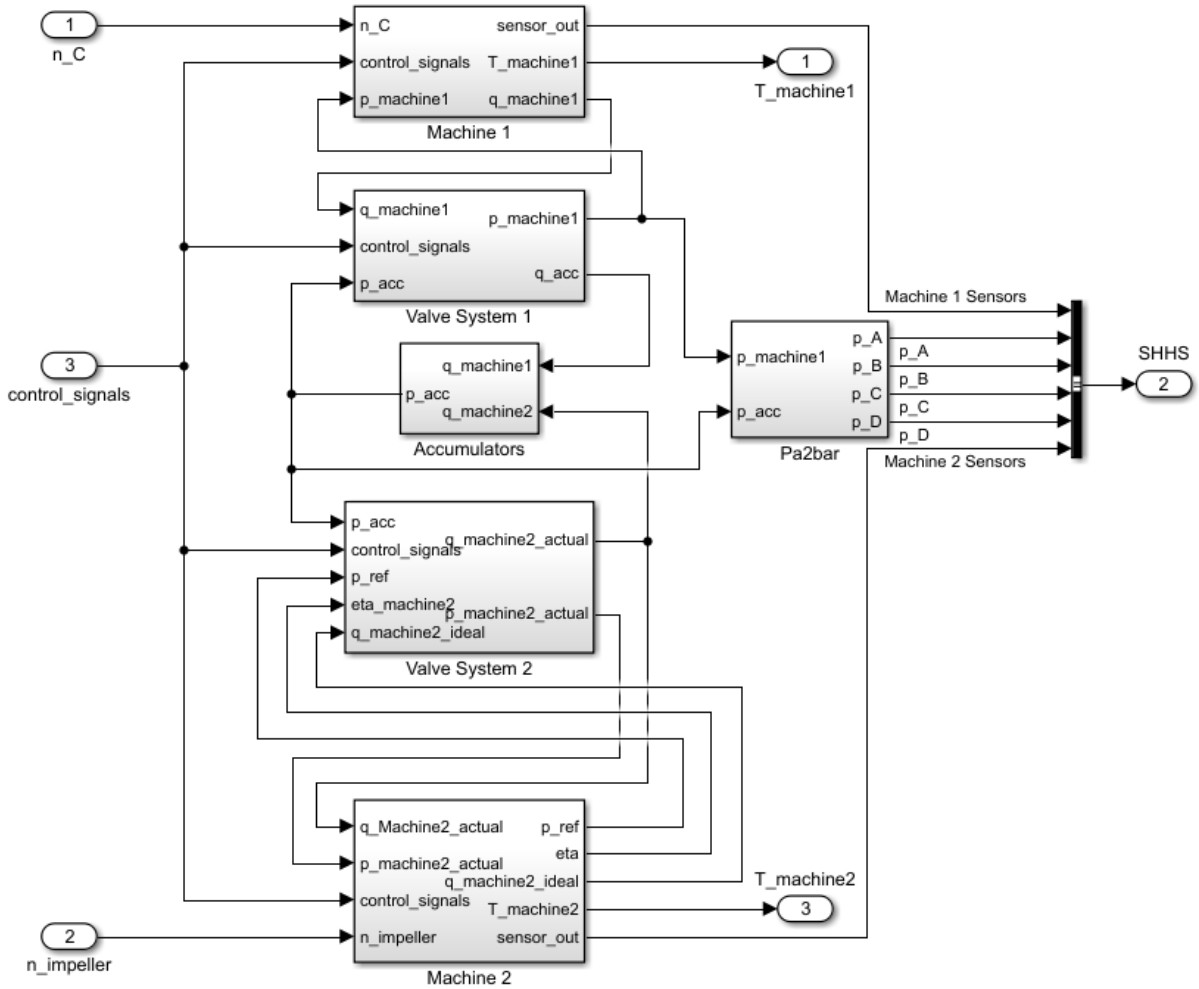


Figure 5.5: Supplementary Hydraulic Hybrid System (SHHS) as modelled in Simulink.

Each component of the SHHS as modelled in Simulink will be further presented in the coming chapters.

### 5.1.4 Machine 1

Machine 1 of the SHHS as modelled in Simulink can be seen in Figure 5.6.

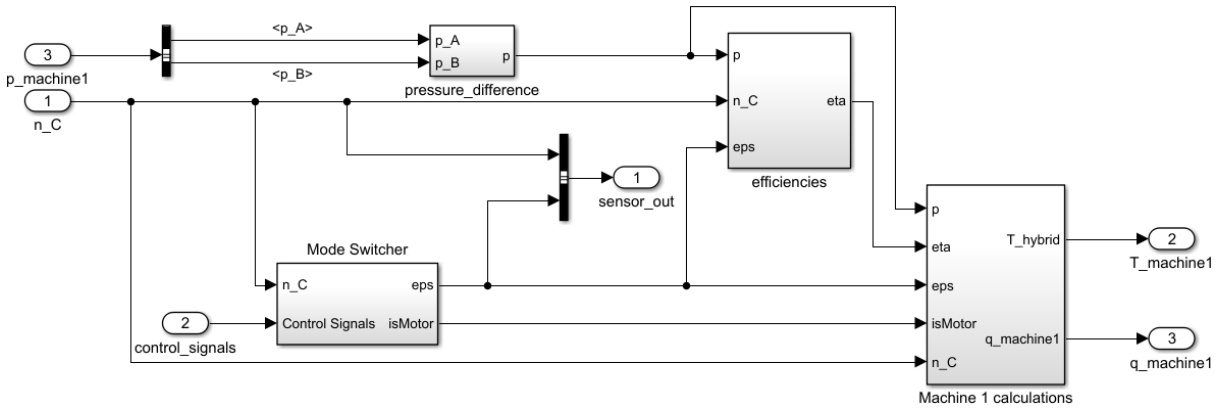


Figure 5.6: Machine 1 of the SHHS as modelled in Simulink.

The Mode Switcher block includes logic which identify if the machine is operating as pump or motor. As mentioned, Machine 1 is displacement controlled and thus dependent on a $\varepsilon$ control signal. The displacement setting, $\varepsilon$, is referred to as eps in the model. In the efficiencies block $\eta_{vol}$ and $\eta_{hm}$ is set by look-up tables which are dependent on three signals, displacement setting (eps), $n_C$ and the pressure drop over Machine 1, see Equation 5.7.

$$\Delta p = |p_A - p_B| \tag{5.7}$$

In the Machine 1 calculations block $T_{m1}$ and $q_{m1}$ is calculated. $T_{m1}$ is calculated with Equation 5.8 and $q_{m1}$ is calculated with Equation 5.9.

$$T_{m1} = \frac{\varepsilon_{m1} \cdot D_{m1}}{2 \cdot \pi} \cdot \Delta p \cdot \eta_{hm}^{isMotor} \tag{5.8}$$

$$q_{m1} = \varepsilon \cdot n_C \cdot D_{m1} \cdot \eta_{vol}^{-1 \cdot isMotor} \tag{5.9}$$

The variable $isMotor$ is in $\eta_{hm}$ and $\eta_{vol}$ exponents. $isMotor$ decide if $\eta_{hm}$ and $\eta_{vol}$ is in the numerator or in the denominator of the equation. If Machine 1 is operating as motor $isMotor = 1$ and if it is operating as pump $isMotor = -1$.

An approximation of Machine 1's displacement dynamics is implemented in the Simulink model, see Figure 5.7. As the machine is of bent axis type, the dynamics can be approximated by a low-pass filter together with a rate limiter as proposed by [33]. The response time is different for displacing from minimum to maximum and maximum to minimum, which is taken into respect with a rate limiter. The low pass filter transfer function can be seen in Equation 5.10.

$$G(s) = \frac{1}{1 + s \cdot \tau_{disp}} \tag{5.10}$$

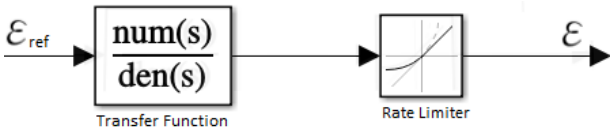


Figure 5.7: Displacement dynamics of Machine 1 as modelled in Simulink

As mentioned, the efficiencies, $\eta_{hm}$ and $\eta_{vol}$ for Machine 1 is found using look-up tables. See Figure 5.8 and 5.9 where they are displayed using normalized values. Inputs to the look-up tables are $\Delta p$, $n_C$ and $\varepsilon$ as can be seen in Figure 5.6. The look-up tables are defined for all operating points of Machine 1.

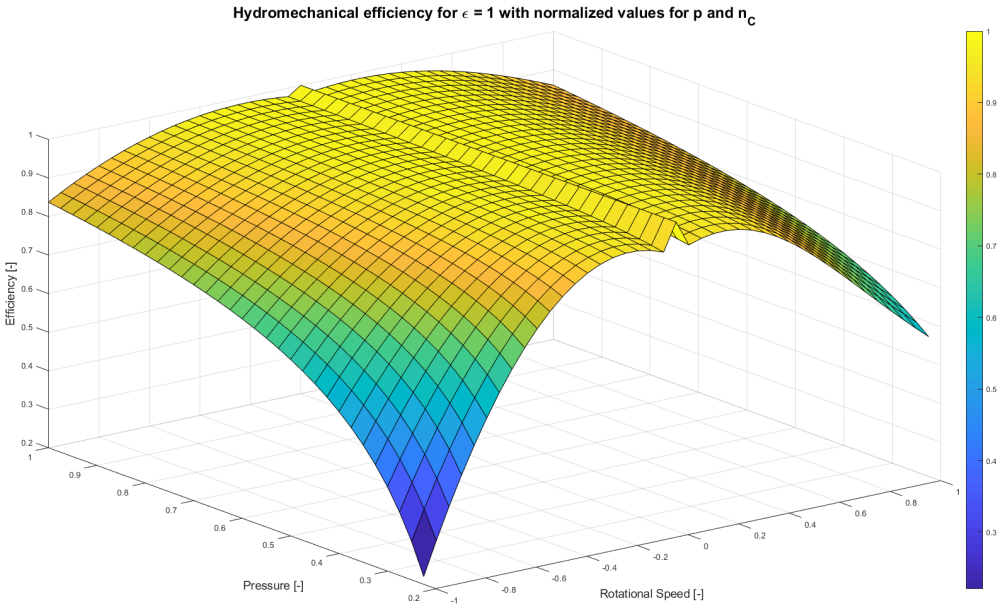


Figure 5.8: $\eta_{hm}$ look-up table for Machine 1 implemented in Simulink, the look-up table is defined for all $\varepsilon$ settings, in the figure $\varepsilon = 1$ can be seen. The values for $\Delta p$ and $n_c$ are displayed with normalized values. The data is acquired from the pump manufacturer.

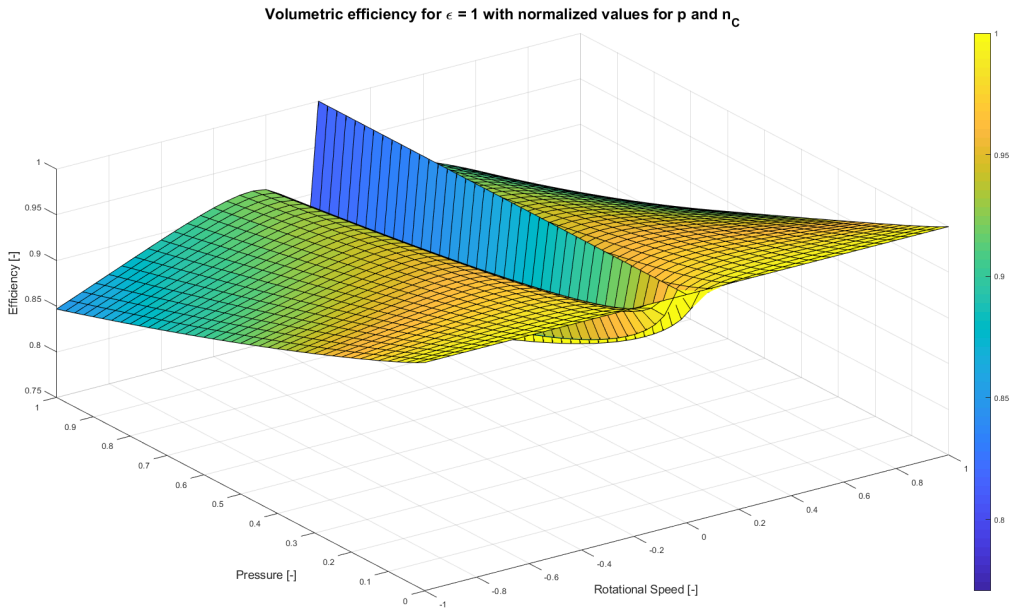


Figure 5.9: $\eta_{vol}$ look-up table for Machine 1 implemented in Simulink, the look-up table is defined for all $\varepsilon$ settings, in the figure $\varepsilon = 1$ can be seen. The values for $\Delta p$ and $n_c$ are displayed with normalized values. The data is acquired from the pump manufacturer.

### 5.1.5 Machine 2

Machine 2 of the SHHS as modelled in Simulink can be seen in Figure 5.10.

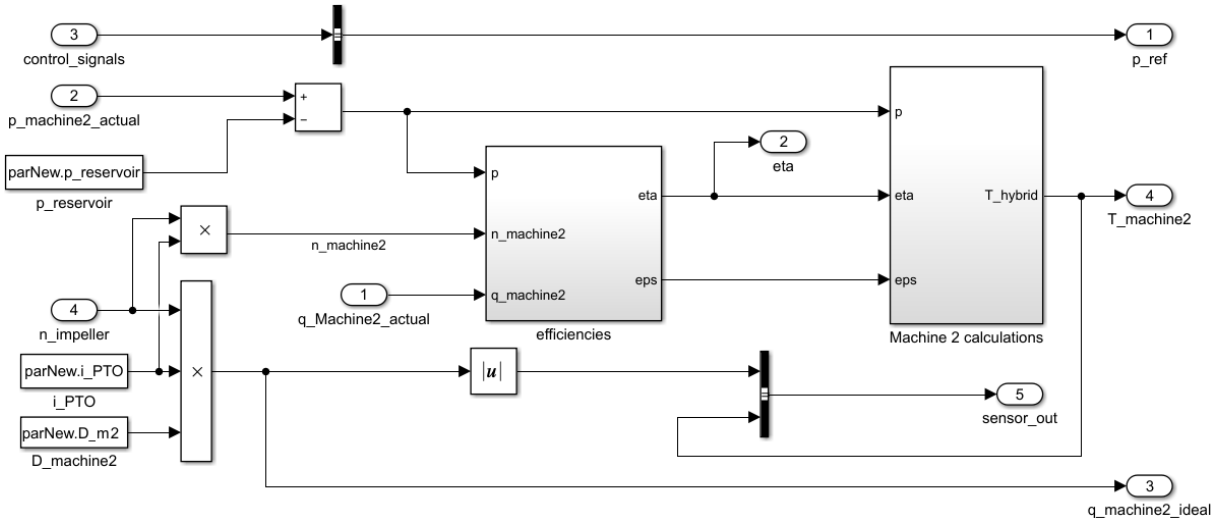


Figure 5.10: Machine 2 of the SHHS as modelled in Simulink.

Machine 2 is pressure controlled, and therefore the flow and torque calculation approach is slightly different from Machine 1. A reference pressure, which has been set by the control system is sent to the valve system. An ideal flow is also calculated and sent to the valve system for comparison. The ideal pump flow $q_{m2,ideal}$ is calculated according to Equation 5.11

$$q_{m2,ideal} = n_{impeller} \cdot D_{m2} \cdot i_{PTO} \tag{5.11}$$

$T_{m2}$ is calculated by Equation 5.12.

$$T_{m2} = \frac{\varepsilon_{m2} \cdot D_{m2}}{2 \cdot \pi} \cdot \Delta p \cdot \frac{1}{\eta_{hm}} \tag{5.12}$$

Which is similar to Equation 5.8, apart from the parameters are for Machine 2. $\eta_{hm}$ is always in the denominator due to Machine 2 is only operated as pump in this configuration. As Machine 2 is pressure controlled the displacement setting is a consequence of the current pressure. And to be able to calculate Machine 2's torque using Equation 5.12, the displacement setting is required. Therefore Machine 2's $\varepsilon_{m2}$ is found using a look-up table. Another difference is that Machine 2's $\Delta p$ is calculated using Equation 5.13.

$$\Delta p = |p_{m2,actual} - p_{reservoir}| \tag{5.13}$$

As for Machine 1, Machine 2's $\eta_{hm}$ and $\eta_{vol}$ is found using look-up tables. An additional look-up table is also required for $\varepsilon_{m2}$. All three look-up tables have three inputs, $\Delta p$, $n_{m2}$ and $q_{m2,actual}$ as can be seen in Figure 5.10. Machine 2's $\eta_{hm}$ and $\eta_{vol}$ look-up tables can be seen in Figure 5.11 and Figure 5.12 with normalized values.

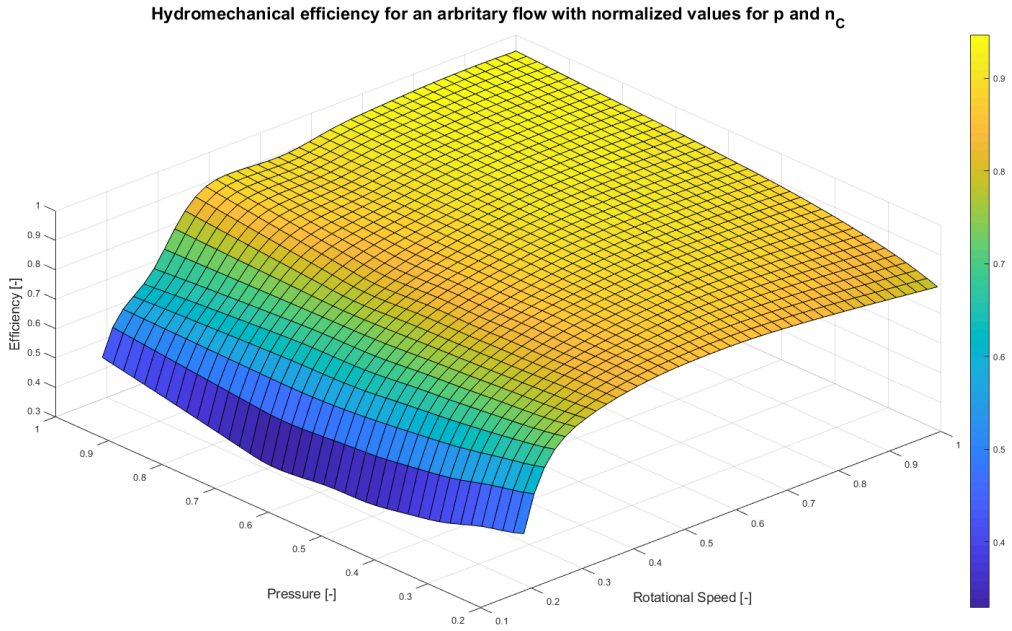


Figure 5.11: $\eta_{hm}$ look-up table for Machine 2 implemented in Simulink, the look-up table is defined for all $q_{m2,actual}$, in the figure an arbitrary flow is used. The values for $\Delta p$ and $n_{m2}$ are displayed with normalized values. The data is acquired from the pump manufacturer.

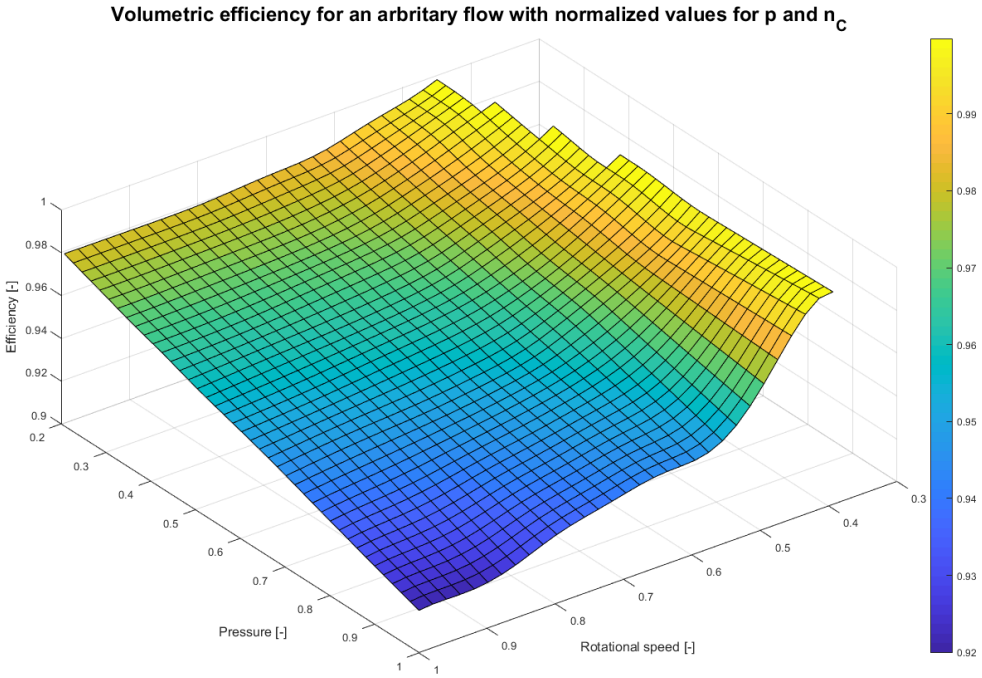


Figure 5.12: $\eta_{vol}$ look-up table for Machine 2 implemented in Simulink, the look-up table is defined for all $q_{m2,actual}$, in the figure an arbitrary flow is used. The values for $\Delta p$ and $n_{m2}$ are displayed with normalized values. The data is acquired from the pump manufacturer.

In Figure 5.13 the look-up table for $\varepsilon_{m2}$ for an arbitrary $q_{m2,actual}$ is displayed with normalized values.

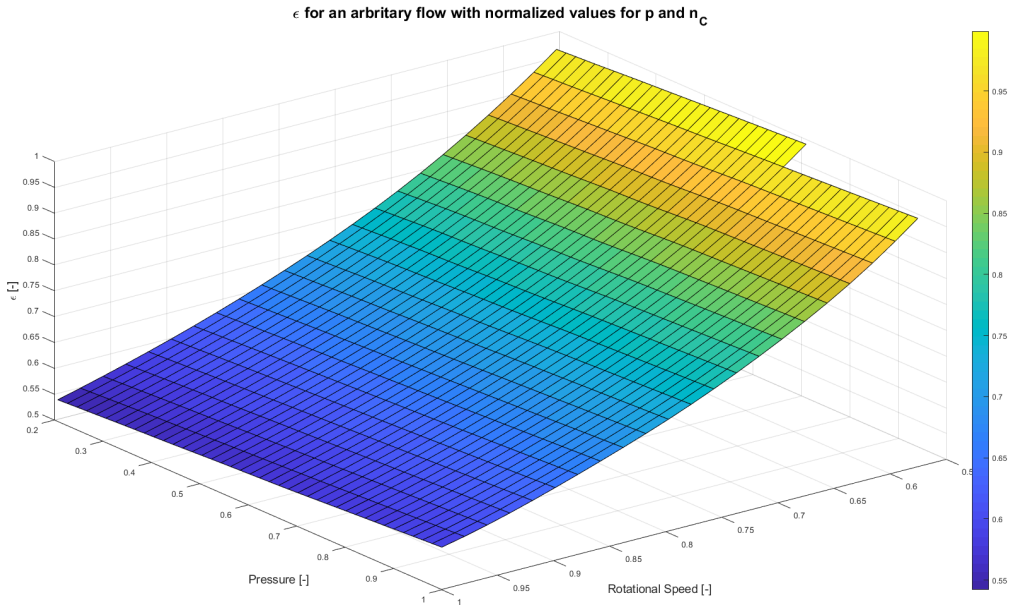


Figure 5.13: $\varepsilon$ look-up table for Machine 2 implemented in Simulink, the look-up table is defined for all $q_{m2,actual}$, in the figure an arbitrary flow is used. The values for $\Delta p$ and $n_{m2}$ are displayed with normalized values. The data is acquired from the pump manufacturer.

The look-up tables requires flow and pressure as input, therefore values from the last iteration must be used. A start value also has to be set, 0.9 is considered to be a reasonable start value for $\eta_{hm}$ and $\eta_{vol}$ and 0.0 for $\varepsilon_{m2}$. Hence, the current efficiencies $\eta_{hm}$ and $\eta_{vol}$ as well as $\varepsilon$ will be calculated with the previous time steps which will induce some computational errors. However the computational errors will be relatively small as the simulation model has small time step size. The efficiencies block of Machine 2 can be seen in Figure 5.14.

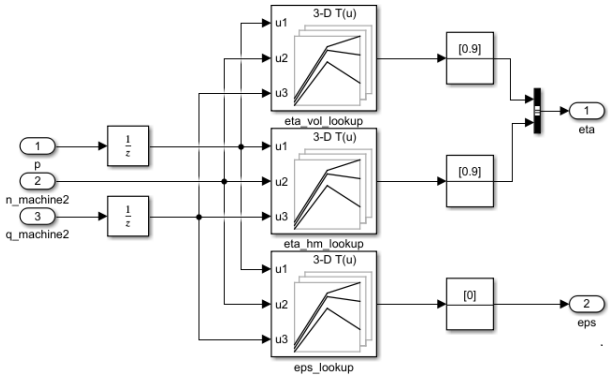


Figure 5.14: Look-up tables for Machine 2 as implemented in Simulink.

### 5.1.6 Valve System 1

Valve System 1 of the SHHS as modelled in Simulink can be seen in Figure 5.15. The valve system includes a mode switcher block which inputs control signals from the control system which decide the opening and closing of Valve 1-4. The block also includes logic which sets pressures of node A and B and flow of node C and D depending on the active valve configuration.

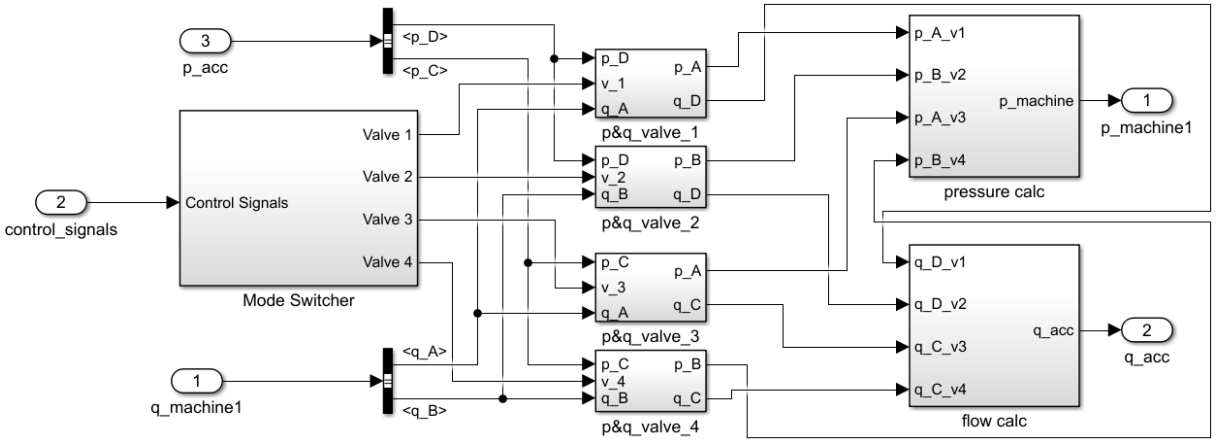


Figure 5.15: Valve System 1 of the SHHS as modelled in Simulink.

The four valves of Valve System 1 are all based on the same logical approach. The approach will be explained by examining Valve 1 see Figure 5.16.

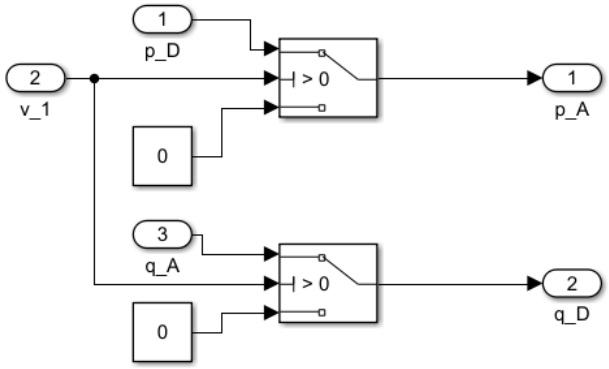


Figure 5.16: Valve 1 of Valve System 1 as modelled in Simulink.

If Valve 1 is open, the pressure of node D, i.e the accumulator pressure $p_{acc}$ is passed on to the node at the other side of the valve, in this case node A. The same approach is used for the flow, the flow at the node A is passed to node D.

### 5.1.7 Valve System 2

Valve System 2 of the SHHS as modelled in Simulink can be seen in Figure 5.17. In this block, the actual flow and pressure delivered by Machine 2 is calculated.

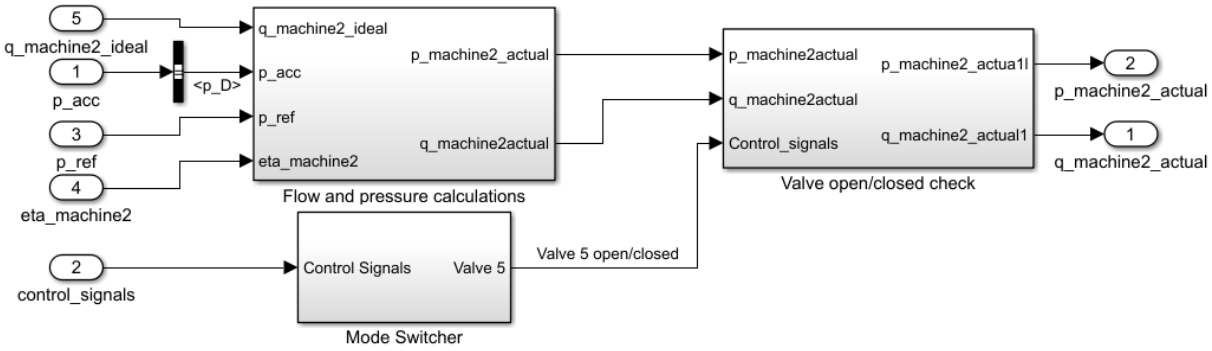


Figure 5.17: *Valve System* 2 of the SHHS as modelled in Simulink.

The block has five inputs; $p_{acc}$, a control signal from the control system which decide the opening and closing of Valve 5, $p_{ref}$ which is the pressure reference of Machine 2, efficiencies $\eta_{m2}$ as well as $q_{m2,ideal}$. One approach to calculate the flow over Valve 5 is to use Equation 5.14.

$$q_{Valve5} = C_q \cdot A \cdot \sqrt{\frac{2}{\rho} \cdot (p_{ref} - P_{acc})} \tag{5.14}$$

The larger the pressure drop over the valve, the greater the flow according the equation. To ensure that the flow over the valve is not greater than the ideal flow of Machine 2, the flow obtained from Equation 5.14 is saturated with the ideal Machine 2 flow.

After the flow has been saturated Machine 2's efficiency $\eta_{vol}$ is taken into account using Equation 5.15.

$$q_{m2,actual} = q_{m2} \cdot \eta_{vol} \tag{5.15}$$

The actual pressure of Machine 2's high pressure side is found using a look-up table which capture the valve's characteristics depending on the flow over it. If Valve 5 is open, Machine 2's flow is fed to the accumulators block. Both the flow and pressure are also fed back to the Machine 2 block for calculations of the next iteration's efficiency.

### 5.1.8 Accumulators

The accumulators as modelled in Simulink can be seen in Figure 5.18. PRVs are implemented which redirects incoming flows to an arbitrary tank if maximum system pressure is reached. According to the principle of the simulation model in Figure 5.3 the flows from the machines are summarized before being sent to the accumulators. Depending on magnitude of the flow to/from the accumulators the pressure at nodes C and D are calculated. The calculation approach is different for the high pressure and low pressure accumulator. Benedict-Webb-Rubin (BWR) equations are used for the high pressure accumulator due to its superior accuracy compared to the ideal gas law in pressure regions over 250 Bar according to [34]. Another study also states that the ideal gas law has a limited range of applicability as it uses only one coefficient, the polytropic exponent, $n$ [35]. The BWR equations uses more coefficients, which are determined empirically, to describe the behaviour of the gas more accurately at high pressures and fast processes when differences in temperature cannot be neglected. For the low pressure accumulator, ideal gas law is sufficient as its operating pressure is relatively low, computational cost is also lower using the ideal gas approach as it uses far less coefficients compared to BWR equations.

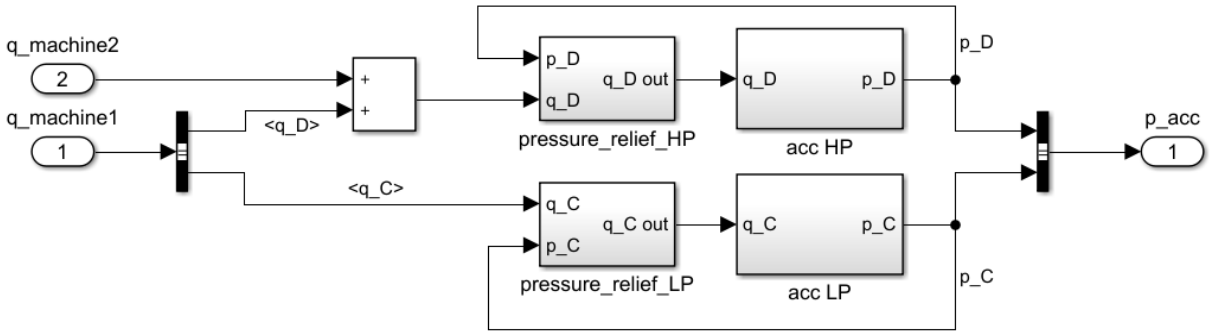


Figure 5.18: Accumulators of the SHHS as modelled in Simulink.

The high pressure accumulator as modelled in Simulink can be seen in Figure 5.19.

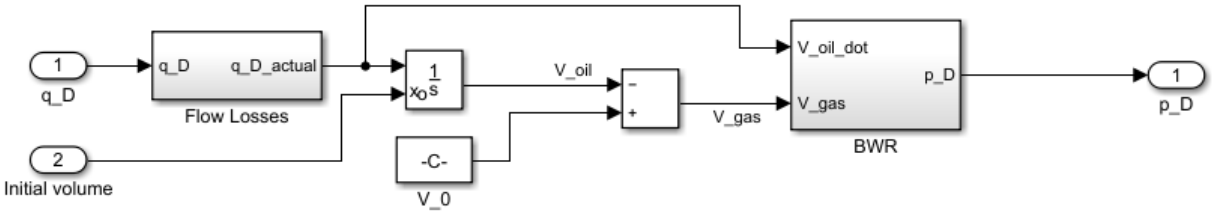


Figure 5.19: High pressure accumulator of the SHHS as modelled in Simulink.

For both the BWR equations and the ideal gas calculation, the flow to and from the accumulators are integrated over time. Depending on the magnitude of flow, the oil volume in the accumulators $V_{oil}$ at each iteration is calculated. Assuming that there is no leakage from the accumulator, Equation 5.16 can be used.

$$\Delta V_g + \Delta V_{oil} = 0 \tag{5.16}$$

The oil volume is integrated over the course of the simulation, see Equation 5.17. Where the integral is calculated between $[t_0, t]$ which is the length of one time step. For the high pressure accumulator, the $j$ variable is used to determine if $\eta_{acc}$ should be in the nominator or denominator of the equation. For charging, $j = 1$ and for discharging $j = -1$.

$$V_{oil} = V_{oilprevious} + \int_{t_0}^{t} q_{oil} \cdot \eta_{acc}^{j} dt \tag{5.17}$$

Since the oil volume is proportional to the gas volume, Equation 5.18 can be used to describe gas volume $V_g$ in the accumulator.

$$V_g = V_0 - V_{oil} \tag{5.18}$$

### 5.1.9 High pressure accumulator with BWR equations

The implementation of BWR equations for the high pressure accumulator in Simulink can be seen in Figure 5.20.

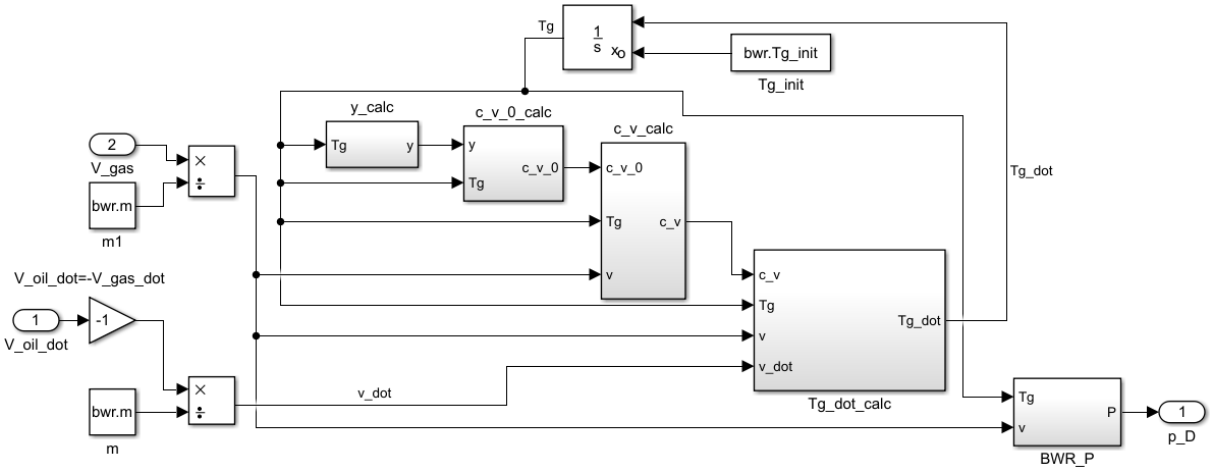


Figure 5.20: BWR equations as implemented in Simulink to calculate the pressure in the high pressure accumulator.

Equation 5.19, which is derived from the energy equation which can be found in the Appendix is used to describe the temperature of the gas in the accumulator.

$$\dot{T}_g = \frac{T_s - T_g}{\tau_{BWR}} - \frac{T_g(\frac{\delta p}{\delta T_g})\dot{v}}{c_v} \tag{5.19}$$

The BWR $p-v-T$ relationship which can be seen in Equation 5.20 [35]. The Equation is manipulated to use kg instead of kmol.

$$p = \frac{RT_g}{\nu} + \frac{B_0 R \cdot T_g - A_0 - \frac{C_0}{T_g^2}}{\nu^2} + \frac{bRT_g - a}{\nu^3} + \frac{a\alpha}{\nu^6} + \frac{c(1+\frac{\gamma}{\nu^2})e^{\frac{-\gamma}{\nu^2}}}{\nu^3 T_g^2} \tag{5.20}$$

Differentiating Equation 5.20 with respect to $T_g$ results in Equation 5.21.

$$\frac{\delta p}{\delta T_g} = \frac{R}{\nu} + \frac{B_0 R}{\nu^2} + \frac{2C_0}{T_g^3 \nu^2} + \frac{bR}{\nu^3} - \frac{2c(1+\frac{\gamma}{\nu^2})e^{\frac{-\gamma}{\nu^2}}}{\nu^3 T_g^3} \tag{5.21}$$

Combining Equation 5.19 and 5.21 yields Equation 5.22.

$$\dot{T}_g = \frac{T_s - T_g}{\tau_{BWR}} - \frac{\dot{\nu}}{c_\nu}\left(\frac{T_g R}{\nu} + \frac{T_g B_0 R}{\nu^2} + \frac{2C_0}{T_g^2 \nu^2} + \frac{T_g bR}{\nu^3} - \frac{2c(1+\frac{\gamma}{\nu^2})e^{\frac{-\gamma}{\nu^2}}}{\nu^3 T_g^2}\right) \tag{5.22}$$

Which can be rewritten into Equation 5.23 [36].

$$\dot{T}_g = \frac{T_s - T_g}{\tau_{BWR}} - \frac{\dot{\nu}}{c_\nu}\left(\frac{T_g R}{\nu}\Big(1+\frac{b}{\nu^2}\Big) + \frac{1}{\nu^2}\Big(T_g B_0 R + \frac{2C_0}{T_g^2}\Big) - \frac{2c}{\nu^3 T_g^2}\Big(1+\frac{\gamma}{\nu^2}\Big)e^{\frac{-\gamma}{\nu^2}}\right) \tag{5.23}$$

Equation 5.23 is implemented in Simulink, see Figure 5.20. To use Equation 5.23 the nitrogen gas specific constants are used to determine the ideal gas specific heat including a pressure correlation, described by [36], see Equation 5.24. The ideal gas constants and the BWR constants $(N_1 - N_9)$ can be found in the Appendix.

$$c_v^0 = R\left(\frac{N_1}{T_g^3} + \frac{N_2}{T_g^2} + \frac{N_3}{T_g} + (N_4 - 1) + N_5 T_g + N_6 T_g^2 + N_7 T_g^3 + \frac{N_8 \frac{N_9}{T_g} e^{\frac{N_9}{T_g}}}{(e^{\frac{N_9}{T_g}} - 1)^2}\right) \tag{5.24}$$

As the specific heat of the ideal gas is known, the specific heat of the real gas can be calculated using Equation 5.25 [36].

$$c_v = c_v^0 + \frac{6}{T_g^3}\left(\frac{C_0}{\nu} - \frac{c}{\gamma}\right) + \frac{3c}{T_g^3}\left(\frac{2}{\gamma} - \frac{2}{\nu^2}\right)e^{-\frac{\gamma}{\nu^2}} \tag{5.25}$$

By combining 5.25 and 5.23 the change in gas temperature can be calculated. The mass of the nitrogen gas is also required for the BWR Equationas can be seen in Figure 5.20.

The ideal gas law combined with the specific volume of nitrogen at atmospheric pressure can be used [35]. See Equation 5.26

$$m_{nitrogen} = \frac{p_0 \cdot V_0}{\nu_{atmosperic} \cdot p_{atmosperic}} \tag{5.26}$$

### 5.1.10 Low pressure accumulator with the ideal gas law

For the low pressure accumulator the ideal gas law is used to determine the pressure. The process is assumed to be isentropic which enabels the use of Equation 5.27.

$$p_g \cdot V_g^n = p_0 \cdot V_0^n \tag{5.27}$$

By combining Equation 5.18, 5.17 and 5.27, Equation 5.28 is obtained. Which is used to calculate the accumulator pressure at each step of the simulation. The polytropic exponent is often assumed to be $n = 1.4$, [22].

$$p_g = p_0 \left( \frac{V_0}{V_0 - \int_{t_0}^{t} q_{oil} dt} \right)^n \tag{5.28}$$

Before starting the simulations, an initial accumulator oil volume is set. The ideal gas law, Equation 5.27 is combined with Equation 5.29 which is the used to calculate the initial pressure. They form Equation 5.30 which is used to calculate the initial volume of oil in the accumulator.

$$p_{init} = p_0 + (p_2 - p_0) \cdot SOC \tag{5.29}$$

$$V_{init} = V_0 \cdot \left( \frac{p_0}{p_{init}} \right)^{(\frac{1}{n})} \tag{5.30}$$

### 5.1.11 Torque Converter look-up tables

To capture the behaviour of the TC, look-up tables are used, see Figure 5.21. Every combination of torque and speed on the turbine's shaft has a corresponding torque and speed on the impeller which is directly connected to the ICE's output shaft.

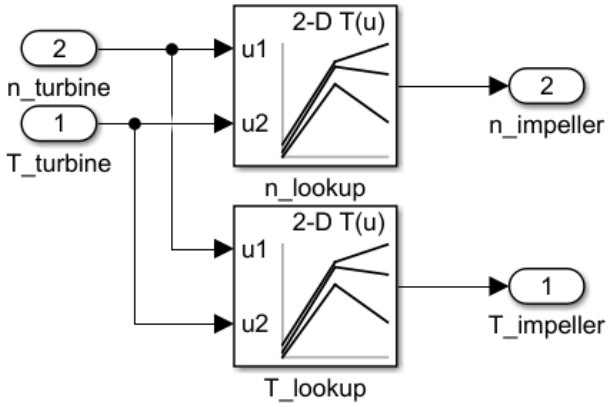


Figure 5.21: TC as modelled in Simulink

### 5.1.12 Internal Combustion Engine and Work Hydraulics

The ICE block as implemented in Simulink can be seen in 5.22. Apart from $T_{ICE}$ and $n_{ICE}$, a control signal with engine speed limit is sent as input to the block. The signal limits the ICE rotational speed to a value defined by the control system.

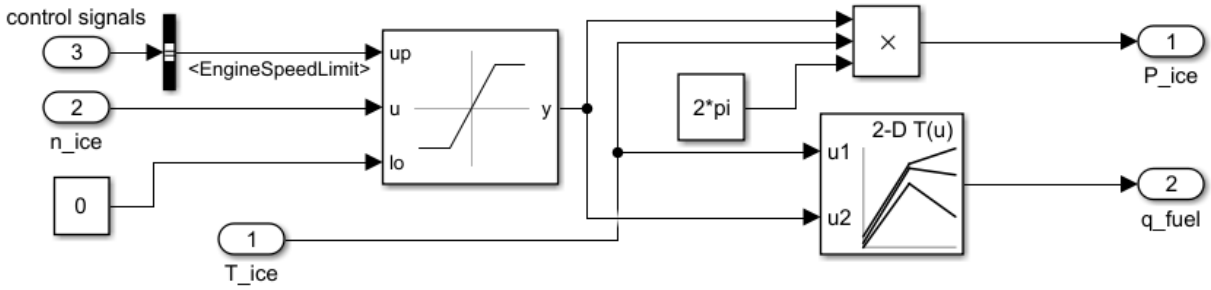


Figure 5.22: ICE as modelled in Simulink.

$T_{ICE}$ is the sum of all torques applied to ICE's shaft according to the simulation principle, see Figure 5.3. To be able to calculate $T_{ICE}$, $T_{WH}$ is calculated using Equation 5.31.

$$T_{WH} = \frac{P_{WH}}{n_{ICE} \cdot i_{WH}} \tag{5.31}$$

$T_{ICE}$ is then calculated using Equation 5.32.

$$T_{ICE} = T_{WH} + T_{impeller} + T_{m2} \tag{5.32}$$

The power required from the engine is calculated with Equation 5.33.

$$P_{ICE} = n_{ICE} \cdot T_{ICE} \cdot 2 \cdot \pi \tag{5.33}$$

A look-up table is used to find the fuel flow required from the engine to fulfill the torque demand from the drive cycle. The fuel flow can then be integrated over time with Equation 5.34 to obtain the accumulated fuel consumption.

$$V_{fuel} = \int_{t_0}^{t} q_{fuel} dt \tag{5.34}$$

### 5.1.13 Sensor signals

Sensor signals is added to the Simulink model, which can be seen in Figure 5.3. The sensor signals provide the basis for decision making in the control system, see Figure 5.1. An example of a signal that is conditioned before sent to the control system is *TrsmOutgoingDir* which indicates the travelling direction of the wheel loader. Another example is the *TrsmChangingDirSt* which indicates if the wheel loader is about to change direction.

## 5.2 Control system

The purpose of the control system is to control the SHHSs hardware and the ICEs speed as desired. Sensor signals from vital components of the wheel loader driveline are fed to the control system for processing. The signals provide the control system with information regarding accumulator pressures, gear selections, shaft speeds and more. The sensor signals are always fed forward through the control system and are present in every subsystem necessary. Based on the sensor signals the control system selects an appropriate EMS state for which a suitable utilization of the SHHS is calculated. Relevant components are then fed with control signals for execution. The logical order of execution can be seen in Figure 5.23.

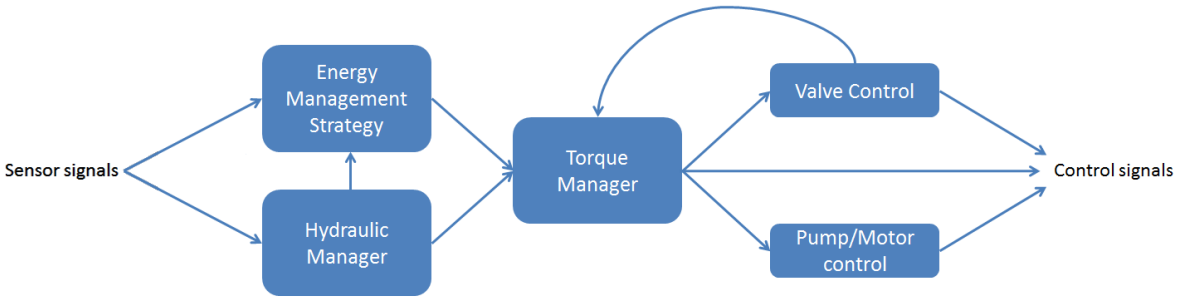


Figure 5.23: Control system architecture with execution order

The control system is modelled in Matlab/Simulink where stateflows serve as a key functionality. State machines are thus utilized in the control system's subsystems.

### 5.2.1 Energy Management Strategy subsystem

The EMS subsystem contain one main stateflow conducting the EMS state machine. A rule-based EMS is utilized as it was stated sufficient for a hydraulic hybrid system in a wheel loader, see Section 4.3. Sensor and SHHS diagnostic inputs serve as basis for decision making to the stateflow. Based on these inputs, the most suitable EMS state is set. The strategy is then being fed further in the control system execution order, as Figure 5.24 visualizes.

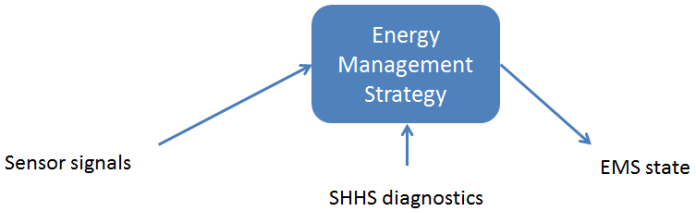


Figure 5.24: Energy Management Strategy subsystem inputs and outputs.

In total, nine states are defined and used for utilizing the SHHS. The states can be seen in Table 5.1 together with a short description. The states named Parallel are, as the

name suggests, operating the SHHS as a Parallel hybrid configuration while the states named Series operate the SHHS as a Series hybrid configuration where some power from the engine is redirected over the SHHS instead of through the TC , see Figure 3.2 and 3.3.

Table 5.1: EMS states

| **State** | **Description** |
|---|---|
| Idle | Hybrid functionality on idle |
| Parallel Direction Change | Energy recuperation by Machine 1 performing pump operation |
| Parallel Drive | Propulsion of the vehicle by Machine 1 performing motor operation |
| Parallel Bucketfill | Propulsion of the vehicle by Machine 1 performing motor operation |
| Parallel Accumulator Charge | Pre-charge of accumulators by Machine 1 performing pump operation |
| Series Direction Change | Energy recuperation by Machine 1 performing pump operation and extra energy stored by Machine 2 performing pump operation |
| Series Drive | Propulsion of the vehicle by Machine 1 performing motor operation and Machine 2 performing pump operation |
| Series Bucketfill | Propulsion of the vehicle by Machine 1 performing motor operation and Machine 2 pump operation |
| Series Accumulator Charge | Pre-charge of accumulators by Machine 2 performing pump operation |

Figure 5.25 illustrates the architecture of the stateflow. All states are reachable from Idle and return to Idle. Rules determine when the strategy is allowed to utilize any other state but Idle, rules also determine if the Parallel or Series configuration should be used. State specific rules determine which state to be used but all states share common diagnostics rules such as parking brake checks, transmission status and engine checks.

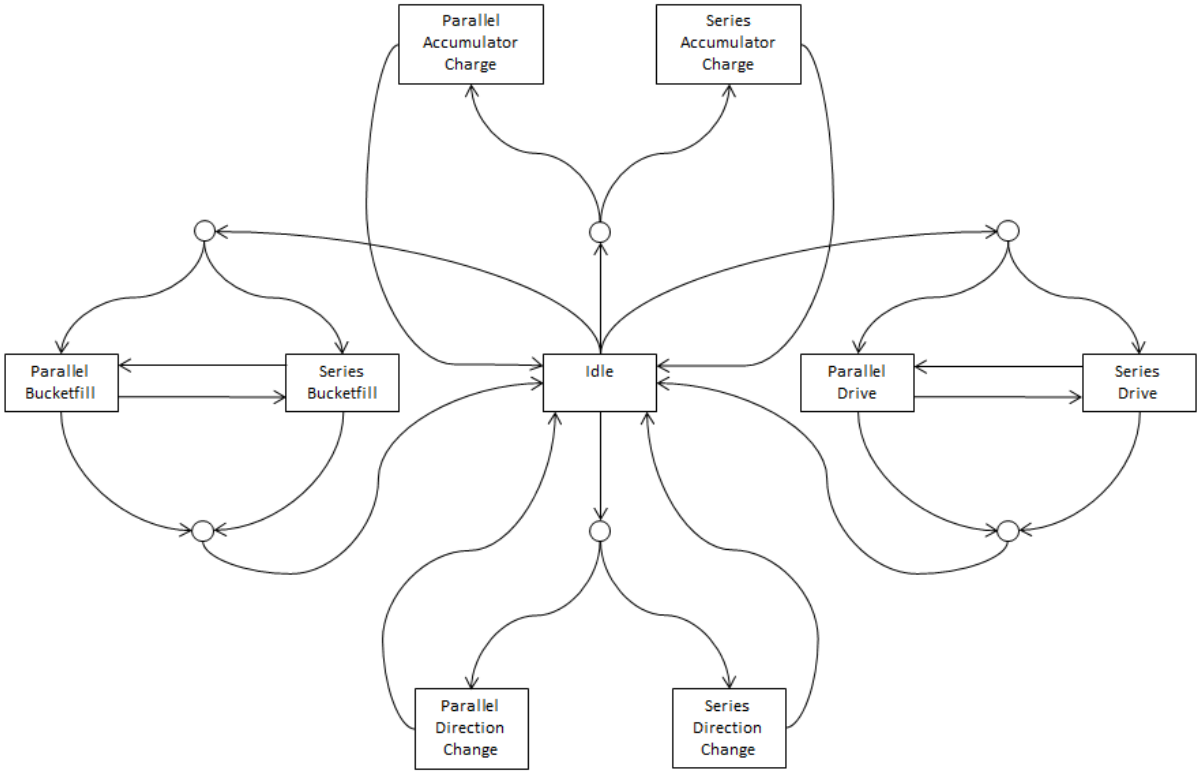


Figure 5.25: EMS stateflow architecture.

The *Bucketfill* states should only be used during the bucketfill phase in the drive cycle. When reaching the gravel pile with the wheel loader kick down is activated, which in turn down shifts the transmission to first gear. Hence a suitable state specific rule for Bucketfill state entry is

- $ActualGear == FirstGear$

When Bucketfill is engaged, the strategy is required to decide whether to use the Parallel or Series configuration. The most favourable outcome is to use all recuperated and stored energy in the accumulator, which is why the Series configuration is not recommended to use unless the accumulator is partly depleted. Hence a suitable state specific rule for Parallel bucketfill is

- $SoC > SoC_{series,Bucketfill}$

Once the accumulator is partly depleted it may be favourable to use the Series configuration to continuously decrease the dependency of the TC and avoid its low efficiency. The Series configuration rule must also take required torque demand into account. If the required torque demand is kept relatively low, so will the displacement setting of Machine 1. Thus, important parameters for the Series bucketfill state rule are SoC and displacement setting. The parameters can be intertwined and expressed as an equation, limiting the number of input rules to one. By introducing Equation 5.35 similar to the straight line equation the parameters can be combined.

$$SoC = \varepsilon_{series} k + SoC_{cut} \tag{5.35}$$

Where $SoC$ is the actual state of charge in the accumulator, $\varepsilon_{series}$ the required displacement setting of Machine 1 to engage the Series configuration, k the incline factor of the line and $SoC_{cut}$ the state of charge in the accumulator at which the line cuts the x-axis. The parameter of interest is the displacement setting as a function of SoC, hence rewriting Equation 5.35 into Equation 5.36. The principles of the line is presented in Figure 5.26.

$$\varepsilon_{series} = \frac{SoC - SoC_{cut}}{k} \tag{5.36}$$

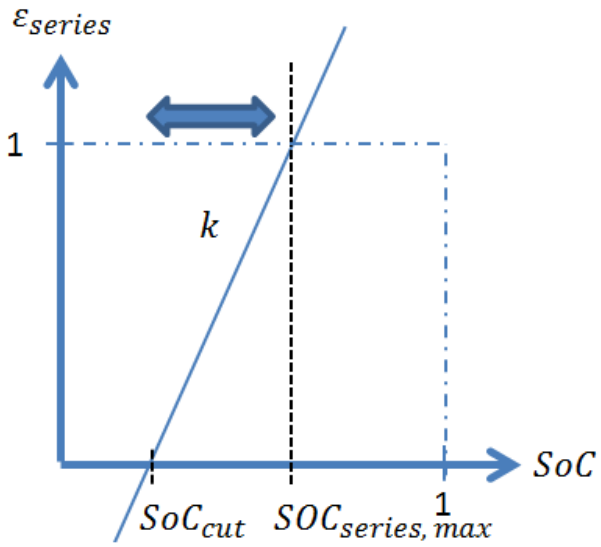


Figure 5.26: Limitation curve for Series bucketfill.

By introducing the boundary conditions in Equation 5.37 and 5.38 the value of $k$ can be calculated for any chosen value of $SoC_{cut}$ and $SoC_{series,max}$.

$$\varepsilon_{series}(SoC_{cut}) = 0 \tag{5.37}$$

$$\varepsilon_{series}(SoC_{series,max}) = 1 \tag{5.38}$$

In practice, the line creates a threshold for usage of the Series configuration. The actual displacement setting of Machine 1 must have a higher value than the calculated $\varepsilon_{series}$ for the system to be allowed to utilize the Series configuration. Values of $\varepsilon_{series}$ will be smaller than zero on the left side of $SoC_{cut}$ and thus whenever the actual SoC is lower than $SoC_{cut}$ the Series configuration is always allowed. Corresponding, values of $\varepsilon_{series}$ will be larger than one on the right side of $SoC_{series,max}$ and thus whenever the actual SoC is larger than $SoC_{series,max}$ the Series configuration is not allowed.

Hence a suitable state specific rule for entering Series bucketfill, independently of previous state equals Idle or Parallel bucketfill, becomes

- $\varepsilon_{m1} > \varepsilon_{series}$

The bucketfill states are to be used as long as bucketfill operation is performed and the SoC is sufficient. Hence suitable conditions for exiting the bucketfill states are

- $ActualGear \neq FirstGear$
- $SoC < SoC_{threshold,Bucketfill}$

The *Direction Change* states are states to be used when the wheel loader changes demanded travelling direction while still in motion. A common way of changing travelling direction with a wheel loader is to change gear from forward to reverse, or vice versa, before stand still and not applying the brakes before changing gear. This action induces negative slip on the TC and dissipates all kinetic energy into heat while exerting wear on the component.

Direction Change state is used to bring the wheel loader to a stop by applying a braking torque with the hybrid system. These states have two major gains; kinetic energy is recuperated and the TC experience negative slip for a decreased period of time, reducing wear. Suitable rules for entering the states are

- $v_{veh} \leq 0$ && $GearState == Forward$
- $v_{veh} > 0$ && $GearState == Backward$

Machine 2 cannot recuperate energy, power provided by the machine instead originates from diesel power. Hence, for energy recuperation Machine 1 is the only suitable machine to operate. However, if it is desirable to reach higher pressures in the accumulator during a direction change Machine 2 can be utilized to increase the rate of charging. Occasions at which higher accumulator pressure may be desirable is when higher brake torque is demanded. One limitation regarding Machine 2 is its maximum operation pressure. Suitable state specific rules for Parallel direction change becomes thus the previous mentioned rules and for Series direction change

- $p_{acc} < p_{m2,max}$

The Directional Change states are no longer desirable to use when the wheel loader has come to a complete stop. Advantages can however be drawn from exiting the states at a certain time before the wheel loader has come to a complete stop. Dynamics in the system may cause pressure drops in the accumulator before the direction is changed. A suitable condition for exiting the states become

- $|v_{veh}| < v_{treshold,DirectionalChange}$

*Drive* is a state used for propulsion of the wheel loader from stand still to a certain velocity. The SHHS do not have enough propulsive torque to enable full hybrid propulsion of the wheel loader, it rather assists the ICE with propulsive torque. Stored energy in the accumulator is converted into kinetic energy as the wheel loader increases in velocity. The Parallel configuration only use stored energy from the accumulator while the Series configuration uses either diesel or stored energy from the accumulator depending on the demanded flow from Machine 1. The Drive state is not suitable for longer distances since a high SoC in the accumulator is desirable at the start of a bucketfill operation. Therefore it is also desirable to keep the SoC in the accumulator as constant as possible. Suitable state specific rules for Series Drive and Parallel Drive are therefore

- $|v_{veh}| < v_{start,Drive}$
- $SoC > SoC_{Threshold}$

A suitable rule for Series Drive is

- $p_{acc} < p_{m2,max}$

Suitable conditions for exiting the states are

- $|v_{veh}| > v_{end,Drive}$
- $SoC < SoC_{threshold}$

The *Charge* states are states mainly used when the wheel loader is started and the accumulator SoC is below the pre-charge pressure. Both Parallel Charge and Series Charge fulfil their purposes without one being superior the other. Parallel Charge displaces Machine 1 and thus applies a braking torque on the wheel loader which in turn charges the accumulator. Series Charge displaces Machine 2 to charge the accumulator. By displacing Machine 2 no braking torque will be applied on the wheel loader, instead power from the ICE is directly used. The wheel loader operator chooses the desired way of charging the accumulators, with the Parallel or the Series configuration. A suitable state specific rule for the Charge state is

- $p_{acc} < p_{acc,Critical}$

If $p_{m2,max} > p_{acc,ChargeLimit}$ a suitable condition for exiting the state is

- $p_{acc} \geq p_{acc,ChargeLimit}$

### 5.2.2 Hydraulic manager subsystem

The objective of the Hydraulic manager is to monitor the SHHS and provide information further down the execution order regarding the state of the SHHS. By feeding sensor signals such as accumulator pressure to the Hydraulic manager the available hydraulic torque which can be utilized for propulsion can be calculated. The hydraulic manager also functions as a safety feature where the strategy is alerted if hybrid operation must be aborted for any reason, e.g prevent the accumulators to reach critically low pressures. Inputs and outputs from the subsystem are presented in Figure 5.27.

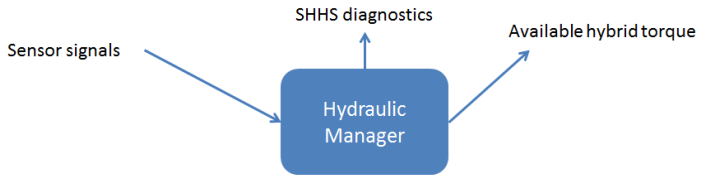


Figure 5.27: Hydraulic Manager subsystem inputs and outputs.

### 5.2.3 Torque control subsystem

The duty of the torque control subsystem is to control the hydraulic hybrid torque as well as determine from where torque should be retrieved, from the ICE or the SHHS. It is not desirable to increase the driveline power output, which for instance happens when the ICE is allowed to operate as usual under the assist of the SHHS. Therefore an engine speed limit signal is sent to the ICE to limit the ICEs speed. However, the ICE rotational speed cannot be limited too low as it may inflict the time it takes to lift the work hydraulic boom, which can cause disturbances in the drive cycle. By feeding the chosen EMS and also SHHS diagnostics to the subsystem, as suggested in Figure 5.28, it may calculate a suitable limitation in ICE rotational speed to keep the driveline power output close to a conventional wheel loader.

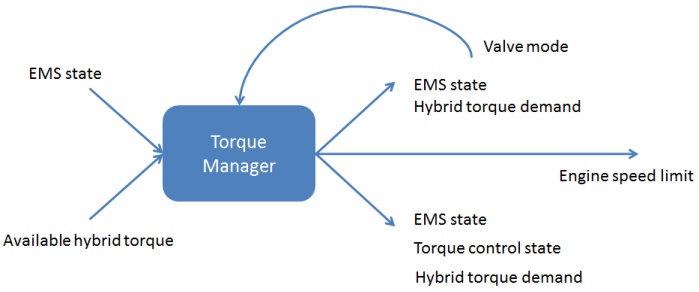


Figure 5.28: Torque Manager subsystem input and outputs.

On a lower level, inside of the torque control subsystem, two more subsystems and a stateflow is present. The logical execution order of these systems is shown in Figure 5.29.

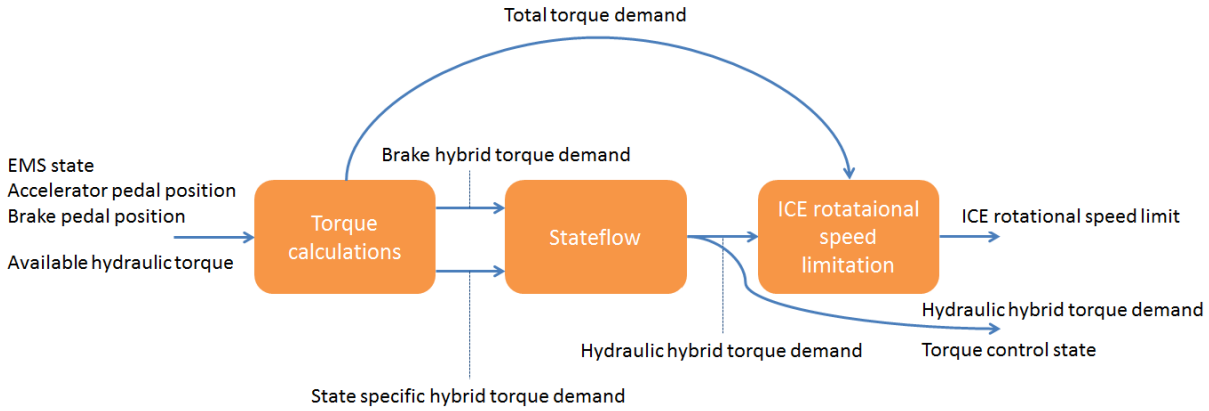


Figure 5.29: Torque Manager subsystem architecture with execution order.

Total torque demand, State specific torque demand and Brake hybrid torque demand are calculated in Torque calculations. State and indirectly actual gear are fundamental for the torque demand as the amplitude of the demand increases with down shifts. Accelerator pedal position is mapped against total torque demand. Combined with state it forms the State specific torque demand. Brake hybrid torque demand functions in the same manner, brake pedal position is mapped against brake torque demand. Figure 5.30 exemplifies the mapping of accelerator pedal to total torque demand and brake pedal to brake torque demand. An important feature is the priority of the Brake torque demand. If a Brake and State specific torque demand is present the Brake torque will always be accounted for by decreasing the State specific hybrid torque. Hence the Hydraulic hybrid torque demand becomes the sum of State specific and Brake torque demand.

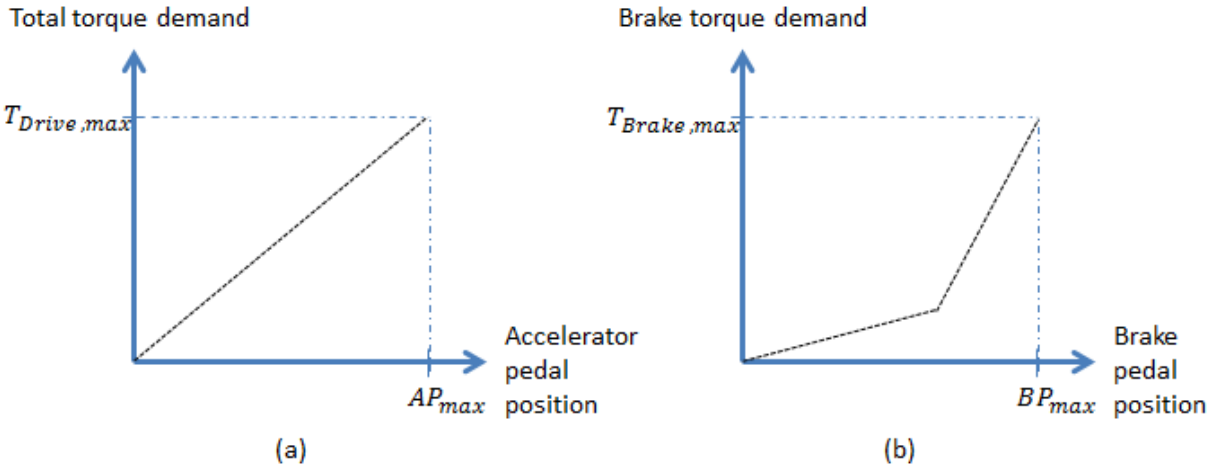


Figure 5.30: Pedal positions against torque demands.

The states along with the stateflow architecture for the torque control are presented in Table 5.2 and Figure 5.31. One torque control state is conducted for each unique major state in the EMS. To reach any of the states in the torque control one of the corresponding EMS states needs to be active as well as the correct valve mode. Deactivated EMS states results in the torque control state eventually returns back to Idle.

Table 5.2: Torque control states

| **State** | **Description** |
|---|---|
| Idle | Torque control on idle |
| Direction Change | Controls the torque dynamics during Direction Change |
| Drive | Controls the torque dynamics during Drive |
| Bucketfill | Controls the torque dynamics during Bucketfill |

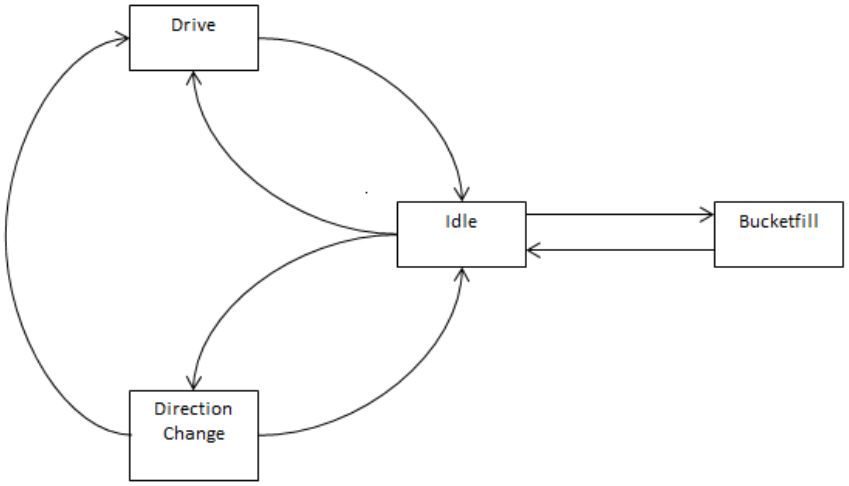


Figure 5.31: Torque Manager stateflow architecture.

Since the hydraulic torque demand signal conducts the foundation for the displacement setting on Machine 1 it is not desirable to create stepping torque demand changes, rather have the demands ramped up and down with certain rates. When ramped a smoother operating experience will be achieved. That is actually the main objective of the torque control stateflow. The principle is presented in Figure 5.32.

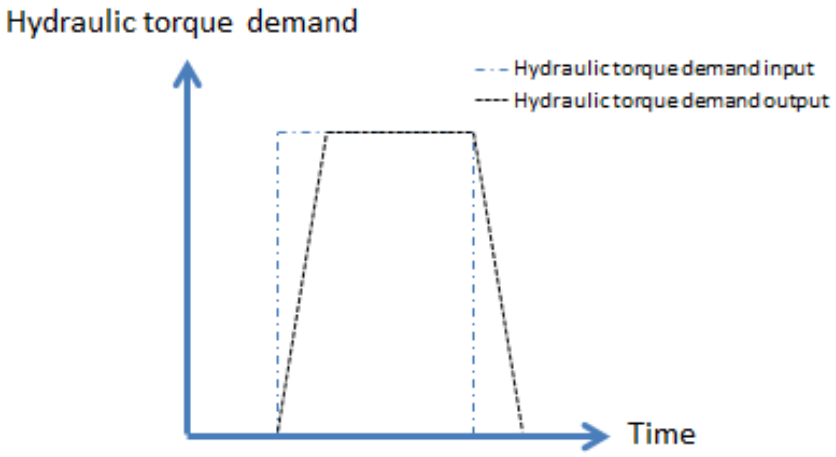


Figure 5.32: Dynamics of hydraulic torque demand.

The limitation of the ICE rotational speed is performed by firstly subtracting the hydraulic torque from the total torque. Once performed it is known how much the ICE need to contribute to the total torque. The torque sum is then mapped against ICE rotational speed in the same manner as accelerator pedal against torque demand.

### 5.2.4 Valve control subsystem

The purpose of the valve control subsystem is to control the valves of the SHHS, as Figure 5.33 suggests. One main stateflow controls which state is active and thus which valve mode used. Valve modes, or states, as well as a description and corresponding valve setup are presented in Table 5.3.

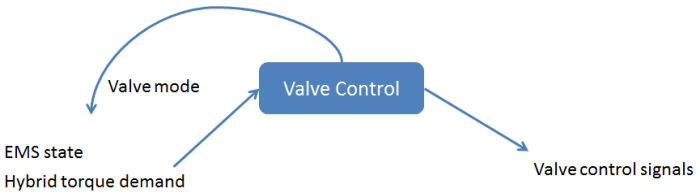


Figure 5.33: Valve Control subsystem input and outputs.

The Parallel Charge state presented in Table 5.1 does not have a corresponding valve mode similar to Series Charge. Parallel Charge can instead utilize the Parallel Positive Torque or Parallel Negative Torque valve modes depending on travelling direction.

Table 5.3: Valve modes

| **Valve mode/State** | **Description** | **Valve Setup** |
|---|---|---|
| Parked | Valves closed during stand still | [0 0 1 1 0] |
| Parallel Positive Torque | Propulsive torque in forward direction | [0 1 0 1 0] |
| Parallel Negative Torque | Propulsive torque in backward direction | [1 0 1 0 0] |
| Transport | Short-circuit when travelling in any direction | [0 0 0 0 0] |
| Transition Positive Torque | Transition between valve modes | [0 0 0 1 0] |
| Transition Negative Torque | Transition between valve modes | [0 0 1 0 0] |
| Series Positive Torque | Propulsive torque in forward direction | [0 1 0 1 1] |
| Series Negative Torque | Propulsive torque in backward direction | [1 0 1 0 1] |
| Series Charge | Pre-charge of accumulator | [0 0 0 0 1] |

The stateflow requires transition conditions to reach other valve modes. Positive and Negative torque valve modes are reachable when a torque demand is present and exited when the torque demand cease. The states requires the Transition valve modes as intermediate states. Transition states prevents undesirable pressure drops in the accumulator during valve closing by assuring the high pressure accumulator valves to always be closed before opening the low pressure accumulator valves. A time delay is always present after a Transition valve mode to ensure sufficient time for the valves to open or close. EMS state determines if Parallel or Series valve modes should be used. EMS state is also the criteria to enter the Charge valve mode. The Parked valve mode is used at stand still, hence actual velocity determines if it should be entered or exit. The architecture of the stateflow can be seen in Figure 5.34.

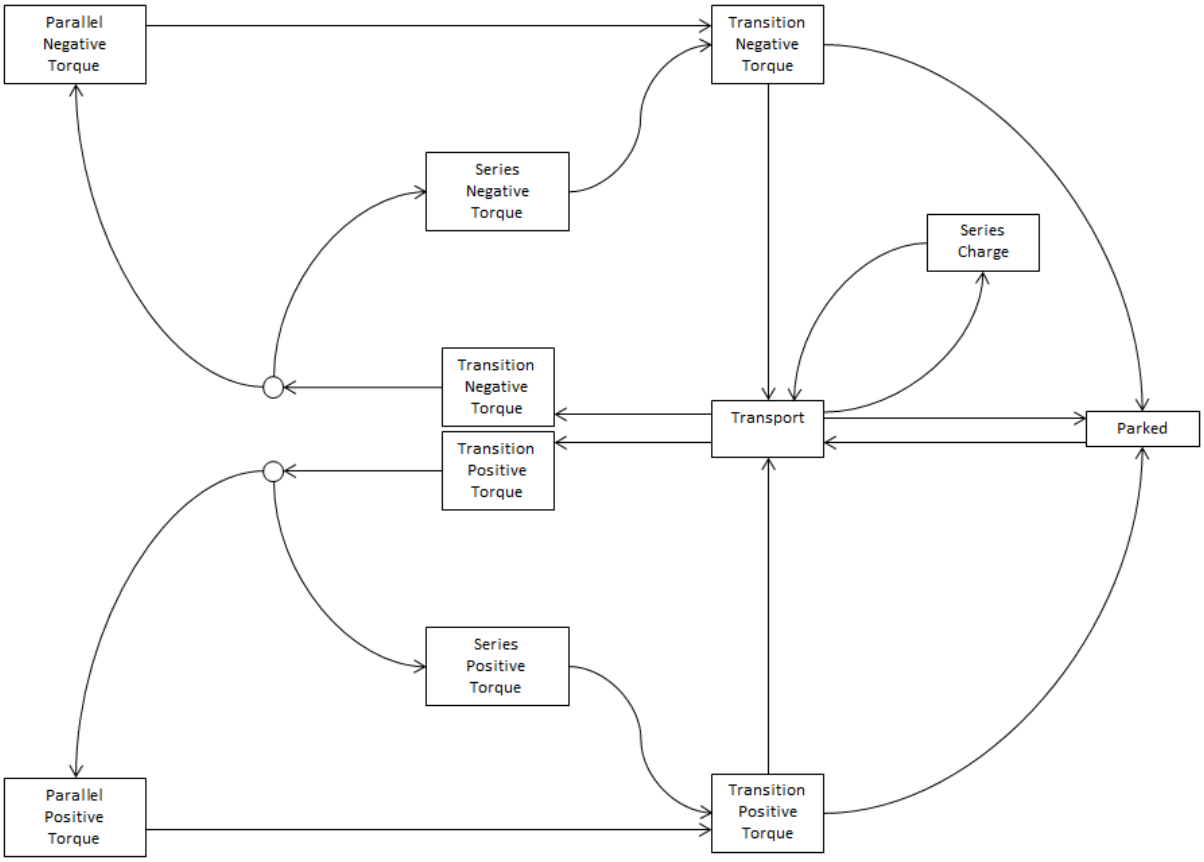


Figure 5.34: Valve Control stateflow architecture.

### 5.2.5 Pump/motor control subsystem

The pump/motor control system acts to displace Machine 1 and provide Machine 2 with a desired reference pressure. No stateflow is used in the subsystem, only calculation blocks and logical operators. Inputs and outputs of the subsystem are presented in Figure 5.35.

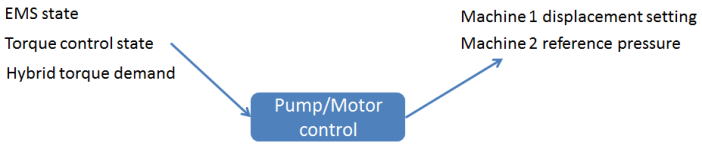


Figure 5.35: Pump/Motor Control subsystem input and outputs.

Machine 1's displacement setting is calculated by Equation 5.39 derived from Equation 2.7.

$$\varepsilon_{m1} = T_{m1} \frac{2\pi}{D_{m1} \Delta p \eta_{hm}} \tag{5.39}$$

The reference pressures provided to Machine 2 are pre-determined and state dependent. Hence the reference pressures acts on the EMS state and Torque control state inputs. Table 5.4 presents the reference pressures for the different EMS states. The EMS states are the only states actually changing to reference pressure value. Torque control states are only present to avoid turning Machine 2 on if the SHHS is not ready.

Table 5.4: Reference pressure for Machine 2 for different EMS states

| **EMS state** | **Reference pressure [bar]** |
|---|---|
| Idle | 0 |
| Parallel Direction Change | 0 |
| Parallel Drive | 0 |
| Parallel Bucketfill | 0 |
| Parallel Accumulator Charge | 0 |
| Series Direction Change | 350 |
| Series Drive | 350 |
| Series Bucketfill | 240 |
| Series Accumulator Charge | 350 |

The maximum pressure of Machine 2 is equal to 350 bar, hence three out of four states uses its maximum capacity. Series bucketfill, the state which is not using its maximum capacity, has a different approach with regards to reference pressure. While all three states with maximum pressure all desire as much flow as possible, Series bucketfill does not. Since Machine 2 is pressure controlled it will displace as much as needed to reach the desired pressure level. In practice this results in a provided flow from the hydraulic machine to the accumulator whenever there is a difference between actual and reference pressure. Series direction change, Series Drive and Series Accumulator Charge all desire as much flow as possible to charge the accumulator, or simply prevent discharging. In the case of bucketfill however, the state strives to use all stored energy in the accumulators, it is not desirable to increase the accumulator pressure.

The bucketfill reference pressure is calculated by studying a bucketfill operation in a conventional wheel loader and the TC turbine torques provided at different ICE rotational speeds. The general idea is to minimize the power flow through the TC and instead redirect it over the SHHS once the stored energy is used. Introducing two torque variables, one as a function of average ICE rotational speed during bucketfill for a conventional wheel loader and one for the minimum ICE rotational speed preventing the work hydraulics to choke, see Equations 5.40 and 5.41.

$$T_{avg} = f(n_{ICE,avg}) \tag{5.40}$$

$$T_{min} = f(n_{ICE,min}) \tag{5.41}$$

The torque difference presented in Equation 5.42 becomes thus the magnitude of torque needed from the SHHS if the ICE rotational speed during bucketfill is kept at the minimum rotational speed.

$$\Delta T = T_{avg} - T_{min} \tag{5.42}$$

Pressure level in the SHHS becomes the key variable as it is linear to the supplied or absorbed torque. Deriving Equation 5.43 from 2.7 allows the desired reference pressure to be calculated.

$$\Delta p = \Delta T_{m1} \frac{2\pi}{\varepsilon_{m1} D_{m1} \eta_{hm}} \tag{5.43}$$

# 6 Results

The SHHS concept is evaluated by simulating the hydraulic hybrid wheel loader model with the developed control system. Firstly, the exchange between hydraulic, kinetic and diesel energy over one SLC is shown to visualize energy flow with the hybrid system. Then the functions of the control system are shown to display the functionality of the hybrid states. The differences between Parallel and Series hybrid operation is also displayed and pointed out. Followed by a comparison of power flows and efficiencies between the conventional driveline versus the SHHS driveline. After which two SLCs are shown to display the system as a whole for comparison of energy efficiency between the Conventional and the SHHS driveline. Finally, a case where the accumulators are down-sized and the SHHS is operated similar to a hydrostatic transmission is displayed. Where it is of interest to study the impact of energy storage size.

## 6.1 Exchange in energy over one SLC

In Figure 6.1 simulated results of one SLC can be seen. The figure visualizes the exchange in energy between hydraulic, kinetic and diesel energy along with strategy state and mass of the wheel loader.

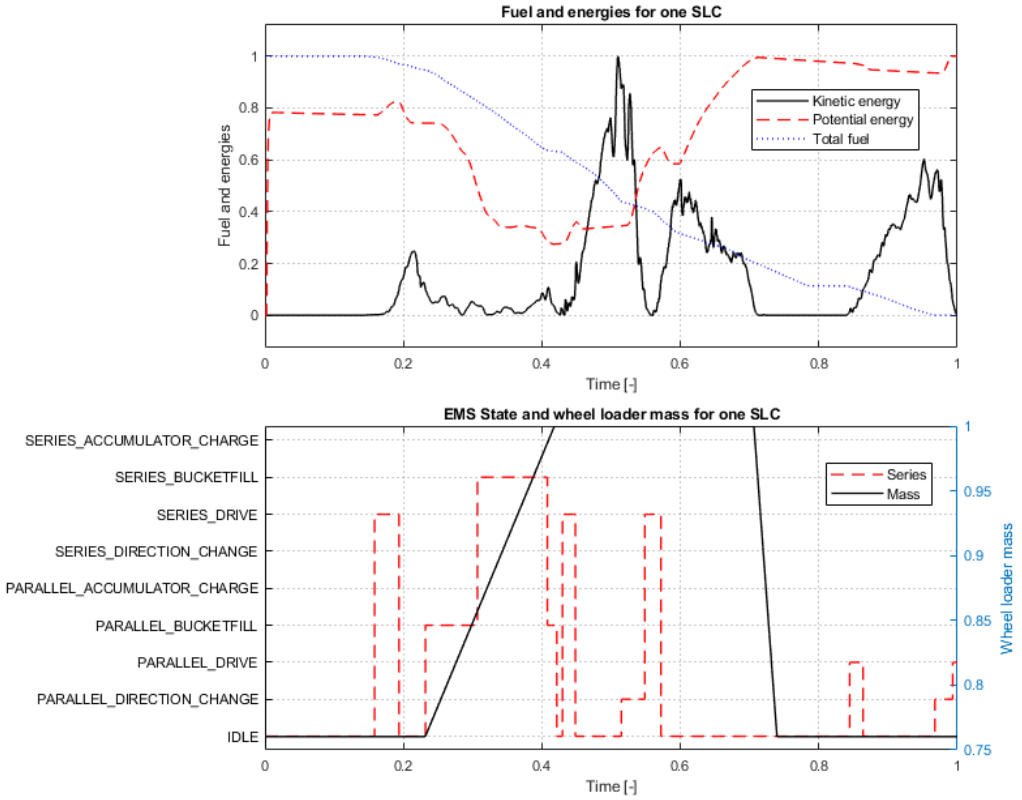


Figure 6.1: Exchange between hydraulic, kinetic and diesel energy for Parallel and Series configuration for one SLC.

The SLC will be explained, step by step to analyse general behaviours of the hybrid system, recall the SLC from Section 2.2. The cause of SoC characteristics will only briefly be pointed out in this section, further explanation will be given in Sections 6.2-6.6. The cycle starts with a Drive, it can be observed that the kinetic energy increases as the wheel loader is set into motion. SoC is converted into kinetic energy and some diesel energy is also required for propulsion. As the wheel loader reaches the pile, Bucketfill state is engaged and SoC is converted into kinetic energy. Extensive diesel energy is also required for propulsion as high transient translational forces acts on the wheel loader during bucketfill. When bucketfill is completed, the slope of the diesel energy is levelled out. The wheel loader reverses from the pile with a Drive, the Drive SoC characteristic can be observed once again. It can also be noted that more diesel energy is required for this Drive, due to less propulsive torque available from the SHHS and the wheel loader's mass has increased several tonnes by filling the bucket. A Direction Change is then made which enables recuperation of kinetic energy. The diesel energy curve is almost horizontal during the direction change (low fuel consumption). Another Drive is made. Then, the operator press the brake and accelerator pedal at the same time to brake the wheel loader before the hauler while providing sufficient power flow to the work hydraulics. Diesel energy is recuperated into hydraulic energy during the braking. When the wheel loader reaches zero kinetic energy, SoC is at its maximum level. By unloading the bucket, the load's mass no longer affect the wheel loader. A Drive is once again made to reverse from the hauler, the same SoC characteristic as for the previous Drives can be observed. Another Direction Change is made to approach the pile. During this Direction Change, some energy is dissipated through the PRV as SoC is already maximum. One last Drive is then made before the wheel loader has completed the cycle. The slight decrease in SoC that can be observed when SoC is high is due thermodynamic losses in the accumulators, captured by the BWR equations.

## 6.2 Direction Change

In Figure 6.2 simulated results of the Direction Change state can be seen. The figure displays the functionality of the state for both the Parallel and Series configuration.

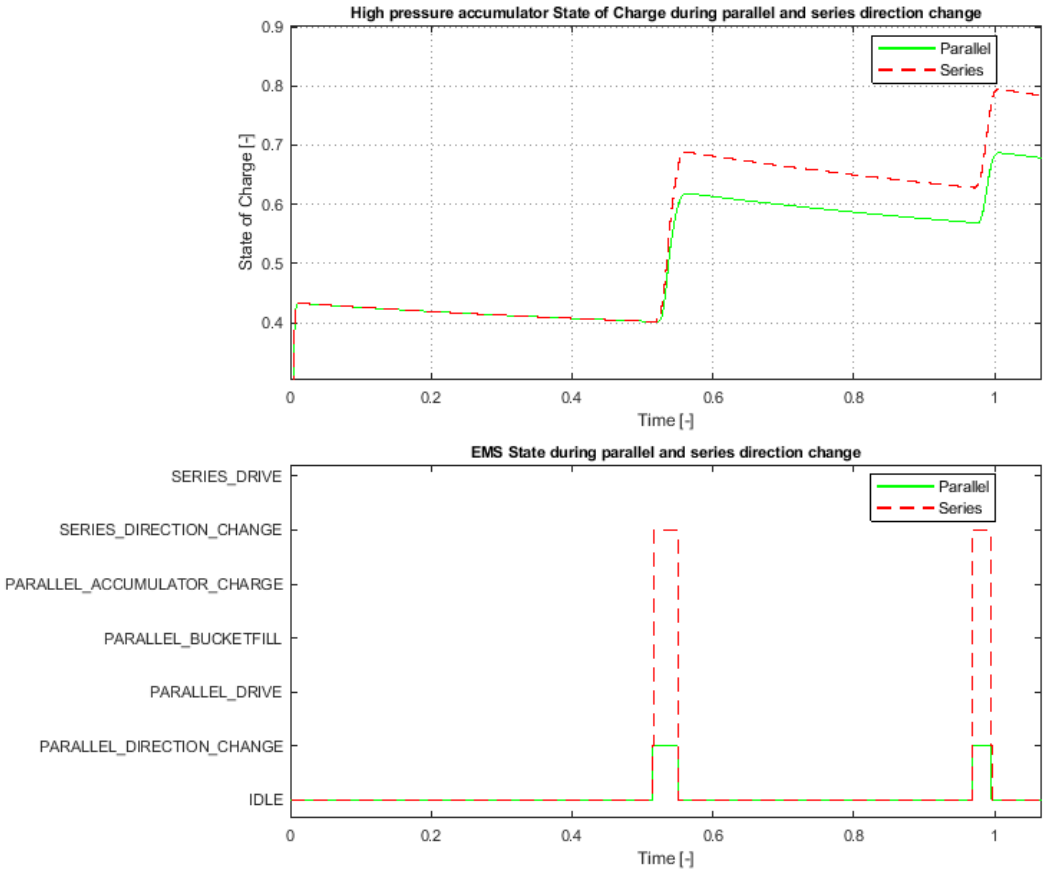


Figure 6.2: Simulated result of the Direction Change state for both Parallel and Series configuration.

As the Direction Change state is engaged, SoC in the high pressure accumulator increase. It can be observed that there is a difference in final SoC between Parallel and Series hybrid operation. If Series hybrid operation is used, SoC increases an additional ∼0.07 SoC units during the first direction change and ∼0.11 units during second compared to the Parallel configuration. This means that more energy is stored in the accumulator with Series Direction Change. However, as Machine 2 utilizes power from the ICE the extra increase in SoC for the Series configuration is diesel energy and not recuperated energy. Hence the Series Direction Change state will lead to a higher SoC but also slightly higher fuel consumption.

## 6.3 Drive

In Figure 6.3 simulated results of the Drive state can be seen. The figure displays the functionality of the state for both the Parallel and Series configuration.

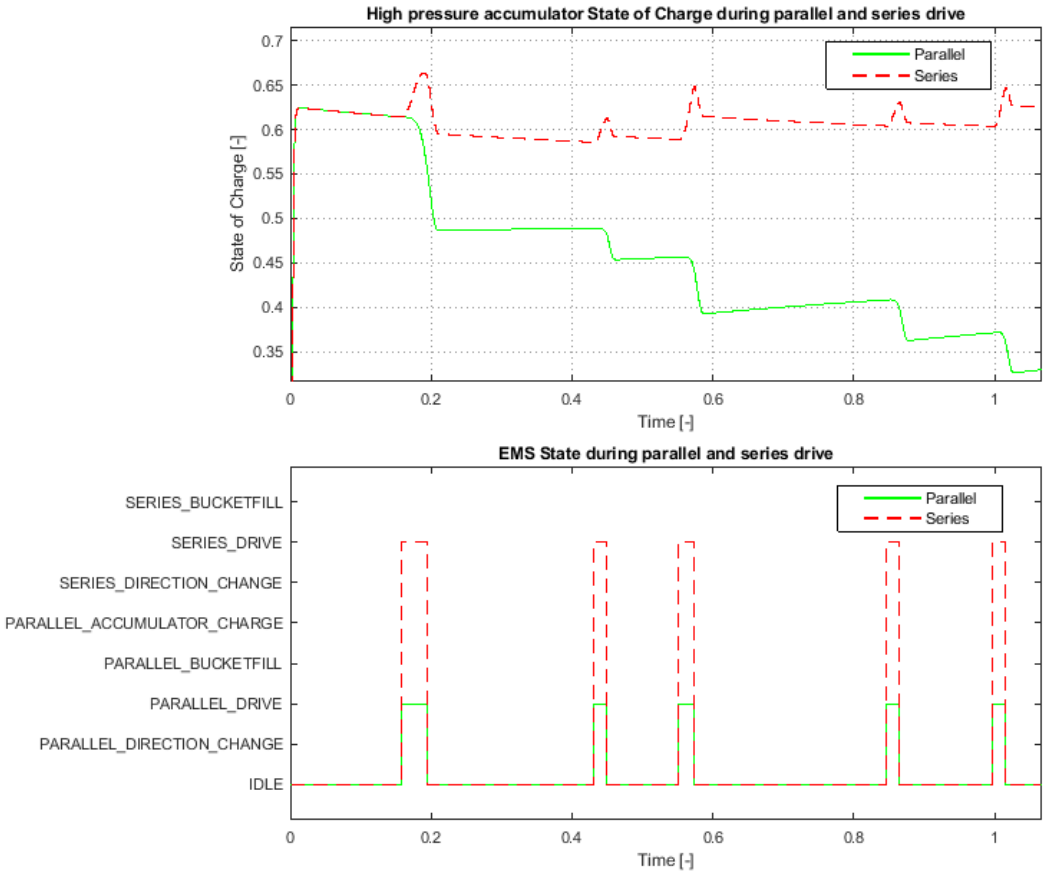


Figure 6.3: Simulated result of the Drive state for both Parallel and Series configuration.

Differences between Parallel and Series hybrid operation can be observed. For the Series configuration the SoC after the drive is approximately the same as before the Drive. The SoC also has a peak characteristic. In the start of the Drive, a small increase in SoC can be observed. This indicates that Machine 2 delivers more flow than Machine 1 can consume. At the peak, the delivered flow from Machine 2 is the same as the consumed for Machine 1. After the peak the SoC starts to decrease, this indicates that Machine 1 consumes more flow than Machine 2 can deliver which leads to oil from the accumulator has to be utilized to satisfy Machine 1's flow demand. For the Parallel Drive, a decrease in SoC always occur. The depletion for the Parallel configuration in the Drive state is between $\sim$0.04 to $\sim$0.13 SoC units. It can be observed that length of the Drive affects the depletion, a longer Drive results in a higher degree of depletion.

## 6.4 Bucketfill

In Figure 6.4 simulated results of the Bucketfill state can be seen. The figure displays the functionality of the state for Parallel, Series and Combined configuration. ∼0.8 is set as initial SoC value for all configurations.

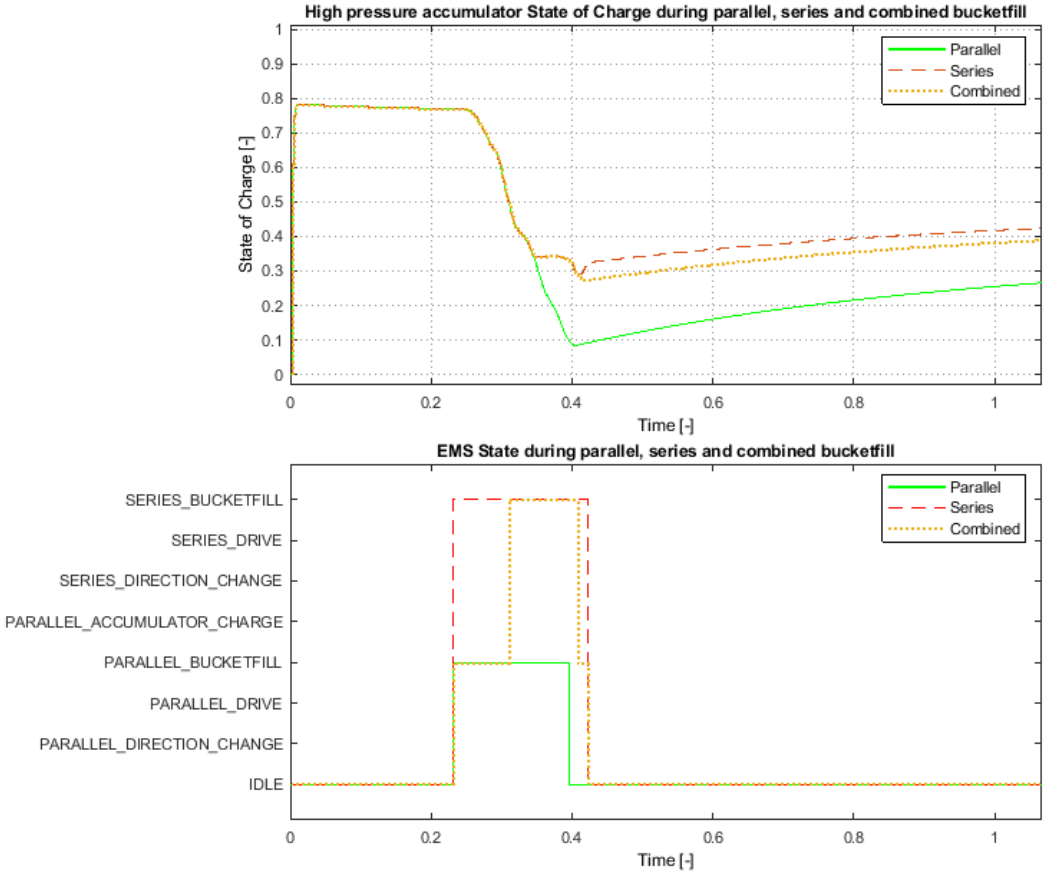


Figure 6.4: Simulated result of the Bucketfill state with an initial SoC of ∼0.8 for Parallel, Series and Combined configuration.

All configurations enter Bucketfill at the same time, the Parallel and Combined configuration enter Parallel Bucketfill state and Series configuration enter the Series Bucketfill state. When Bucketfill is engaged SoC starts to decrease in the same rate for all configurations. It can be observed that the final SoC is ∼0.1 for Parallel operation and ∼0.3 for the Series and Combined configuration. The Parallel configuration exits the Bucketfill state due to low SoC while Series and Combined configuration continue operation using Series Bucketfill state.

For the Series configuration, Machine 2 engage Series Bucketfill state immediately when Bucketfill is triggered. However, as the reference pressure for Machine 2 is set to a value corresponding to 0.35 in SoC Machine 2 will not be able to deliver any flow while the SoC is above that value. Hence, Series and Combined configuration has the same SoC characteristic. Another observation is that the Combined configuration switches to the Series Bucketfill state when the criteria for Series Bucketfill is fullfilled, $\varepsilon_{m1} \geq \varepsilon_{series}$. Series Bucketfill is active until the criteria is no longer fulfilled, $\varepsilon_{m1} < \varepsilon_{series}$, see Figure 6.5 and recall Equation 5.36 for calculation of $\varepsilon_{series}$. The result is that the combined configuration's final SoC is slightly lower than pure Series configuration for which the criteria is not used.

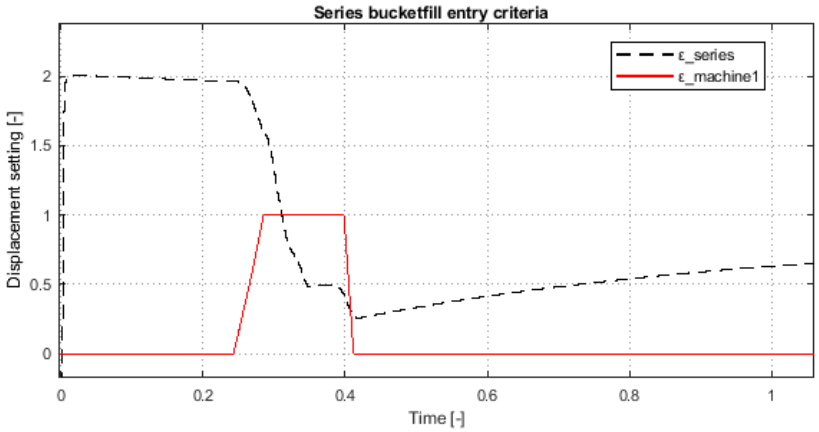


Figure 6.5: Series Bucketfill entry criteria, $\varepsilon_{series}$ is the entry criteria to engage in Series Bucketfill. Series Bucketfill is allowed when $\varepsilon_{m1} \geq \varepsilon_{series}$, recall Equation 5.36.

In Figure 6.6 another simulated result of the Bucketfill state can be seen, now with an initial SoC of ∼0.5. The length of the bucketfill is exactly the same as for the simulation in Figure 6.4. By comparing the simulations, one difference that can be observed is that the Parallel configuration is active for a shorter period of time when ∼0.5 is set as initial SoC. Another difference is that the Combined configuration switch to the Series Bucketfill state faster than in the simulation with ∼0.8 as initial SoC due to that the criteria for Series Bucketfill is fulfilled earlier. It can be seen that when the threshold is reached, the SoC characteristics of the Series and Combined configuration are the same as for the simulation with ∼0.8 as initial SoC.

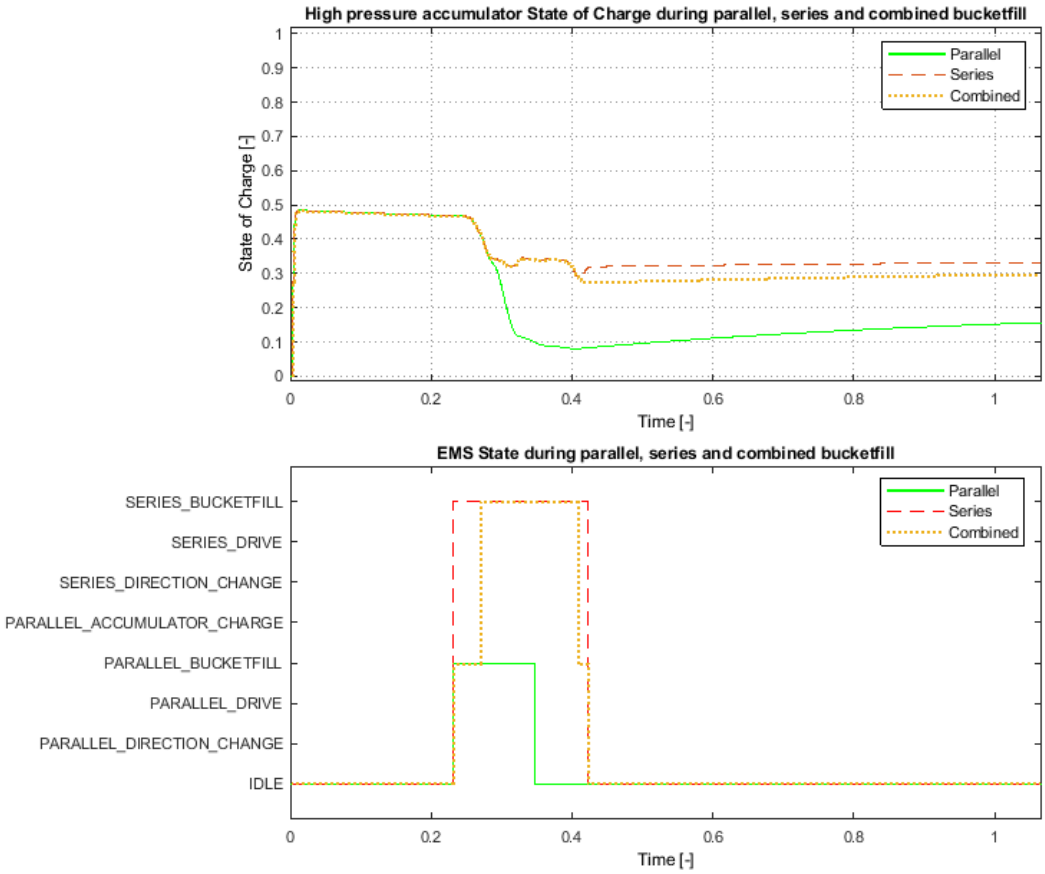


Figure 6.6: Simulated result of the Bucketfill state with an initial SoC of 0.5 for Parallel, Series and Combined configuration.

## 6.5 Brake

In Figure 6.7 simulated results of the Hybrid Brake can be seen. Vehicle velocity is also plotted.

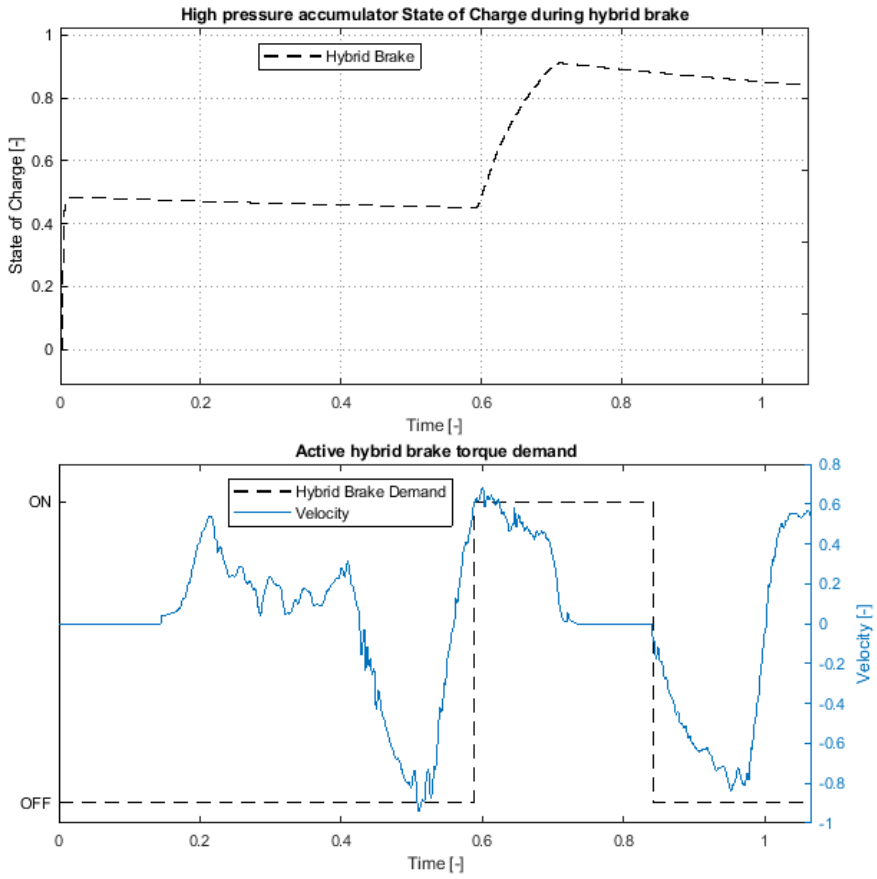


Figure 6.7: Simulated result of the Hybrid Brake, vehicle velocity is also plotted.

It can be seen that the SoC increases from ∼0.5 to ∼0.9 during the brake state which occur when the wheel loader approaches the hauler. SoC increases while the vehicle velocity is still above zero. When the wheel loader reaches stand still SoC cease to increase even though the Hybrid Brake is still active. The reason being that the wheel loader's kinetic energy is 0, i.e Machine 1's speed, $n_C$, is 0. Thus no flow can be delivered from Machine 1.

## 6.6 Direction Change to Drive in sequence

Drive is often used after a Direction Change which is why it is of interest to study the behaviour when these states occur in immediate sequence. After a Direction Change the displacement setting of Machine 1 is 1, therefore no ramp of $\varepsilon_{m1}$ is required. Maximum propulsive torque for the current pressure level can therefore be exerted by Machine 1 immediately. Simulation results from each of the four possible combinations of Direction Change to Drive can be seen in Figure 6.8. An initial SoC of ∼0.43 is set for all configurations.

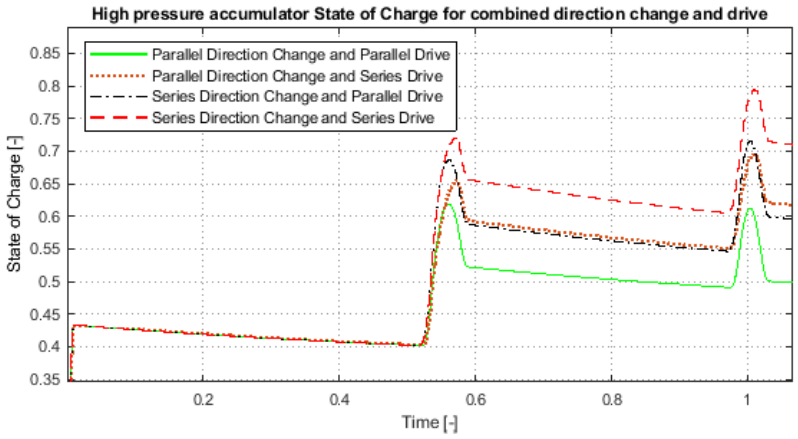


Figure 6.8: Simulated result of Direction Change to Drive in sequence for the four possible sequential combinations.

It can be observed that the slope of both Series Direction Change combinations increase in the same rate, the difference between the two combinations occurs when the Drive state is engaged. The configuration which engages Parallel Drive has lower amplitude of the SoC peak and a lower final SoC compared to the configuration which engages in Series Drive. This is due that no flow is delivered by Machine 2 using the Parallel drive. The same characteristic can be observed for both the Parallel Direction Change combinations. The rate of SoC increase is the same for both configurations but the configuration which engages Parallel Drive has lower amplitude of the SoC peak and a lower final SoC compared to the configuration which engages in Series Drive. Moreover, it can be observed that the combination Parallel Direction Change to Series Drive and Series Direction Change to Parallel Drive reach approximately the same final SoC value, Parallel Direction Change to Series Drive has slightly higher. Another observation is that there is approximately a gap of ∼0.14 SoC units between the two extremes, Parallel Direction Change to Parallel Drive and Series Direction Change to Series Drive. The combinations Parallel Direction Change to Series Drive and Series Direction Change to Parallel drive final SoC is placed in the middle between the two extremes with a difference of ∼0.07 SoC to each extreme.

## 6.7 Power flows and efficiencies

Power flows and efficiencies are affected by the SHHS, which will be exemplified and stated in this section. The results will be clarified by studying one full Series bucketfill without stored energy. Energy losses during hybrid operations, hence during Bucketfill and Drives, over the course of one SLC will then be presented.

In Figure 6.9 simulated results of a Series Bucketfill can be seen. ∼0.2 in SoC is set as initial value of the Bucketfill.

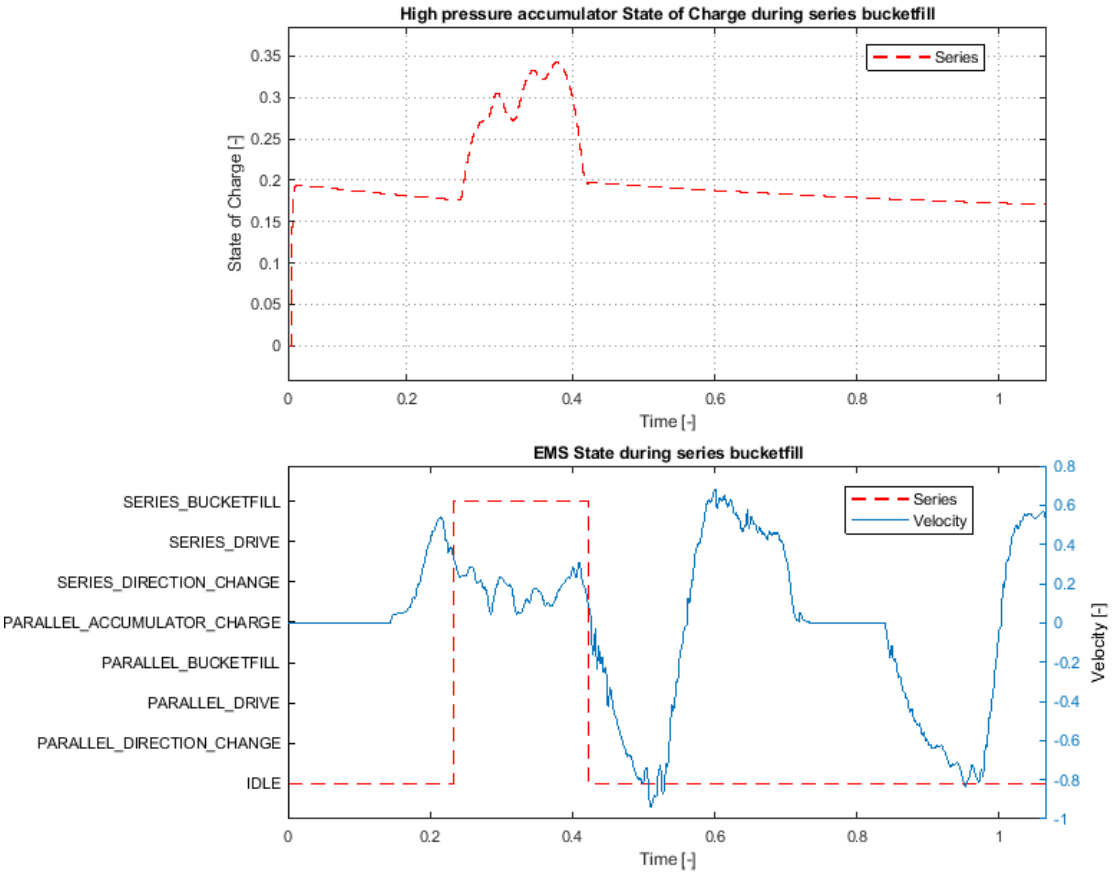


Figure 6.9: Simulated result of the Bucketfill state with an initial SoC of ∼0.2, i.e there is no recuperated energy.

When Bucketfill state is engaged, the reference pressure for Machine 2 is set to a value corresponding to 0.35 in SoC. It can be seen that the SoC increases from the start of the state, hence the flow delivered from Machine 2 is greater than Machine 1's consumed flow. The oscillations in SoC are caused by variations of the vehicle velocity as Machine 1's output axle is mechanically linked to the wheels. Variations in vehicle velocity is proportional to $n_C$ which is proportional to the flow consumed by Machine 1. In this case, vehicle speed increases towards the end of the bucketfill which results in a final SoC value which is slightly higher than the initial SoC.

A comparison of efficiencies for the TC and the hybrid loop during bucketfill is presented in Figure 6.10. Three efficiency plots can be seen, one for the conventional driveline

where only TC efficiency is present and two for the Series configuration where both TC and hybrid efficiencies are present.

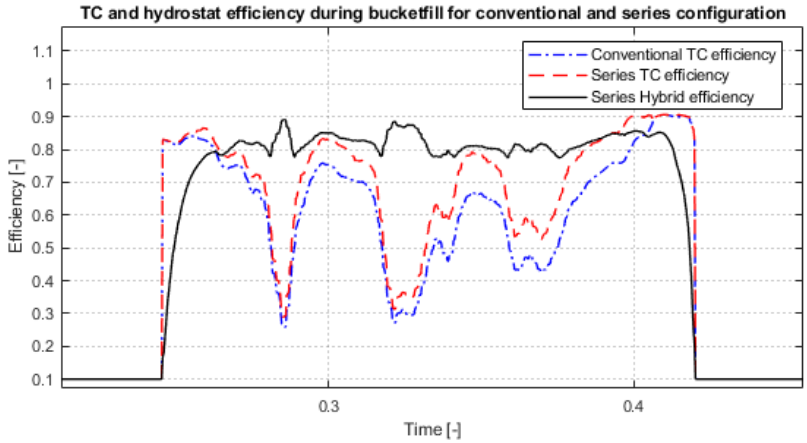


Figure 6.10: Simulated result of the TCs and the hybrids's efficiency for a bucketfill with an initial SoC of ∼0.2.

It can be observed that the hybrid's efficiency is significantly better than the TC's efficiency for most part of the Bucketfill except during the start and end of the bucketfill. The reason for occasionally low hybrid efficiency is the displacement setting being ramped up-/down to obtain a smooth transition between conventional and hybrid propulsion. Moreover, it can be seen that the TC's efficiency is slightly higher using the Series configuration compared to the Conventional driveline for most part of the bucketfill. Hence, the total efficiency of the driveline with the SHHS is higher compared to the Conventional driveline. To gain an better understanding of how the increased efficiency obtained with the SHHS affects the wheel loaders energy efficiency it is of interest to study the power input and power losses for the TC and the SHHS.

In Figure 6.11 normalized input power during bucketfill for Conventional and Series configuration can be seen. TC input power is significantly lower for the Series configuration compared to the Conventional configuration. The SHHS's input power is dependent on the size of Machine 2, which is about half of the TC's input power for the studied case. It can be observed that the total input power is slightly lower for the Series configuration for the most part of the bucketfill phase.

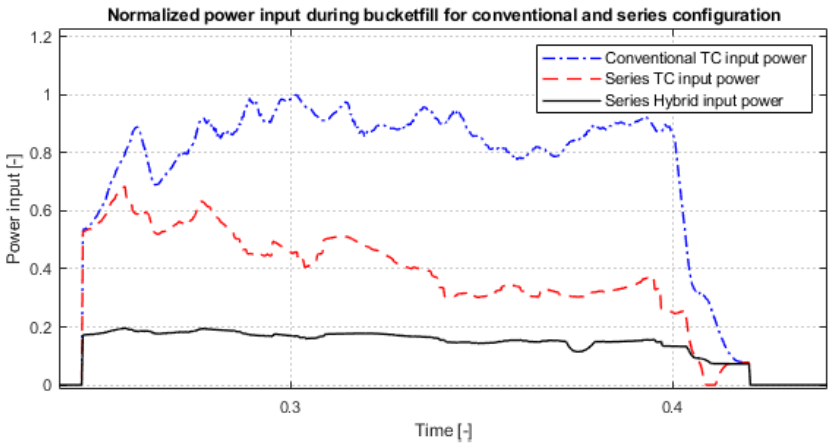


Figure 6.11: Simulated result of the TCs and the hybrid's normalized input power for a Bucketfill with an initial SoC of ∼0.2.

By multiplying input power presented in Figure 6.11 by the corresponding efficiencies presented in Figure 6.10, power losses for each power path is obtained, see Figure 6.12.

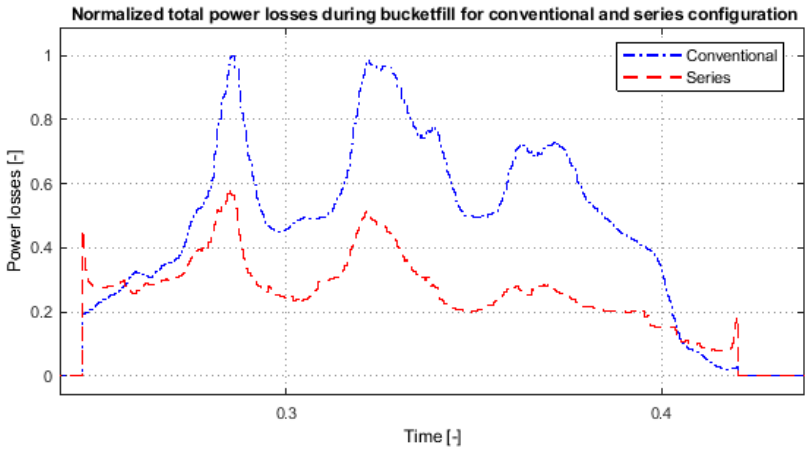


Figure 6.12: Simulated result of the TC's and the hybrid's normalized power losses for a bucketfill with an initial SoC of ∼0.2.

It can be observed that the power losses through the driveline are significantly lower for the Series configuration compared to the Conventional configuration. This result is a consequence of the redirected power flow through the SHHS, bypassing the TC. As the SHHS has superior efficiency compared to the TC, power losses will be lower and thus energy efficiency will increase.

In Figure 6.13 accumulated energy losses during Bucketfill and Drive for the Conventional driveline compared to the SHHS driveline over the course of one SLC can be seen. The bar graph is divided into three sections, one for the Bucketfill state, one for the Drive states and one for the total accumulated losses of these two states. The Conventional configuration is represented by the bars to the left and the Series configuration is represented by the bars to the right for each specific state.

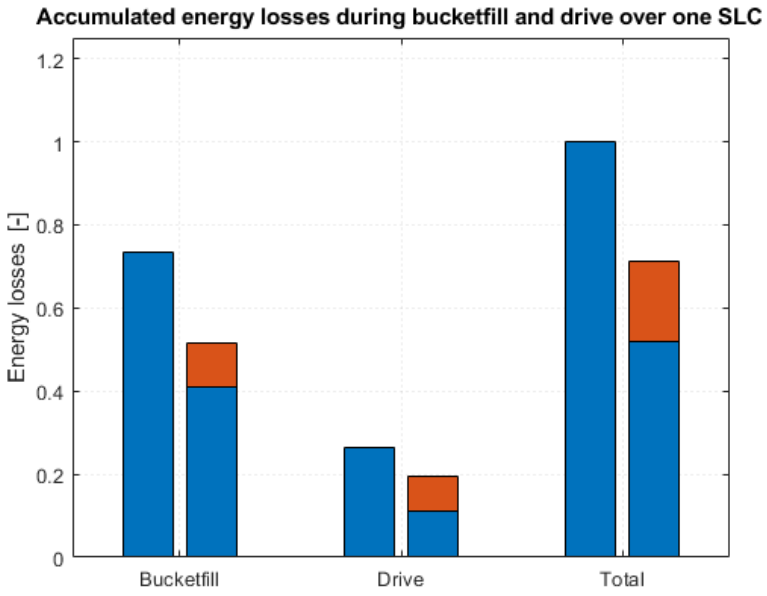


Figure 6.13: Accumulated energy losses for the Conventional configuration (bars to the left) and the SHHS driveline (bars to the right) for one SLC with an initial SoC of ∼0.8.

It can be observed that the total accumulated energy losses are approximately 30 % lower for the Series configuration compared to the Conventional configuration. For the Bucketfill state the accumulated energy losses are approximately 22 % lower for the Series configuration, for the Drive state the accumulated energy losses are approximately 8 % lower.

## 6.8 Energy efficiency

How the SHHS driveline compares to the Conventional driveline in terms of total energy losses and thus energy efficiency is a key interest of this study. Therefore, a simulation of two SLCs in sequence for each configuration is conducted and the energy losses is measured.

### 6.8.1 With accumulators

In Figure 6.14 SoC and EMS state for the three hybrid configurations; Parallel, Series and Combined can be seen. ∼0.8 in SoC is set as initial value for all configurations. For the Parallel and Combined configurations Parallel Direction Change is used since its charge is considered sufficient. Series Direction Change results in abundant SoC and wasted energy in the context of full SLCs, which moreover constitutes the reason for Parallel Direction Change being considered redundant for the Combined configuration and thus not used.

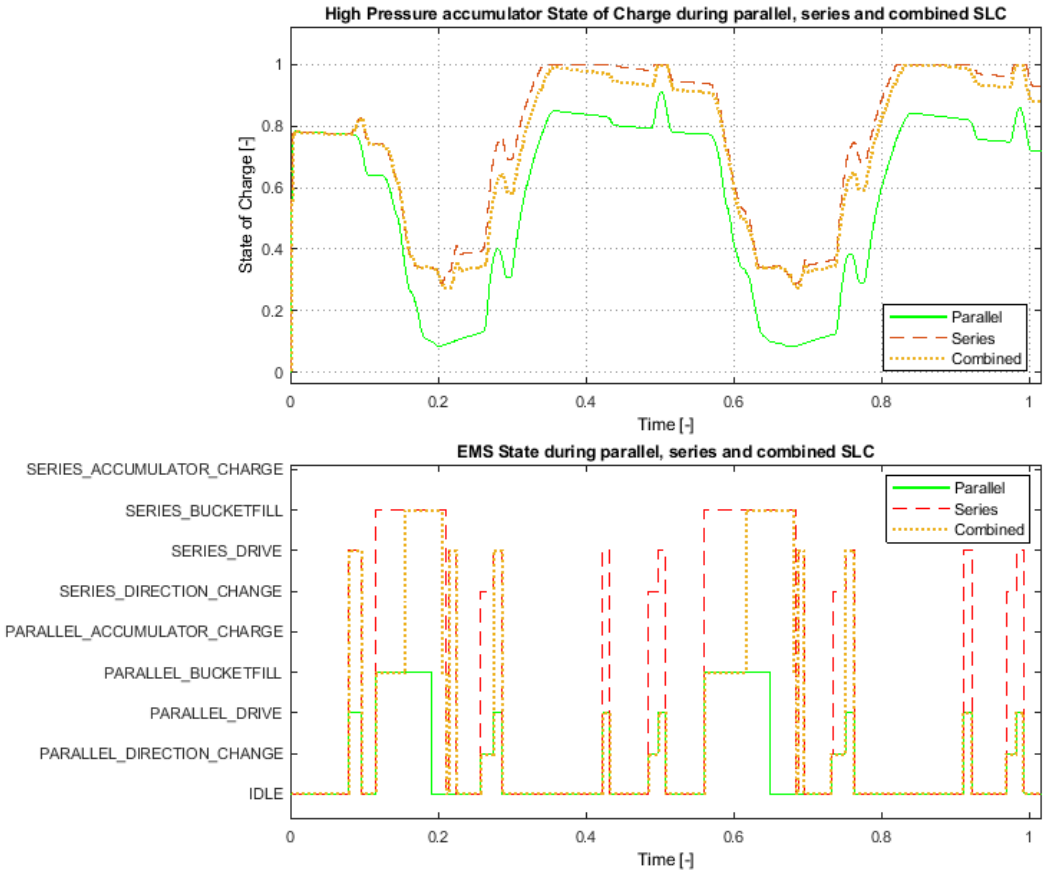


Figure 6.14: Simulated result of SoC and EMS state over the course of two SLC:s with an initial SoC of ∼0.8 for Parallel, Series and Combined configurations.

Energy losses when using the Conventional configuration serves as a benchmark for evaluating the hybrid configurations. The hybrid configurations all perform relatively equal, Combined configuration performs best, then Series and lastly Parallel configuration. Based on the results obtained in Figure 6.15, a comparison of energy losses in relative numbers between the Conventional and the hybrid configurations can be seen in Table 6.1.

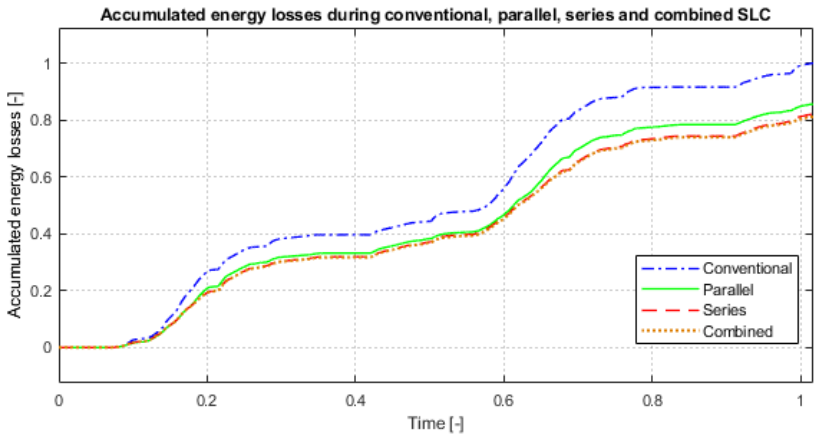


Figure 6.15: Simulated result of the accumulated energy losses over the course of two SLCs with an initial SoC of ∼0.8 for Parallel, Series and Combined configurations.

Table 6.1: Energy efficiency for two SLCs, with Conventional as reference

| Configuration | Improved energy efficiency [%] |
|---|---|
| Conventional | 0 |
| Parallel | 14.35 |
| Series | 17.96 |
| Combined | 18.82 |

### 6.8.2 Without accumulators

It has been presented how the wheel loader performs in terms of energy efficiency when adding the SHHS to the Conventional driveline. Included in the scope is also to investigate how the size of the accumulator affects the energy efficiency. This is performed by decreasing the accumulator size to a size sufficient for only adding capacitance to the system i.e no energy recuperation is possible.. Figure 6.16 presents the accumulated energy losses over the course of two full SLCs. Table 6.2 presents the energy efficiency improvement for the Series configuration without accumulators compared to the Conventional configuration.

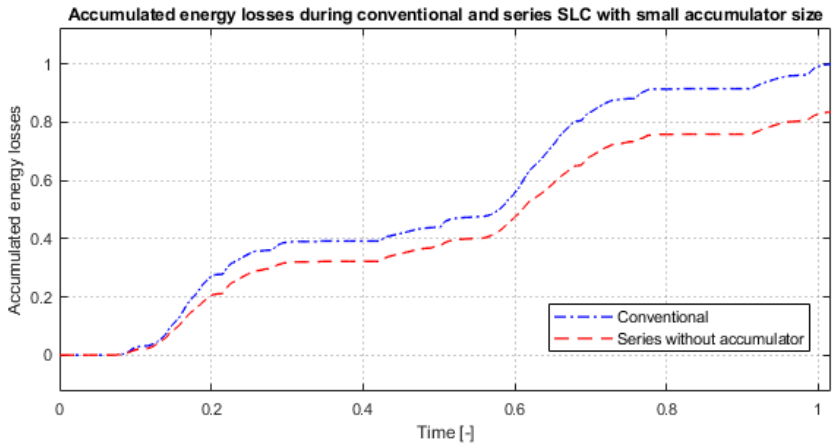


Figure 6.16: Simulated result of the accumulated fuel consumption over the course of two SLCs for the Conventional and Series without accumulator configuration.

Table 6.2: Energy efficiency for two SLCs using no energy storage, with Conventional as reference

| Configuration | Improved energy efficiency [%] |
|---|---|
| Conventional | 0 |
| Series without accumulator | 16.40 |

# 7 Discussion

The simulated results shows functionalities which correlate with the intended outcome of each operation mode. Direction Changes increase the high pressure accumulator SoC as kinetic energy is converted into hydraulic energy and stored for later usage. Even higher SoC is obtained when diesel energy is simultaneously converted into hydraulic energy. Drive convert hydraulic energy into kinetic energy, hence discharging the accumulator as long as diesel energy is not provided, which is the case for the Parallel configuration. As much recuperated kinetic energy as possible is utilized to assist during Bucketfills and when the stored energy is depleted, additional diesel energy is provided. Lastly, excessive diesel energy, necessary for the work hydraulics, is recuperated by braking with the hybrid system as it approaches the hauler and thus charging the accumulators.

The SHHS evaluated over two complete short loading cycles indicates significant energy savings in the driveline where the Combined configuration shows the best improvement, as expected. A cycle utilizing the Combined configuration will only allow Machine 2 to contribute at selected operating points to avoid unnecessary usage, for example when the SoC is high or when the accumulator pressure is above Machine 2's maximum pressure. Only utilizing the Series configuration allows this type of unnecessary usage, hence higher energy losses for the Series configuration compared to Combined configuration. Another reason may also be that Series Direction Change state considered redundant for the Combined configuration since more than enough kinetic energy can be recuperated through braking during a SLC. Which is also the reason for excluding Series Direction Change from the Combined configuration. Other type of drive cycles such as the *Load and Carry* cycle may however benefit from Series Direction Change regardless since longer accelerations to higher velocities are conducted.

Not only does the Combined configuration result in a better energy efficiency compared to the Parallel configuration but it also finish the cycles with higher SoC. Which consequently results in the Combined configuration possessing more stored energy in forms of diesel and hydraulic energy. Likewise does the Series configuration. The difference in SoC should therefore also be taken into account when considering energy efficiency improvements. However, the difference between the Combined and Series configurations are not as significant as the comparison with the Parallel configuration since both configurations reaches maximum SoC during braking.

Given the fact that energy efficiency is improved while assuring high SoC at the end of each drive cycle makes the Combined configuration pre-eminent. Judging from the Bucketfill results the Combined configuration, and the Series configuration for that matter, also entails a more redundant system. Bucketfills with low starting SoC will benefit from the Series configuration. While the Parallel configuration will inevitable be forced to supply power through the TC, the Combined and Series configurations are able to further reduce the dependency of the TC by bypassing it. This provides a rather forgiving hybrid system from which many operators, independent of skill level, should be able to draw benefits from.

The results from the simulation with no accumulators gives clarity in how much the hydraulic energy storage actually contribute to the energy efficiency. The results indicate some beneficial gains with an energy storage. As previously explained, kinetic energy can be recuperated and used at later occasions which will lower the overall fuel consumption. However, the relatively small difference in energy efficiency improvements between the configurations indicate that larger benefits come from bypassing the TC and thus avoiding operating points with bad efficiency. The Bucketfill power flow results show that the input power of the hybrid system is less than half of the TC input power. Which in turn indicates that power losses could be further decreased if additional power could be redirected through the hybrid system. It could therefore be of interest to investigate if the size of Machine 1 and Machine 2 could be increased. Utilizing a hybrid system with smaller accumulators would also imply a smaller investment cost. Moreover, potential issues with mounting space and increased weight with large accumulators would be simplified.

## 7.1 Control system

The EMS decides at which occasions and with what configuration the hybrid system should be utilized. Along with the hydraulic machine and accumulator dimensions, the EMS lay the foundation for potential energy savings. The control systems architecture is found to have a negligible impact on energy efficiency since the sample time can be set to fractions of a second. Consequently the control system itself will only cause delay equal to a couple of milliseconds from the moment a state is engaged until torque is realized. Other type of EMS would however most probably show further improvements in energy efficiency compared to the rule-based EMS. Dynamic programming, for example, would provide the possibility to find optimal reference pressure levels for Machine 2. Moreover, the Combined configuration could be analysed to find the optimal usage of the hybrid configurations, i.e when charging/discharging should occur as well as when Series configuration should be engaged or disengaged. Since optimal controllers such as Dynamic programming can't practically be used in online applications sub-optimal controllers such as Equivalent-Consumption Minimization Strategy may be a viable choice. It is however hard to predict if ECMS can achieve further energy efficiency improvements compared to the rule-based EMS in this application. Mainly due to previous studies concluding a simple rule-based strategy to be robust and adequate in a hydraulic hybrid wheel loader.

## 7.2 Simulation model

Although simulations indicate improved energy efficiency other relevant aspects are difficult to capture with the backward-facing simulation approach. Aspects such as reduced brake wear due to hybrid braking, reduced cooling fan power due to lower power losses and partly reduced transmission wear due to a lower degree of usage can not be evaluated with the conducted simulations. Yet, they are important to consider when evaluating the hybrid system as a whole. Also, productivity is one crucial aspect to consider but difficult to simulate with backward facing simulation. All of these aspects emphasize on the importance of evaluating the concept with machine tests.

Charges and discharges of the accumulator is basically ingoing and outgoing flows of power. Under the assumption that the drive cycle is accurate regarding velocities and traction forces, validation of the results is made easy, especially for the Parallel configuration case. The mechanical connection between the SHHS and the wheels conducts no uncertainties regarding flow of power for the Parallel configuration, as long as losses are correctly accounted for. However, the Series configuration has no mechanical connection to the wheels, therefore another degree of freedom is obtained in the simulation, namely the ICE rotational speed. Which in turn may leave uncertainties regarding simulation results. Power provided by the Series configuration is for the most part exclusively dependent on the drivers behaviour due to the mechanical connection between Machine 2 and the ICE and thus the accelerator pedal. ICE rotational speed, in the case of backward simulation, is rather a consequence of actual wheel loader velocity and traction force instead of accelerator pedal position, which directly affect the power provided by Machine 2. Consequences that this entail is uncertainties in the power provided by Machine 2. However, the simulation approach may be more favourable in terms of energy efficiency as backward simulation calculates only what is necessary for the ICE to provide rather then providing what is demanded by a driver. Hence the most dubious part of the results is the behaviour of a driver, which is not captured when backward simulation is utilized.

Specific improvements that can be made on the simulation model regards Machine 2. No dynamics are implemented for Machine 2 causing it to provide power instantaneous after the reference pressure is set. Behaviours such as response time as well as pressurizing the small volume between Machine 2 and Valve 5 should be captured for a more accurate simulation result. Both the response time and the pressurizing is however only a matter of tenths and should not affect the overall outcome of the results.

## 7.3 Hydraulic hybrid concept

The power through the hybrid system, i.e the power that is bypassed the TC is relatively low but shows great potential in lowering the overall energy losses and thus reducing fuel consumption. Machine 1 is absolute determiner of the magnitude of power that can be exerted by the hybrid system. While Machine 2 is absolute determiner of the input power to the hybrid system. Hence, the machines are highly dependent on each other as Machine 1 can not output more power than Machine 2 can input. Thus, to increase the overall transmitted power through the hybrid system both machines should be increased in size. Or, as issued previously, the overall pressure could be increased, but at the cost of efficiency. An interesting concept would be to increase the size of the hybrid system to a point where all propulsive power is allowed to bypass the TC. Such a concept would even allow the TC to be removed completely from the driveline. The TC can instead be replaced with a clutch mechanically connecting the shafts at operating points when the hydraulic pump and motor are running at the same rotational speeds. The functionality would show similarities to TC lock-up. Advantages of such a system would be good efficiency when high power demands occur, such as during bucketfill and accelerations. Similar efficiencies during constant speeds would also be achieved. A challenge that might occur when implementing such a system is to control the hybrid system so that acceptable operability is maintained.

The speed limitation of the ICE would also need research before implemented on a real machine application. As explained, when backward simulating the engine speed will not increase more than necessary and rarely reach levels above the engine speed limitation, causing the limitation to be redundant in the simulations. In a real machine application however, the driver determines the engine speed by the accelerator pedal, hence allowing higher engine speeds than necessary and thus causing the limitation to be a vital part of the control system. The engine speed is always limited determined by how much hybrid torque is available and provided. However, a lower saturation for the limitation is always present to secure the functionality of the work hydraulics. In practice this will at some occasions conclude in an increase of output power which may or may not be favourable. From an operability point of view it may be found pleasant with a higher acceleration and the productivity could increase, it may however shorten the life time of the machine due to higher strains on each cycle. To overcome this issue limitations should be done in steps of two. First limiting the engine speed and then, if necessary, limiting the hybrid torque. Another, more extensive solution, could be downsizing the engine to a size sufficient for providing work hydraulics with enough engine speed and power without increasing the output power of the driveline.

Previous research has shown large deviations in energy efficiency between operators. Which also reasonably indicates that the hydraulic hybrid system performance is dependent on the operator's ability to utilize the system. This insight combined with the fact that the SLC is highly repetitive makes the hydraulic hybrid concept an interesting subject for automation and autonomous technology. With an autonomous hydraulic hybrid wheel loader, each state of the hybrid system could be used to its full potential to optimize energy efficiency as the uncertainty regarding operator ability can be neglected. Moreover, operability would not have to be considered. Hence Machine 1 could be controlled with a very high displacement setting rate, theoretically only limited by the dynamics of the machine itself. Thus, high efficiency would be achieved faster which in turn lead to increased energy efficiency.

## 7.4 Operability

Driver operability is of key importance when introducing supplementary propulsive systems to a conventional wheel loader design. The supplementary propulsive system must be implemented in a way that maintains the operability while still being superior compared to the prior driveline, often with regards to fuel consumption, energy efficiency or productivity. Generally, efficiencies for hydraulic machines are highly dependent on the displacement setting. Low displacement settings inflicts low efficiencies and are thus unfavourable. From the simulations, it can be observed that the hybrid system's efficiency do not always outperform the TC. In fact, intervals when the TC efficiency outweigh the hybrid system's efficiency are intervals for which driver operability are assured sufficient. Hence, displacing hydraulic machines to max at a high rate is favourable from an efficiency point of view. However, rapid displacement rate of hydraulic machines might inflict jerky behaviour of the wheel loader and conclude in an affected operability. Therefore it is always a trade-off between high efficiency and acceptable operability when controlling hydraulic hybrid vehicles in general. By this fact, the most efficient Drive is actually

obtained directly after a Direction Change. Both from an efficiency and an operability point of view since the relevant hydraulic machine at this point is already fully displaced. Another challenge is to obtain high predictability and operator feeling of the brake pedal as the magnitude of braking torque is dependent on the pressure level in the accumulator as well as displacement setting of the hydraulic machine.

# 8 Conclusion

The proposed hydraulic hybrid concept for wheel loaders with torque converters show promising results. The conducted simulations show that significant energy savings can be made by adding a supplementary hydraulic hybrid system to the conventional driveline. Moreover, the results indicate that stored energy in the accumulators have a rather small impact on the energy efficiency. Instead of increasing the size of the accumulators, more power should be redirected through the hybrid system as its efficiency is superior when the torque converter experience high slip. The backward facing simulation approach is sufficient for evaluation of the concepts in terms of energy efficiency but does not capture all dynamic behaviours or the drivers actions. To capture these aspects machine tests or forward facing simulations should be conducted. Additionally, downsizing of the combustion engine is made possible by adding a hydraulic hybrid system. Referring to the research questions addressed in Section 1, the following specific conclusions may be drawn:

**Q1:** Backward simulations over the course of a short loading cycle indicates energy savings of 14.4 % for the Parallel configuration, 18.0 % for the Series configuration and 18.8 % for the Combined configuration compared to the conventional driveline. Moreover, removing the accumulators show energy savings equal 16.4 % compared to the conventional driveline.

**Q2:** The operability of the wheel loader can be preserved by assuring smooth transitions between conventional and hybrid operation. Smooth transitions can be achieved by limiting the internal combustion engine's power output as well as controlling the rate of which displacement setting is changed for the hydraulic machine connected to the wheels. Moreover, regards to work hydraulic power demand must be taken into consideration when limiting the internal combustion engine's power output.

**Q3:** The EMS decides when the energy storage should be charged/discharged. Generally the energy storage should be charged whenever energy can be recuperated, hence during Directional Change and when approaching hauler. During Bucketfill the energy storage should be depleted of stored energy. State of charge in the energy storage should strive to be preserved during Drive, mainly to assure sufficient stored energy for Bucketfill. The best strategy for charging/discharging is the Combined configuration.

**Q4:** The control system architecture seen in Figure 5.23, based on a rule-based EMS, is found to be a suitable architecture for a hydraulic hybrid wheel loader.

# 9 Future work

To be able to draw further conclusions, machine tests should be conducted to evaluate operability and performance in field. Once conducted, further development of the engine speed limitation should be made to ensure an even output power. Such improvements should not limit the possibilities of downsizing the engine, which is also an interesting aspect to study. A larger leap towards fuel efficient wheel loaders would be smaller engines while assuring a maintained performance which could be feasible when utilizing the supplementary hydraulic hybrid system. Sufficient knowledge about hydrostatic transmission may even enable utilizing the current transmissions with the torque converter excluded.

To further explore the possibilities for hydraulic hybrid drivelines in wheel loaders another supplementary energy carrier such as electricity could be added. A beneficial synergy could be achieved by utilizing the advantages of each of the three energy carriers. Which theoretically could improve fuel economy for wheel loaders. However, a rather complex control system is required to realize such a hybrid system.

# References

[1] Achten, P. 2008. *A serial hydraulic hybrid drive train for off-road vehicles.* p. 1 51st, National conference on fluid power; 2008; Las Vegas, NV

[2] Rydberg, K. 2009. *Energy Efficient Hydraulic Hybrid Drives.* The 11th Scandinavian International Conference on Fluid Power, SICFP'09, June 2 − 4, 2009, Linköping, Sweden

[3] Guzzella, L., Sciarretta, A. 2013. *Vehicle Propulsion Systems.* ISBN: 9783642359125

[4] Uebel, K., Raduenz, H., Krus, P., de Negri, VJ. 2018. *Design Optimisation Strategies for a Hydraulic Hybrid Wheel Loader.* p. 1-3 Proceedings of the BATH/ASME 2018 Symposium on Fluid Power and Motion Control FPMC2018 September 12−14, 2018, Bath, UK

[5] Rohdin, M. Öijwall, S. 2015. *Development of Control Strategies for a Hydraulic Hybrid Wheel Loader - with a focus on energy efficiency.* ISRN: LIU-IEI-TEK-A- -16/02529- -SE

[6] Nationalencyklopedin. 2019. *hjullastare (wheel loaders).* `http://www.ne.se.e.bibl.liu.se/uppslagsverk/encyklopedi/lång/hjullastare`

[7] Volvo Construction Equipment, 2018, *L60H, L70H, L90H Volvo Wheel loaders*

[8] Frank, B. 2018. *On Optimal Control for Concept Evaluation and System Development in Construction Machines.* ISBN: 978-91-88934-91-8 or 978-91-88934-90-1

[9] Harishbabu, B. Rajesh Kumar, P. Prabu, P. Thiruselvan, Mg. 2014. *Design Optimisation of Counter Weight of Front End Loader Through Dynamic Mass Balancing.* International Journal of Engineering Research & Technology (IJERT)

[10] Singh, S. 2006. *Factors affecting the productivity of loaders in surface mines.* International Journal of Mining Reclamation and Environment, March 2006

[11] VanGelder, K. 2014. *Fundamentals of Automotive Maintenance and Light Repair.* Jones & Bartlett Learning

[12] Gordon, J. 2006. *Beyond Fluid Couplings Torque Converters.* Motor Age

[13] Uebel, K. 2017. *Conceptual Design of Complex Hydromechanical Transmissions.* ISBN 978-91-7685-447-1

[14] Thai do, Hoang. 2018. *Energy Management of Parallel Hydraulic Hybrid Wheel Loader.* URN:urn:nbn:se:kth:diva-246097 OAI: oai:DiVA.org:kth-246097 DiVA, id: diva2:1295780

[15] Volvo Construction Equipment, 2010, *Optishift for L150F, L180F and L220F*

[16] Nezhadali, V. Eriksson, L 2013. *Optimal Control of Wheel Loader Operation in the Short Loading Cycle Using Two Braking Alternatives.* 2013 IEEE Vehicle Power and Propulsion Conference (VPPC)

[17] Chapple, Peter. 2014 *Principles of Hydraulic Systems Design.* ISBN-13: 978-1606504529 ISBN-10: 1606504525

[18] Larsson, L V. 2017. *Control Aspects of Complex Hydromechanical Transmissions.* ISBN: 978-91-7685-483-9

[19] Baseley, S. Ehret. C, Greif, E. Kliffken, M.G. 2014. *Hydraulic Hybrid Systems for Commercial Vehicles.* SAE 2007 Commercial Vehicle Engineering Congress & Exhibition

[20] Pettersson, K. Heybroek, K. 2015. *Hydrauliskt Hybridsystem för Anläggningsmaskiner - Delat Energilager är Dubbelt Energilager.* Hydraulikdagarna, Linköping, Sverige, 16 – 17 mars 2015

[21] Ericson, L., Rydberg, K-E. 2016. *Basic fluid power, components and systems.* ISBN: 9789177735489

[22] Department of Management and Engineering, Linköping University. 2016. *Formula Book for Hydraulics and Pneumatics.* LiTH

[23] Trinkel, B. 2007. *Fluid Power Basics.* `https://www.hydraulicspneumatics.com/fluid-power-ebook-edition-1/chapter-1-fundamentals-fluid-power`

[24] Larsson, L V., Larsson K V. 2014. *Simulation and Testing of Energy Efficient Hydromechanical Drivelines for Construction Machinery.* ISRN: LIU-IEI-TEK-A- -14/01882- -SE

[25] B. Armstrong, C.C. de Wit, 1995. *Friction Modeling and Compensation.* The Control Handbook. Editor Williams S. Levine, pp. 1369 – 1382, CRC Press and IEEE Press, 1996.

[26] Mathworks. 2007. *Translational Friction.* `https://se.mathworks.com/help/physmod/simscape/ref/translationalfriction.html#bqkz188-1`

[27] Thoma, J.U. 1990. *Simulation by bondgraphs – Introduction to a Graphical Method.* ISBN 978-3-642-83922-1

[28] Wu, B. Lin, C. Filipi, H, Assansis, D. 2004. *Optimal Power Management for a Hydraulic Hybrid Delivery Truck.* Vehicle System Dynamics Vol. 42, Nos 1 – 2, p.23 – 40

[29] Bellman, R. 1954. *The Theory of Dynamic Programming.* Bull. Amer. Math. Soc., Volume 60, Number 6 (1954), 503 – 515.

[30] Bertsekas, D.P. 1995. *Dynamic Programming and Optimal Control.* Athena scientific Belmont

[31] Musardo, C. Rizzoni, G. Guezennec, Y. Staccia, B. 2005. *A-ECMS: An Adaptive Algorithm for Hybrid Electric Vehicle Energy Management.* European Journal of Control, Volume 11, Issues 4 – 5, 2005, Pages 509 – 524

[32] Liermann, Matthias, 2012, *Backward simulation - A tool for designing more efficient mechatronic systems.* Conference: 9th International MODELICA Conference, Munich, Germany

[33] Larsson, V., Uebel, K., Krus, P. 2015 *Mode Shifting In Hybrid Hydromechaincal Transmissions.* Proceedings of the ASME/BATH 2015 Symposium on Fluid Power and Motion Control FPMC2015 October 12 – 14, 2015, Chicago, Illinois, USA, pages 1 – 13.

[34] Rydberg, K. 1984. *Gas-Charged Accumulators as Energy Storage Devices in Hydrostatic Drives.* Technical report, Division of Fluid Power Department of Mechanical Engineering, Linköping University

[35] Yunus A, Çengel. 2016 *Fundamentals of thermal-fluid sciences.* ISBN: 9789814720953

[36] Pourmovahed, A, Otis, D.R., 1990. *Experimental thermal time-constant correlation for hydraulic accumulators.* Journal of Dynamic Systems, Measurement and Control, Transac- tions of the ASME, 112(1) : 116 – 121.

[37] National Bureau of Standards, US. 1990. *Thermophysical properties of nitrogen from the fusion line to 3500 R (1944 K) for pressures to 150 00 PSIA (*$10342x10^5$ *[N/m$^2$].* U.S Department Of Commerce

# Appendix

In this appendix, formulas and constants used in for the BWR equations is presented

Table 9.1: BWR gas constants [35] with recalculated units.

| **Constant** | **Value** | **Unit** |
|---|---|---|
| $a$ | 0.115703387 | $\left(\frac{m^3}{kg}\right)^3 \frac{N}{m^2}$ |
| $A_0$ | 136.0474619 | $\left(\frac{m^3}{kg}\right)^2 \frac{N}{m^2}$ |
| $b$ | $2.96625 \cdot 10^{-6}$ | $\left(\frac{m^3}{kg}\right)^2$ |
| $B_0$ | 0.001454417 | $\left(\frac{m^3}{kg}\right)$ |
| $c$ | $7.3806143 \cdot 10^{-5}$ | $\left(\frac{m^3}{kg}\right)^3 K^2 \frac{N}{m^2}$ |
| $C_0$ | $1.0405873 \cdot 10^{-6}$ | $\left(\frac{m^3}{kg}\right)^2 K^2 \frac{N}{m^2}$ |
| $\alpha$ | $5.7863972 \cdot 10^{-9}$ | $\left(\frac{m^3}{kg}\right)^3$ |
| $\gamma$ | $6.7539311 \cdot 10^{-6}$ | $\left(\frac{m^3}{kg}\right)^2$ |
| $R$ | 296.797 | $\frac{J}{kgK}$ |

Table 9.2: Ideal gas specific heat constants [37].

| **Constant** | **Value** | **Unit** |
|---|---|---|
| $N_1$ | $-735.210$ | $K$ |
| $N_2$ | 34.224 | $K$ |
| $N_3$ | $-0.557648$ | $K$ |
| $N_4$ | 3.5040 | $K$ |
| $N_5$ | $-1.7339e-5$ | $K$ |
| $N_6$ | $1.7465e-8$ | $K$ |
| $N_7$ | $-3.5689e-12$ | $K$ |
| $N_8$ | 1.0054 | $K$ |
| $N_9$ | 3353.4061 | $K$ |

**Energy equation**

The time derivative of the first law of thermodynamics results in Equation 9.1

$$\dot{U} = \dot{Q} - \dot{W} \iff m \cdot \dot{u} = \dot{Q} - \dot{W} \tag{9.1}$$

The heat transfer by convection can be approximated according to Equation 9.2 [36], where the time constant $\tau$ is the time it takes to reach 63 % of the final value.

$$\dot{Q} = \frac{m \cdot c_v \cdot (T_s - T_g)}{\tau} \tag{9.2}$$

The rate of work in the accumulator can be described by Equation 9.3.

$$\dot{W} = p \cdot \dot{V} \tag{9.3}$$

The internal energy per unit mass is described by Equation 9.4.

$$\dot{u} = c_v \cdot \dot{T}_g + \left( T_g \cdot \left( \frac{\delta p}{\delta T_g} \right) - p \right) \cdot \dot{v} \tag{9.4}$$

Combining Equation 9.2, 9.3 and 9.4 into 9.1 yields Equation 9.5.

$$m \cdot \left( c_v \cdot \dot{T}_g + \left( T_g \cdot \left( \frac{\delta p}{\delta T_g} \right) - p \right) \cdot \dot{v} \right) = \frac{m \cdot c_v \cdot (T_s - T_g)}{\tau} - p \cdot \dot{V} \tag{9.5}$$

which can be rewritten into Equation 9.6.

$$\dot{T}_g + \frac{T_g \cdot \left( \frac{\delta p}{\delta T_g} \right) \cdot \dot{v}}{c_v} - \frac{p \cdot \dot{v}}{c_v} = \frac{(T_s - T_g)}{\tau} - \frac{p \cdot \dot{V}}{m \cdot c_v} \tag{9.6}$$

As $\dot{V} = m \cdot \dot{v}$ Equation 9.6 can be formulated as 9.7.

$$\dot{T}_g = \frac{(T_s - T_g)}{\tau} - \frac{T_g \cdot \left( \frac{\delta p}{\delta T_g} \right) \cdot \dot{v}}{c_v} \tag{9.7}$$

**Proof of internal energy equation**

The fundamental thermodynamic relation is written in Equation 9.8

$$\delta U = T \cdot \delta S - p \cdot \delta V \tag{9.8}$$

Where $\delta$ S can be expressed in terms of $\delta$ T and $\delta$ V, which can be seen in Equation 9.9

$$\delta S = \left(\frac{\delta S}{\delta T}\right) \cdot \delta T + \left(\frac{\delta S}{\delta V}\right) \cdot \delta V \tag{9.9}$$

By combining Equation 9.8 and 9.9 and using the fact that $c_v = T \cdot (\frac{\delta S}{\delta T})$ yields Equation 9.10.

$$\delta U = c_v \cdot \delta T + T \cdot \left(\frac{\delta S}{\delta V}\right) \cdot \delta V - p \cdot \delta V \tag{9.10}$$

As $T$ indicates the gas temperature $T = T_g$ and by using the Maxwell relation $(\frac{\delta S}{\delta V}) = (\frac{\delta p}{\delta T})$ Equation 9.11 can be formulated.

$$\delta U = c_v \cdot \delta T_g + \left(T_g \cdot \left(\frac{\delta p}{\delta T_g} - p\right)\right) \cdot \delta v \tag{9.11}$$